

# Novel itinerant transverse spin waves

Author: John Feldmann

Persistent link: <http://hdl.handle.net/2345/994>

This work is posted on [eScholarship@BC](#),  
Boston College University Libraries.

---

Boston College Electronic Thesis or Dissertation, 2009

Copyright is held by the author, with all rights reserved, unless otherwise noted.

Boston College

The Graduate School of Arts and Sciences

Department of Physics

NOVEL ITINERANT TRANSVERSE SPIN WAVES

a dissertation

by

JOHN DELANEY FELDMANN

submitted in partial fulfillment of the requirements

for the degree of

Doctor of Philosophy

December 2009



# NOVEL ITINERANT TRANSVERSE SPIN WAVES

JOHN DELANEY FELDMANN

Dissertation advisor: Prof. Kevin S. Bedell

## ABSTRACT

In 1956, Lev Davidovich Landau put forth his theory on systems of interacting fermions, or fermi liquids. A year later, Viktor Pavlovich Silin described spin waves that such a system of fermions would support. The treatment of the contribution of the molecular field to the spin wave dispersion was a novel aspect of these spin waves. Silin predicted that there would exist a hierarchy of spin waves in a fermi liquid, one for each component of the spherical harmonic expansion of the fermi surface.

In 1968, Anthony J. Leggett and Michael J. Rice derived from fermi liquid theory how the behavior of the spin diffusion coefficient of a fermi liquid could be directly experimentally observable via the spin echo effect [24]. Their prediction, that the diffusion coefficient of a fermi liquid would not decay exponentially with temperature, but rather would have a maximum at some non-zero temperature, was a direct consequence of the fermi liquid molecular field and spin wave phenomena, and this was corroborated by experiment in 1971 by Corruccini, et al. [13].

A parallel advancement in the theory of fermi liquid spin waves came with the extension of the theory to describe weak ferromagnetic metals. In 1959,

Alexei Abrikosov and I. E. Dzyaloshinski put forth a theoretical description of a ferromagnetic fermi liquid [1]. In 2001, Kevin Bedell and Krastan Blagoev showed that a non-trivial contribution to the dispersion of the ferromagnetic current spin wave arises from the necessary consideration of higher harmonic moments in the distortion of the fermi surface from its ground state [8].

In the chapters to follow, the author presents new results for transverse spin waves in a fermi liquid, which arise from a novel ground state of a fermi liquid—one in which an  $l = 1$  harmonic distortion exists in the ground state polarization. It is shown that such an instability can lead to spin waves with dispersions that are characterized by a linear dependence on the wave number at long wavelengths, or can lead to spin waves that are characterized by a square root dependence on the wave number at long wavelength.

The author also presents new results for spin waves in a fermi liquid that has a spin density wave in its ground state. A spin density wave is characterized by a spiral magnetization in the ground state, and is observed to occur in materials such as MnSi.

# Acknowledgments

I would like to thank everyone who made this time at Boston College a great time of learning for me, and a very enjoyable time, as well. First of all, thank you to Professor Rein Uritam for having a hand in admitting me to the program. Thank you to Professor David Broido for initiating me into the world of research. Thanks to Professor Gabor Kalman, who was my first advisor; for giving me free enough reign to think up my own research ideas and to follow them through; for the chance to go to a conference in Moscow, which was a great experience, and a great conference; for his understanding when I decided to switch advisors; for the exceptional example that he set for me in how to properly go about research, and how to pursue all possible avenues when investigating an idea or a research problem, and how to see the research to the end stage of final understanding and representation of what has been found. Thanks to Professor Kevin Bedell, for taking me on as his graduate research assistant, when I decided to switch advisors in my fifth year, and for his understanding in this matter; for allowing me to investigate interesting problems and bring forth my own ideas; for the APS conferences that I attended in New Orleans and Pittsburgh; for setting a great example of how to think about a problem deeply, and to keep searching for a possible way through to the goal of the research. Many thanks to Nancy Chevy, Joyce Light, James Ruppenthal, and Karen Barry.

Thanks to Justin Butler, Al Ward, Frank Bello, Kevin Sullivan, Francis

Niestemski, Lucas Lindsay, Hari Dahal, Bed Poudel, Yang Wang, Liang Niestemski, Jason Jackiewicz, Sergio Gaudio, and hmm...lots of other people, but too many to name. It's been a great 7 years. Thanks for all the good times. See ya around.

# Dedication

To my Dad, Mom, Christen, Gretchen, Kristofer, Mary Clare, and Genevieve.  
For all the years of fun times we've had together, and all of the love and support.



# List of Figures

2.1	The Ginzburg-Landau free energy, in arbitrary units, is plotted as a function of the magnetization fraction $m \equiv (n_{\uparrow} - n_{\downarrow})$ . Notice the stable minimum of the free energy occurs at a non-zero magnetization fraction. This describes a ferromagnetic system. . . . .	8
2.2	(a) A two-dimensional representation of the two fermi surfaces – spin up and spin down—are shown in the case when a small magnetization is present in the system. The larger one is the spin up fermi surface, and the smaller one is the spin down fermi surface. (b) The magnetization density $\sigma_p$ as a function of the momentum $p$ is shown. For small magnetization this function can be assumed to be a delta function at the fermi momentum, $p_F$ . The example of a magnetization fraction equal to 0.1 is shown. . . . .	10
2.3	A single spin-symmetric particle-hole excitation. . . . .	17

2.4	When a quasi particle distribution is perturbed by a spatially varying external field with wave vector $q$ , the single quasi particle excitations are restricted to the region into which the fermi sphere is translated by the wave vector. In the figure, the shaded region corresponds to the allowed particle-hole excitations. . . . .	18
2.5	A single spin-antisymmetric particle-hole excitation in a ferromagnetic fermi liquid. The inner surface (inner solid line) is the spin-down fermi surface, while the outer solid line is the spin-up fermi surface. In this schematic, a spin-down quasi particle that used to lie inside of the spin-down fermi sphere, is excited and becomes a spin-up quasi particle, that must lie outside of the spin-up fermi sphere, because of the Pauli exclusion principle. . . . .	19
3.1	Theoretical ferromagnetic spin modes, $\omega^+(q)$ , in an atomic gas of ${}^6\text{Li}$ atoms. . . . .	29
4.1	A spin distribution function (SDF) that contains only $\sigma_0$ , and thus describes a system in a homogeneous magnetic state. . .	37
4.2	A spin distribution function (SDF) that contains $\sigma_0$ and $\sigma_1$ , and thus describes a system in a homogeneous magnetic state which also has a persistent spin current (PSC) in its ground state. . . . .	38

4.3	The SDF of a system with $\sigma_0$ and $\sigma_1$ in its ground state. The white surface is the spin- $\downarrow$ distribution function, and the shaded surface is the spin- $\uparrow$ distribution function. . . . .	40
4.4	Phase diagram of MnSi. Data taken from Shirane (1983) [37].	42
4.5	Phase diagram of MnP. Data taken from Becerra (1980) [7].	42
4.6	Representations of "spiral" and "screw" SDW magnetic structures. . . . .	44
5.1	Approximate solutions from [8] for $qv_F \ll F_1^a$ . The values of the LPs are $F_1^a = 1$ and $F_1^a = -0.5 \dots 0.5$ . . . . .	50
5.2	General solution to the cubic equation for the SC mode of a QEQ system, including $l = 2$ in the perturbation. The values of the LPs are $F_1^a = 1$ and $F_1^a = -0.5 \dots 0.5$ . . . . .	51
5.3	$\omega_0^+(q)$ when only $\nu_0, \nu_1, F_0^a, F_1^a$ , and $\sigma_0$ are included. $F_0^a = 1$ , and $F_1^a = -0.5 \dots 0.5$ . . . . .	52
5.4	$\omega_1^+(q)$ when only $\nu_0, \nu_1, F_0^a, F_1^a$ , and $\sigma_0$ are included. $F_0^a = 1$ , and $F_1^a = -0.5 \dots 0.5$ . . . . .	53
5.5	$\omega_0^+(q)$ when $\nu_0, \nu_1, \nu_2, F_0^a, F_1^a, F_2^a$ , and $\sigma_0$ are included. $F_0^a =$ $1$ , and $F_1^a = -0.5 \dots 0.5$ . . . . .	53
5.6	$\omega_1^+(q)$ when $\nu_0, \nu_1, \nu_2, F_0^a, F_1^a, F_2^a$ , and $\sigma_0$ are included. $F_0^a =$ $1$ , and $F_1^a = -0.5 \dots 0.5$ . . . . .	54
5.7	$q^2$ approximation for $\omega_0^+(q)$ when $\nu_0, \nu_1, F_0^a, F_1^a$ , and $\sigma_0$ are included. $F_0^a = 1$ , and $F_1^a = -0.5 \dots 0.5$ . . . . .	54
5.8	$q^2$ approximation for $\omega_1^+(q)$ when $\nu_0, \nu_1, F_0^a, F_1^a$ , and $\sigma_0$ are included. $F_0^a = 1$ , and $F_1^a = -0.5 \dots 0.5$ . . . . .	55

5.9	The $l = 0$ and $l = 1$ spin wave dispersions that result from a fermi liquid that is magnetic and has a spin current in its ground state. The dispersions are proportional to $q^1$ to leading order in $q$ . . . . .	59
5.10	Showing the leading order $q$ behavior of the spin current mode of a fermi liquid that is magnetic and has a spin current in its ground state. The dispersion is proportional to $q^1$ as $q \rightarrow 0$ . .	59
5.11	The two spin waves that arise from a spin current being in the ground state of a fermi liquid that does not have homogeneous magnetization. The dispersion is proportional to $q^{1/2}$ . . . . .	62
5.12	Calculated Landau parameters, $F_0^a$ and $F_1^a$ , for a gas of $^6\text{Li}$ atoms in the appropriate high-field seeking spin states near the 834-Gauss Feshbach resonance. The horizontal axis is the inverse of the bare scattering length $a_s$ times the fermi wave vector $k_F$ . The quantities plotted are dimensionless. . . . .	67
5.13	SC and SP modes near a Feshbach resonance for a polarized Fermi liquid, for $F_0^a = 0 \dots 10$ . Dashed lines correspond to $F_0^a = 0$ .	69
5.14	SP mode near a Feshbach resonance for an unpolarized PSC Fermi liquid, for $F_0^a = 0 \dots 10$ . Dashed line corresponds to $F_0^a = 0$ .	70
5.15	SC mode near a Feshbach resonance for an unpolarized PSC Fermi liquid, for $F_0^a = 0 \dots 10$ . Dashed line corresponds to $F_0^a = 0$ .	71
5.16	SP mode near a Feshbach resonance for a polarized PSC Fermi liquid, for $F_0^a = 0 \dots 10$ . Dashed line corresponds to $F_0^a = 0$ . . .	72
5.17	SC mode near a Feshbach resonance for a polarized PSC Fermi liquid, for $F_0^a = 0 \dots 10$ . Dashed line corresponds to $F_0^a = 0$ . . .	72

5.18 Spin wave modes of a spiral SDW fermi liquid. The linear modes are the paramagnon modes, and the quadratic modes are the SP and SC transverse spin wave modes. . . . .	75
---	----

# Contents

<b>1</b>	<b>Motivation</b>	<b>1</b>
<b>2</b>	<b>Introduction</b>	<b>3</b>
2.1	Quasi particles (and Quasi holes) . . . . .	4
2.2	Distribution Function . . . . .	5
2.3	Landau Parameters . . . . .	9
2.4	Stability of the fermi surface . . . . .	13
2.5	Precession of spin magnetic moment . . . . .	14
2.6	Collective modes . . . . .	14
2.7	Particle-hole continuum . . . . .	16
2.8	Spin Current . . . . .	20
2.9	Useful Integrals . . . . .	21
<b>3</b>	<b>Spin waves</b>	<b>23</b>
3.1	Kinetic equation . . . . .	23
3.2	Paramagnetic spin waves . . . . .	25
3.3	Ferromagnetic spin waves . . . . .	27
<b>4</b>	<b>New ground states in fermi liquid theory</b>	<b>31</b>

4.1	Additional harmonics in the ground state . . . . .	32
4.1.1	Spontaneous spin current in the ground state . . . . .	32
4.1.2	Induced spin current in ground state . . . . .	34
4.1.3	Induced spin current in ground state . . . . .	35
4.1.4	$l=2$ spherical harmonic distortion in the ground state .	39
4.2	Non-homogeneous polarizations . . . . .	40
<b>5</b>	<b>New spin waves</b>	<b>45</b>
5.1	Equilibrium and Quasi-equilibrium . . . . .	46
5.2	Including $l=2$ in the perturbation . . . . .	48
5.3	Spin waves in a PSC system . . . . .	55
5.4	Non-polarized PSC spin waves . . . . .	58
5.5	Paramagnetic . . . . .	63
5.6	Spin waves in dilute atomic gases . . . . .	64
5.7	Spin waves near a Feshbach resonance in an atomic gas . . . .	65
5.8	Spin waves in SDW materials . . . . .	73
<b>6</b>	<b>Summary and Conclusions</b>	<b>76</b>
	<b>Appendix A</b>	<b>78</b>
A.1	Substitutions . . . . .	78
A.2	Parameter Values . . . . .	79
	<b>Appendix B</b>	<b>80</b>
	<b>Appendix C</b>	<b>84</b>
C.2.1	Spherical Harmonic Projection . . . . .	89

C.2.2	$\nu_0, \nu_1, \sigma_0, f_0^a, f_1^a \neq 0$	94
C.2.3	$\nu_0, \nu_1, \nu_2, \sigma_0, f_0^a, f_1^a, f_2^a \neq 0$	96
C.2.4	$\nu_0, \nu_1, \sigma_0, \sigma_1, f_0^a, f_1^a \neq 0$	98
C.2.5	$\nu_0, \nu_1, \sigma_1, f_0^a, f_1^a \neq 0$	99
C.2.6	$\nu_0, \nu_1, \nu_2, \sigma_0, \sigma_1, f_0^a, f_1^a, f_2^a \neq 0$	100
C.2.7	$\nu_0, \nu_1, \nu_2, \sigma_0, \sigma_1, f_0^a, f_1^a, f_2^a \neq 0$	102
C.2.8	$\nu_0, \nu_1, \nu_2, \sigma_1, f_0^a, f_1^a, f_2^a \neq 0$	103
C.2.9	$\nu_0, \nu_1, \nu_2, \sigma_0, \sigma_2, f_0^a, f_1^a, f_2^a \neq 0$	103
<b>Appendix D</b>		<b>105</b>
<b>Appendix E</b>		<b>111</b>
E.3	Specific Heat	111
E.3.1	Specific Heat for $\omega_0(q) \sim q^{1/2}$ spin mode	112
E.3.2	Specific Heat for $\omega_0(q) \sim q^1$ spin mode	113



# Chapter 1

## Motivation

This thesis was originally motivated by experiments in the 1970's on MnSi, MnP, and other itinerant helical magnets. The spiral and fan magnetism found to be exhibited in itinerant magnets has been traditionally explained theoretically in terms of spin orbit coupling and crystal field interaction [39]. However, this research was initially taken up with the intent of alternatively explaining this phenomenon within the framework of fermi liquid theory. The intent was to recast the transverse magnetization components in terms of the spherical harmonic distortions of the fermi surface, which are central concepts in fermi liquid theory. It was thought that the inclusion of higher harmonic orders in the ground state would represent some sort of symmetry breaking, and that this could account for the small anisotropy gap that is observed in the spin wave dispersions of e.g. MnSi. Unfortunately, this connection has not been made, and given the outcome of our research to date, it is in serious doubt that there is such a connection at all. However, as often happens in science, our results from this investigation turned out

to be novel and significant in another field of physics, via a different (and valid) physical interpretation of the higher spherical harmonic distortion of the fermi surface in the ground state.

Our current physical interpretation of our results—that we are in fact introducing a spin current by including the  $l = 1$  distortion in the ground state—led us to consider cold atomic gases as a possible experimental setup where our findings might be observable. Cold atomic gases provide a clean testing ground for spintronic applications and collective phenomena, among other things. Free of lattice effects and band structures, etc..., and offering complete control of spin states of individual atoms, cold atomic gases have been increasingly attracting researchers who formerly were confined to more conventional condensed matter systems, namely electrons. It should be possible to construct an experimental setup in which there exists a spin current that is constant in time, i.e. a part of the ground state. In this setup, our new spin waves would be observable.

Another type of system in which our results would be observable is one in which there is a persistent current in the ground state. Such systems have close ties to spintronics and the spin Hall effect, and are found widely in solid state physics, including semiconductors and superconductors. Thus, these materials provide excellent possibilities for experimentally observing our new spin waves.

# Chapter 2

## Introduction

This introductory chapter is intended only as a brief overview of the theory and concepts of Landau's theory of fermi liquids. There are many books, articles, monographs, and theses that deal extensively with fermi liquid theory from the most basic concepts to the most complex derivations [33, 31, 18, 6, 10, 19, 15]. These works are entirely sufficient for the curious reader to become well-acquainted with the theory. Therefore, the present introduction will be concerned with introducing the concepts that are sufficient to allow the reader to grasp the thesis of the present work. For a much deeper understanding of Landau's theory, the author refers the reader to the above cited materials.

The first section of this chapter will introduce the concept of a quasi particle, the second, the distribution function, and the third will deal with Landau parameters. Next, the stability of the fermi surface will be discussed, as this is an important consideration in the present work. Sections 4, 5, and 6 will introduce the formalism for calculations that occur in this thesis. Finally,

in section 8, there are provided useful integrals that are required for many of the calculations in this thesis.

## 2.1 Quasi particles (and Quasi holes)

In the context of fermi liquid theory, a quasi particle (quasi hole) is a spin- $1/2$  particle state in an interacting fermi system that corresponds to a spin- $1/2$ , single-particle (-hole) state in the low-temperature non-interacting fermi system that lies outside (inside) of the fermi sphere. It is different, however, from the corresponding state in the non-interacting system in that it is a state that is "dressed" via interactions with the other quasi particles and quasi holes. The interactions lead to a different energy spectrum for the quasi particle, just as interactions in a solid lead to a different energy spectrum for the electrons (i.e. different from  $E = p^2/2m$ ). Also, the lifetime of a quasi particle state is dependent on its proximity to the fermi surface.

In what follows, the quasi particle states will be restricted to lie on the fermi surface, thus they can be assumed to be well-defined states with an infinite lifetime, and therefore can be treated as collisionless. For a finite-temperature treatment, collisions can be added, but the present work will only be concerned with the zero-temperature limit, in which collisions can be completely neglected.

The creation of a quasi particle and quasi hole on the fermi surface corresponds to an excited state of the interacting system. Since this creation occurs on the fermi surface, the usual method of studying deviations of the fermi surface from the ground state (fermi sphere) is to expand the devia-

tions in terms of spherical harmonics. This ensures that all quasi particles and quasi holes lie directly on the fermi surface, and thus are well-defined, long-lived excitations. This expansion also allows for a systematic solution to the transport equation, which, as derived in detail in the Landau kinetic equation section below, describes the collective modes that result from these deviations from the ground state.

## 2.2 Distribution Function

The distribution of quasi particles and quasi holes for an isotropic, translationally invariant fermi liquid at zero temperature is a perfect sphere in momentum space. This is evident from the equation for the distribution of fermions, which is derived from statistical considerations,

$$n_{\varepsilon_p} = \frac{1}{1 + e^{(\varepsilon_p - \mu)/k_B T}} \quad (2.1)$$

At low temperature, fluctuations occur on the fermi surface, and the system is perturbed from its ground state. For very low temperature, i.e.  $T \ll E_F/k_B$ , the quasi particle states reorganize themselves on the fermi surface, and can be considered to not leave the fermi surface at all. In this case, the distribution function can be expanded in terms of spherical harmonics. The dynamics of the system is determined by the states only on the fermi surface, and a treatment of the low-lying states is unnecessary.

If a spin degree of freedom is included in the Hamiltonian, for instance if a magnetic field is present, or if the system is ferromagnetic, then the

distribution function is described by a two-by-two matrix in spin space.

$$[n_p] = \begin{bmatrix} n_p + \sigma_{p,z} & \sigma_{p,x} - i\sigma_{p,y} \\ \sigma_{p,x} + i\sigma_{p,y} & n_p - \sigma_{p,z} \end{bmatrix} \quad (2.2)$$

A quasi particle can be either spin up or spin down, which can locally determine the quantization axis. However,  $x$  and  $y$  components arise from the possibility that the spin quantization axis can vary with position throughout the system, which is determined by the local field at that position. Thus, a spin density wave with a spiral structure or a fan structure in the ground state would be such a system in which the quantization axis for the quasi particles would vary as one travelled along a certain crystalline axis.

If there is a net magnetization present, then there is necessarily a population difference in the two fermi surfaces, spin up and spin down. The relative volume of the two fermi surfaces is determined by the equilibration of the two chemical potentials. A population imbalance can be caused by two different mechanisms. One mechanism is an external magnetic field, which changes the energy of the spin degree of freedom by an amount

$$E_{\uparrow} - E_{\downarrow} = -\hbar\sigma \cdot H. \quad (2.3)$$

where  $E_{\uparrow(\downarrow)}$  is the energy of a quasi particle with spin up (down),  $\sigma$  is the spin state of the quasi particle, and  $H$  is the external magnetic field. The chemical potential of each spin species changes by an identical amount, and in order to reach equilibrium, some spin down quasi particles must flip to spin up quasi particles.

The second mechanism by which a spin population imbalance can occur is a ferromagnetic instability in the system. In this case, the system possesses an interaction between the quasi particles that makes the ferromagnetic phase lower in energy than the non-ferromagnetic phase. In fermi liquid theory, this occurs with a violation of a Pomeranchuk stability condition (see section: Stability of the fermi surface), namely the  $l = 0$  condition, where  $F_0^a < -1$ . This instability portends a ferromagnetic phase. However, if this were the whole story, then this fermi liquid would saturate to full polarization, and one spin species would be completely depopulated. In order to achieve a small magnetization, it must be assumed that there exists a higher order term of the magnetization (higher than second order, which can be determined to leading order in FLT) in the free energy that saves the system from full polarization. This is seen in Ginzburg-Landau phase-transition theory, and it is in this theory where it can be understood that such a phase, with small polarization can be realized.

In Ginzburg-Landau theory, a free energy expansion near a critical point, in terms of the order parameter, is assumed to exist in the form of a power series. Thus, near a magnetic phase transition, the free energy can be expanded in terms of the magnetization,

$$F(m) = am + bm^2 + cm^3 + dm^4 + em^5 + \dots \quad (2.4)$$

However, due to symmetry considerations, in a ferromagnetic system, the free energy cannot be an odd function of the magnetization, since the systems we consider here must have full rotational symmetry in spin space. Thus,

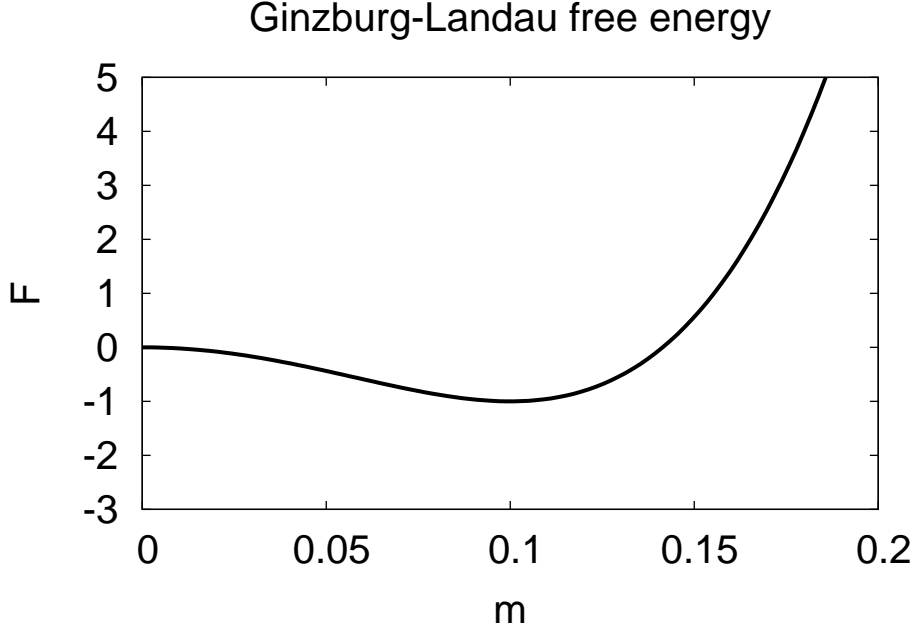


Figure 2.1: The Ginzburg-Landau free energy, in arbitrary units, is plotted as a function of the magnetization fraction  $m \equiv (n_{\uparrow} - n_{\downarrow})$ . Notice the stable minimum of the free energy occurs at a non-zero magnetization fraction. This describes a ferromagnetic system.

the free energy expansion must be restricted to containing only even powers of the magnetization, and the expansion must take the form,

$$F(m) = bm^2 + dm^4 + \dots \quad (2.5)$$

The coefficient  $b$  can be determined in terms of fermi liquid parameters, while the coefficient  $d$  cannot. However, the signs of each coefficient must be that  $b < 0$  and  $d > 0$ , in order for a small magnetization to be achieved in a system. This is obvious if the free energy is plotted as a function of the magnetization fraction,  $m \equiv (n_{\uparrow} - n_{\downarrow})$ , as in Fig. (2.1). In the figure, the stable ground state would possess a magnetization fraction of 0.1.



It is essential that the magnetization fraction remain small, or equivalently, that the population imbalance between the two species remains small compared to the total number of quasi particles. This makes it possible to treat the Landau parameters and fermi velocities of the two species as being identical. If there were a large difference in the two fermi momenta, then the dependence of the interaction (Landau parameters) on momentum would have to be taken into account, since the interaction of quasi particles with different momenta would now play a role, and the spherical harmonic expansion of the Landau parameters would no longer be a useful tool.

In Fig. (2.2) the situation is graphically displayed. The two fermi surfaces are so close, the quasi particles that lie on each are considered to possess negligibly different momenta, and furthermore, the region where the magnetization is non-zero is in such a small region, it can be considered to first order to be a delta function in terms of the momentum. This greatly facilitates the analysis of the transport equation for spin, which leads to the dispersion law for the transverse spin components.

## 2.3 Landau Parameters

The interaction parameter of quasi particles and quasi holes is called the f-function, or Landau parameter, and is represented by the notation  $f_{p\sigma p'\sigma'}$ , where the  $p\sigma p'\sigma'$  denote the specific momentum,  $p$ , and spin state,  $\sigma$ , of a quasi particle-quasi particle, quasi particle-quasi hole, or quasi hole-quasi hole pair.  $f_{p\sigma p'\sigma'}$  is a phenomenological parameter that contains all of the information concerning how quasi particles and quasi holes interact. For

(a)

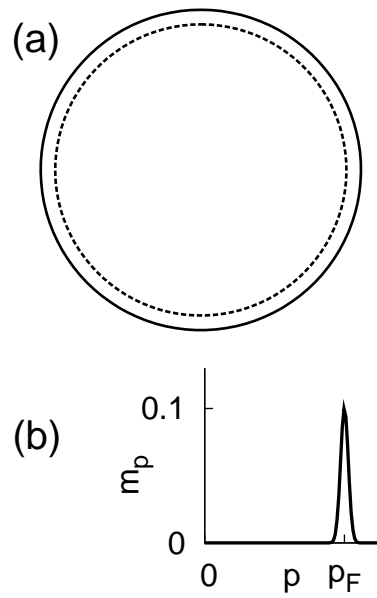


Figure 2.2: (a) A two-dimensional representation of the two fermi surfaces – spin up and spin down – are shown in the case when a small magnetization is present in the system. The larger one is the spin up fermi surface, and the smaller one is the spin down fermi surface. (b) The magnetization density  $\sigma_p$  as a function of the momentum  $p$  is shown. For small magnetization this function can be assumed to be a delta function at the fermi momentum,  $p_F$ . The example of a magnetization fraction equal to 0.1 is shown.

example, in a charged fermi liquid, where  $Z$  is the charge state of the quasi particle or quasi hole, the Landau interaction parameter could be as simple as a bare Coulomb potential,

$$f_{\vec{p}\sigma p'\sigma'} = \frac{kZZ'}{\hbar|\vec{p}-\vec{p}'|^2} \quad (2.6)$$

which depends only on the relative size of the momenta. This would correspond to a repulsive interaction, if the charges of the fermions were the same, which would mean that  $f_{p\sigma p'\sigma'}$  would be positive. A simple Coulomb potential is, however, rarely sufficient to study real systems of fermions. Thus  $f_{p\sigma p'\sigma'}$  is usually much more complicated, and is dependent on the spins of the interacting quasi particles.

Because of the way that Landau parameters are defined, there are infinitely many of them. This is because  $f_{p\sigma p'\sigma'}$  is always expanded in terms of Legendre polynomials, as a function of only the angle between  $\vec{p}$  and  $\vec{p}'$ , and this sum runs from zero to infinity. It is only a function of the angle between the two vector momenta that label the states, because, as Landau pointed out, the qp's and qh's all lie on the fermi surface, and it is only these states that are allowed to interact—the low-lying states, deep within the Fermi sea, are forbidden from interacting, because they are restricted by the Pauli exclusion principle from changing their momentum to some other state, since all other states around them are occupied. Therefore, interactions are restricted to occurring on the fermi surface, where states exist into which qp's can scatter. Thus the interaction parameter  $f_{p\sigma p'\sigma'}$  is only a function of the fermi momentum (the radius of the fermi sphere in momentum space),

the angle between the two interacting momentum states in momentum space, and the spins of each state.

While there are formally infinitely many Landau parameters, only the first few spherical harmonic moments in the expansion of the Landau parameters are assumed to be relevant. This assumption is made for at least three reasons. First of all, only the first two moments of the expansion are able to be determined directly by experiment, and it is comforting to think that that an experiment would be able to supply the parameters that are necessary for a theoretical model. Second, keeping more terms than these leads to higher order coupled equations in calculating, for example, the dispersion laws for density and spin fluctuations. This is not only messy, but provides dispersion laws that would most likely never be observable experimentally. Finally, and perhaps most importantly, by definition an expansion of a quantity in terms of a parameter is always made with the hope that not all of the terms are relevant. This implies that there should be some cutoff after which the terms can be neglected, since they are of higher and higher order in terms of the parameter, and hopefully contain less and less of the essential physics of the system. And, usually in physics, with some famous exceptions, of course, if using only the first term of the expansion is not sufficient, then using the second usually is, and employing the third is when one begins to question whether the expansion is worth it. Thus it is with Landau parameters. The first and second terms, corresponding to the  $l = 0$  and  $l = 1$  spherical harmonic moments, are usually sufficient. However, the experimental data for  $^3\text{He}$  suggests that the cutoff of the expansion after the  $l = 1$  term may be a bit arbitrary and may be missing some of the physics, since at a pressure

of 0 atmospheres, the values found for the Landau parameters are  $F_0^s = 9.15$ ,  $F_1^s = 5.27$ ,  $F_0^a = -0.70$ , and  $F_1^a = -0.55$  [20].

## 2.4 Stability of the fermi surface

In order for the fermi surface to be stable against fluctuations in the distribution function, the variation of the energy with respect to a variation in the distribution must be positive. In other words, it must cost energy to change the distribution function from the ground state. The variation in the energy is given by

$$\delta E = \sum_p \varepsilon_p \delta n_p + \sum_{pp'} f_{pp'} \delta n_p \delta n_{p'} \quad (2.7)$$

where  $\delta n_p$  is the variation in the distribution function. If  $\delta E$  is less than zero, then the fermi surface will find some other ground state that minimizes the energy.

If we expand the Landau parameters and distribution function in terms of Legendre polynomials and spherical harmonics, respectively, then the condition of stability of the fermi surface leads to the Pomeranchuk stability conditions, which are

$$F_l > -(2l + 1) \quad (2.8)$$

Each of these conditions must be met in order to ensure a stable fermi surface.

In the chapters to follow, however, one or more of these conditions will be violated. This is a common tool used to create a spontaneous molecular field

in a fermi liquid [1]. While such a violation does create an instability in the fermi surface, the instability is arrested and stabilized by the introduction of a positive quartic term in Ginzburg-Landau phase transition theory. The coefficient of this term can not be determined completely in terms of Landau parameters, but it is necessary for a theory of ferromagnetism in fermi liquid theory (see Landau Parameters section).

It should be noted here, that there are some systems that possess an instability in the fermi surface, and the system changes to a completely new ground state, with no arresting quartic term to keep the order parameter small. For example, in a conventional superconductor an effective attractive interaction between the quasi particles leads to pairing of the fermions and to a collapse of the fermi surface. The pairs of quasi particles act like bosons, and the lowest energy configuration in momentum space is no longer a sphere, but a point at zero temperature, since there is no limit for the number of bosons that can occupy the same quantum mechanical state.

## **2.5 Precession of spin magnetic moment**

## **2.6 Collective modes**

The collective modes of a fermi liquid can be derived and understood in two different ways. The first method is through consideration of the transport equation. The second is through response theory, in examining the poles of the response function, which supply modes of the system for which there is required no initial perturbation—in other words, the system supports these

collective modes without an external perturbation. Both of these treatments lead to the same results.

In a system that is initially slightly out of equilibrium, collective modes arise as an attempt to restore equilibrium. Thus, in a fermi liquid, if there exists a spatial gradient in the density or spin projection of quasi particles, then collective modes will form at certain frequencies and wave vectors that are resonant to the system. When one derives the collective mode structure of a system, it is these resonant frequencies and wave vectors that are derived.

Considering a volume of phase space, which is a six dimensional space, one dimension for each component of momentum (3) and each spatial component (3). If we consider the number of quasi particles flowing into and out of this volume, the time rate of change of the number of quasi particles inside this volume must be equal to the difference of the number that flow out and the number that flow in. (We are neglecting collisions throughout this thesis. Taking collisions into account, this would be another mechanism which would also change the number of quasi particles in the volume of phase space.) This is just the particle conservation law. From this simple consideration, we immediately arrive at the transport equation

$$\frac{\partial}{\partial t}n = \sum_i \left( \frac{\partial n}{\partial q_i} \frac{\partial \varepsilon}{\partial p_i} - \frac{\partial n}{\partial p_i} \frac{\partial \varepsilon}{\partial q_i} \right) \quad (2.9)$$

It is shown in explicit detail how this equation is linearized in terms of the variation of the distribution function, and thus leads to the derivation of the collective modes (spin waves) of a fermi liquid.

As mentioned above, the collective modes can also be derived from con-

sideration of the response function. As an example, the magnetic response function, i.e. magnetic susceptibility, is considered, from which the spin wave spectrum is derived.

In response to a perturbing magnetic field that varies slowly in space and time, a fermi liquid with a spin degree of freedom will respond by polarizing in the direction of the perturbing field, by an amount determined by the dynamic susceptibility,  $\chi(q, \omega)$ .

## 2.7 Particle-hole continuum

What is referred to as the particle-hole continuum of excitations, or the Stoner continuum, is the energy, as a function of the wave vector  $q$ , that is required to make a single quasi particle-quasi hole pair excitation. An exemplary situation is shown in Fig. 2.3.

The spectrum of the single particle-hole excitations is significant in fermi liquid theory, because they have the effect of dampening the collective excitations that happen to have the same energy as such an excitation. This means that any collective excitation, whether density fluctuation or spin fluctuation, will be dampened to some degree (the degree to which they will be dampened varies, but this won't be considered in this thesis).

The particle-hole dispersion is easily understood in the context of fermi surfaces in momentum space, and in energy space. It is simply the union of all possible single particle-hole excitations. Thus, for the spin-symmetric particle-hole dispersion, it is the energy required to move a quasi particle that lies within the fermi sphere to an allowed region that lies outside of the



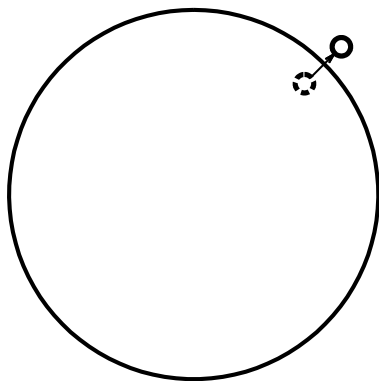


Figure 2.3: A single spin-symmetric particle-hole excitation.

fermi sphere (without changing the spin, i.e. spin-symmetric).

The allowed region is determined by the momentum that is being transferred to the system by some external perturbation. When an external probe is introduced to the system, it introduces a perturbing external potential that is a function of the spatial coordinate,  $\mathbf{r}$ , and time,  $t$ . If this external potential is Fourier transformed with respect to space and time, then the perturbation becomes a function of the wave-number,  $\mathbf{q}$ , and the frequency,  $\omega$ . As a result of this perturbation, the single particle-hole excitations are only allowed to occur from the region in energy space that the fermi surface occupied before the perturbation, to the region in space that the fermi surface occupies after the perturbation. This is much more economically shown graphically, as in Fig. 2.4. In this figure, the shaded region is the region of

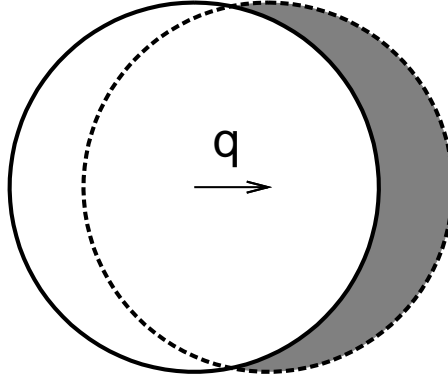


Figure 2.4: When a quasi particle distribution is perturbed by a spatially varying external field with wave vector  $q$ , the single quasi particle excitations are restricted to the region into which the fermi sphere is translated by the wave vector. In the figure, the shaded region corresponds to the allowed particle-hole excitations.

allowed particle-hole excitations

where  $\omega_L$  is the Larmor frequency. It must be remembered that in a fermionic system there usually exist two fermi surfaces, one for each spin projection (unless the system is fully polarized). Thus there exists the possibility for a spin-antisymmetric excitation to occur, in which the spin of the quasi particle is changed during the excitation. The spin-antisymmetric particle-hole dispersion is understood in a very similar way as the spin-symmetric dispersion. The only difference is that the quasi particle's spin must be changed in creating the excitation, and thus more care must be taken to obey the Pauli exclusion principle.

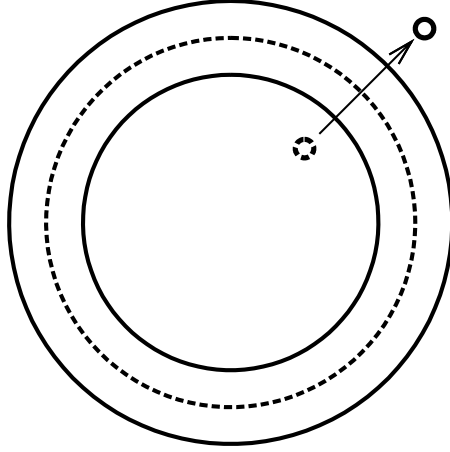


Figure 2.5: A single spin-antisymmetric particle-hole excitation in a ferromagnetic Fermi liquid. The inner surface (inner solid line) is the spin-down Fermi surface, while the outer solid line is the spin-up Fermi surface. In this schematic, a spin-down quasi particle that used to lie inside of the spin-down Fermi sphere, is excited and becomes a spin-up quasi particle, that must lie outside of the spin-up Fermi sphere, because of the Pauli exclusion principle.

The dispersion of the single particle-hole excitations for a spin-flip process is given by the relation,  $\hbar\omega_{ph} = \varepsilon_{p+q}^{\uparrow} - \varepsilon_p^{\downarrow}$ , or

$$\omega_{ph} = \omega_L - \frac{2mF_0^a}{\hbar N(0)} + \mathbf{q} \cdot \mathbf{v}_p \quad (2.10)$$

Such an excitation is shown in Fig. 2.5 for  $q = 0$ .

## 2.8 Spin Current

A spin current is the transport of a spin projection in spin space along a certain direction with respect to the crystalline axis. For example, the  $z$ -projection of a spin can travel along the  $x$ ,  $y$ , or  $z$  cartesian axis, or any combination thereof, and the same goes for the  $x$  and  $y$  projections of a spin. If there exists a spatial gradient of some spin projection, then this gradient can produce a spin current.

We must note here that there are systems where there exists a predisposition for such a gradient to exist in the ground state, namely materials that possess a spin density wave in their ground state—for instance  $\text{ZrZn}_2$  and  $\text{MnSi}$ . These two materials are itinerant magnets that possess a non-homogeneous spin structure in their ground state in a certain temperature and pressure range.

Nevertheless, a spin current can still be set up in any fermi liquid that possesses rotational and translational degrees of freedom. Experimentally a spin current can be produced by introducing a perturbation in the local magnetic field. This perturbation is then transmitted away from this point as the system attempts to restore local (and global) equilibrium. This transmission of a local magnetic perturbation throughout the system is what is called a spin current.

The net spin conservation law in fermi liquid theory is

$$\frac{\partial \sigma(\mathbf{r}, t)}{\partial t} + \frac{\partial}{\partial r_i} j_{\sigma, i}(\mathbf{r}, t) = \gamma \sigma(\mathbf{r}, t) \times H(\mathbf{r}, t) \quad (2.11)$$

where the spin current is

$$j_{\sigma,i}(\vec{r}, t) = 2 \int \frac{d^3p}{(2\pi\hbar)^3} \left( \frac{\partial \varepsilon_{\mathbf{p}}}{\partial p_i} \sigma_{\mathbf{p}} + \frac{\partial \mathbf{h}_{\mathbf{p}}}{\partial p_i} n_{\mathbf{p}} \right) \quad (2.12)$$

## 2.9 Useful Integrals

$$\begin{aligned} I. \quad & \int_0^\infty dp \, p^2 \left( -\frac{\partial n_p^0}{\partial \varepsilon_p} \right) \\ II. \quad & \int_0^{2\pi} \int_0^\pi d\theta_p \, d\phi_p \, \sin \theta_p \, Y_l^{m*}(\theta_p, \phi_p) Y_{l'}^{m'}(\theta_p, \phi_p) Y_{l''}^{m''}(\theta_p, \phi_p) \end{aligned}$$

For integral  $I$  the solution is obtained by noting that  $-(\partial n_p^0 / \partial \varepsilon_p) = \delta(\varepsilon_{p\sigma} - \mu)$ , and  $\varepsilon_{p\sigma} - \mu \approx v_F \cdot (p - p_F)$ . This second step is used, because it is necessary to get the delta function in terms of the integral variable, which in this case is  $p$ . Thus the solution is

$$\begin{aligned} & \int_0^\infty dp \, p^2 \left( -\frac{\partial n_p^0}{\partial \varepsilon_p} \right) = \int_0^\infty dp \, p^2 \, (\delta(\varepsilon_{p\sigma} - \mu)) \\ & = \int_0^\infty dp \, p^2 \, (\delta(v_F \cdot (p - p_F))) \\ & = \frac{1}{v_F} \int_0^\infty dp \, p^2 \, (\delta(p - p_F)) = \frac{1}{v_F} p_F^2 = \boxed{p_F m^*} \end{aligned}$$

For integral  $II$ , the example will be

$$\begin{aligned}
& \int_0^{2\pi} \int_0^\pi d\theta_p d\phi_p \sin \theta_p Y_2^0(\theta_p, \phi_p) Y_1^0(\theta_p, \phi_p) Y_1^0(\theta_p, \phi_p) \\
&= \int_0^{2\pi} \int_0^\pi d\theta_p d\phi_p \sin \theta_p \left( \frac{\sqrt{5}}{\sqrt{16\pi}} (3 \cos^2 \theta_p - 1) \right) \left( \frac{\sqrt{3}}{\sqrt{4\pi}} \cos \theta_p \right) \left( \frac{\sqrt{3}}{\sqrt{4\pi}} \cos \theta_p \right) \\
&= \frac{3\sqrt{5}}{8\sqrt{\pi}} \int_0^\pi d\theta_p \sin \theta_p \left[ 3 \cos^4 \theta_p - \cos^2 \theta_p \right] \\
&= -\frac{3\sqrt{5}}{8\sqrt{\pi}} \left[ \frac{3}{5} \cos^5 \theta_p \Big|_0^\pi - \frac{1}{3} \cos^3 \theta_p \Big|_0^\pi \right] \\
&= \frac{3\sqrt{5}}{8\sqrt{\pi}} \left[ \frac{6}{5} - \frac{2}{3} \right] \\
&= \frac{1}{\sqrt{5\pi}}
\end{aligned}
\tag{2.13}$$

# Chapter 3

## Spin waves

### 3.1 Kinetic equation

The starting point for calculating spin wave dispersions in fermi liquid theory is the Landau kinetic equation (LKE). Below is a derivation of the LKE, and an explanation of the nuances and differences between it and other kinetic equations.

Generally speaking, a kinetic equation is derived from phase space arguments, where the conservation of a certain quantity leads to an expression relating a change in time of the quantity to a change in space of the same quantity.

In the case of the particle distribution function, if each particle is represented by a point in phase space, which is specified by three momentum components and three spatial components, then the time derivative of the number of particles in a volume of phase space,  $dV = dp_x dp_y dp_z dx dy dz$ , is equal to the number of particles flowing into the volume minus the number of

particles flowing out of the volume, and also plus/minus the number of particles that undergo a collision that abruptly brings them into/takes them out of the volume (by changing their momentum components). Mathematically, this relation is represented by a kinetic equation in the following form,

$$\frac{\partial n_p}{\partial t} + \frac{\partial n_p}{\partial \vec{x}} \cdot \frac{\vec{p}}{m} + \frac{\partial n_p}{\partial \vec{p}} \cdot \vec{f} = \frac{\partial n_p}{\partial t}|_{coll}. \quad (3.1)$$

where  $n_p$  is the distribution function. This is the Boltzmann equation, and it is a first order differential equation. In this thesis we ignore collisions, which is a valid approximation as the temperature  $T \rightarrow 0$ .

For spin waves in fermi liquid theory, it is sufficient to treat the deviation of the quasi particle distribution from the ground state (fermi sphere) as linear. Thus, the distribution function is represented by a ground state distribution,  $\sigma_p^0$ , and a deviation,  $\delta\sigma_p$ ,

$$\sigma_p \equiv \sigma_p^0 + \delta\sigma_p \quad (3.2)$$

where  $\sigma_p$  is the spin distribution function, and it is equal to  $n_{p\uparrow} - n_{p\downarrow}$ , i.e. the difference of the distribution functions of the two spin species. Thus, the spin distribution function parametrizes the polarization properties of a fermi liquid, and it has its own kinetic equation, from which spin waves are derived (density waves are derived from the kinetic equation for  $n_p$ ). Since  $\sigma_p^0$  is the ground state distribution function, it does not vary with time. Throughout this thesis we assume that the polarization is small, so that the Landau parameters in the polarized state can be assumed to be equal to the LP's in the unpolarized state [24]. If the polarization is not small, then the



dependence of the Landau parameters (interaction parameters)  $f_{pp'\sigma\sigma'}$  on the difference in magnitude of the momentum,  $|\mathbf{p} - \mathbf{p}'|$ , of two interacting quasi particles has to be taken into account, in addition to the angle between the two momentum vectors, and this would greatly enhance the complexity of the theory. The polarization of the system is given by

$$\sigma = \sum_p \sigma_p = \sum_p (n_{p\uparrow} - n_{p\downarrow}) = n_{\uparrow} - n_{\downarrow} \quad (3.3)$$

The form for the spin kinetic equation is

$$\frac{\partial}{\partial t} \vec{\sigma}_p + \vec{v}_p \cdot \vec{\nabla}_r \left( \vec{\sigma}_p - \frac{\partial n_p^0}{\partial \varepsilon_p} \int \frac{d^3 p'}{2\pi\hbar} f_{pp'}^a \vec{\sigma}_p' \right) = -\frac{2}{\hbar} \vec{\sigma}_p \times \vec{h}_p \quad (3.4)$$

It is from this equation that the spin wave dispersions are derived.

## 3.2 Paramagnetic spin waves

Many of the properties of polarized fermi liquids were first investigated by V. P. Silin [38]. Silin derived the behavior of spin density fluctuations in a paramagnetic system. In a homogeneous Fermi liquid ( $q = 0$ ) in the presence of an external magnetic field, there exist a hierarchy of spin waves, one for each harmonic distortion of the fermi surface (distribution function), which are called Silin modes, and are given by

$$\omega_l^{\pm} = \pm \left( \omega_0 - \frac{2}{\hbar N(0)} \sigma_0 \left( F_0^a - \frac{F_l^a}{2l+1} \right) \right) \quad (3.5)$$

If the system is in equilibrium with a homogeneous external magnetic field,  $H$ , then

$$\sigma_0 = \frac{\gamma\hbar}{2} \frac{N(0)}{1 + F_0^a} H \quad (3.6)$$

and the collective modes are

$$\omega_l^\pm = \pm\omega_0 \frac{1 + F_l^a/(2l + 1)}{1 + F_0^a} \quad (3.7)$$

where  $l$  is the polar order of the spherical harmonic component to which each spin wave corresponds (as in  $Y_l^m$ ). The spherical harmonics arise in the decomposition of the kinetic equation in terms of the harmonics of the fermi surface distortion.

In the case of a non-homogeneous perturbation, the spatial gradient of the spin distribution function spawns non-homogeneous spin waves, which are characterized by a certain wavelength  $\lambda$ , and thus a wave vector  $q = \frac{2\pi}{\lambda}$ , and a corresponding frequency  $\omega$ , with which the spin wave propagates for any given  $q$ . The dependence of  $\omega$  on the wave vector  $q$  is the dispersion of the spin wave. The  $\omega$  and  $q$  arise upon Fourier transforming the kinetic equation. The dispersion relations are derived in the Appendix, and for the case of Silin (paramagnetic) spin waves, the first two spin waves are

$$\begin{aligned} \omega_0^+(q) &= \omega_L + \frac{\frac{1}{3}(1 + F_0^a)(1 + \frac{F_1^a}{3})v_F^2 q^2}{\frac{2}{\hbar N(0)}(F_0^a - \frac{F_1^a}{3})\sigma_0} \\ \omega_1^+(q) &= \omega_L - \frac{2}{\hbar N(0)}(F_0^a - \frac{F_1^a}{3})\sigma_0 - \frac{\frac{1}{3}(1 + F_0^a)(1 + \frac{F_1^a}{3})v_F^2 q^2}{\frac{2}{\hbar N(0)}(F_0^a - \frac{F_1^a}{3})\sigma_0} \end{aligned} \quad (3.8)$$

where  $\omega_L$  is the Larmor frequency equal to  $\frac{\gamma\hbar}{2}H$ , where  $H$  is the external magnetic field.

### 3.3 Ferromagnetic spin waves

Transverse spin waves are also realized in the absence of a magnetic field in a ferromagnetic fermi liquid, where the ferromagnetism can arise either from a ferromagnetic instability,  $F_0^a < -1$ , or from a quasi-equilibrium situation, which can be created in a dilute atomic gas either by spin injection or by laser-induced spin transitions.

The only differences between the Silin paramagnetic spin wave dispersions and the ferromagnetic spin wave dispersions are that the Larmor frequency is not present in the latter, since the external field is absent, and the magnetization is no longer given by its equilibrium value in an external field, but rather is determined by the GL free energy in the case of a ferromagnetic instability, or by the rate of spin-flipping processes in the case of laser-induced spin transitions or spin injection.

The quadratic dispersion of the ferromagnetic modes in fermi liquid theory was confirmed by Abrikosov and Dzyaloshinskii [1]. Such a quadratic dispersion was expected, as it was in the paramagnetic case, based on the previous theoretical derivations of spin waves in Heisenberg ferromagnets.

The derivation put forth by Abrikosov and Dzyaloshinskii has been slightly modernized, e.g. [6], by expanding the fermi surface in terms of spherical harmonics (see Appendix). The first two resultant spin waves are

$$\begin{aligned}
\omega_0^+(q) &= \frac{\frac{1}{3}(1 + F_0^a)(1 + \frac{F_1^a}{3})v_F^2 q^2}{\frac{2}{\hbar N(0)}(F_0^a - \frac{F_1^a}{3})\sigma_0} \\
\omega_1^+(q) &= -\frac{2}{\hbar N(0)}(F_0^a - \frac{F_1^a}{3})\sigma_0 - \frac{\frac{1}{3}(1 + F_0^a)(1 + \frac{F_1^a}{3})v_F^2 q^2}{\frac{2}{\hbar N(0)}(F_0^a - \frac{F_1^a}{3})\sigma_0}
\end{aligned} \tag{3.9}$$

These modes are plotted in Fig. 3.1. The first mode is the spin precession mode, and corresponds to the precession of the quasi particle spin about the internal ("molecular") magnetic field. It is a gapless Goldstone mode with a quadratic dispersion. Such a mode usually arises from a continuous degeneracy that is inherent in the ground state energy, and in this case it is no different. The continuous degeneracy that exists in a homogeneous ferromagnetic system is the direction of the magnetization. Since all magnetization directions are equivalent, the result is a continuous degeneracy with respect to the magnetization.

The second mode is called the spin current mode, since the harmonic moment of the fermi surface distortion to which it corresponds ( $l = 1$ ) spawns a spin current, as will be derived in the next section. A spin current is the transport of the spin variable through the system. In this case, the spin current oscillates in space and time. (In the next chapter, a spin current will be allowed to occur in the ground state that is constant in time, and new spin waves will result.)

The detection of these spin waves in metals is hindered by two factors. One, the parameters in the theory are phenomenological, and attempts to

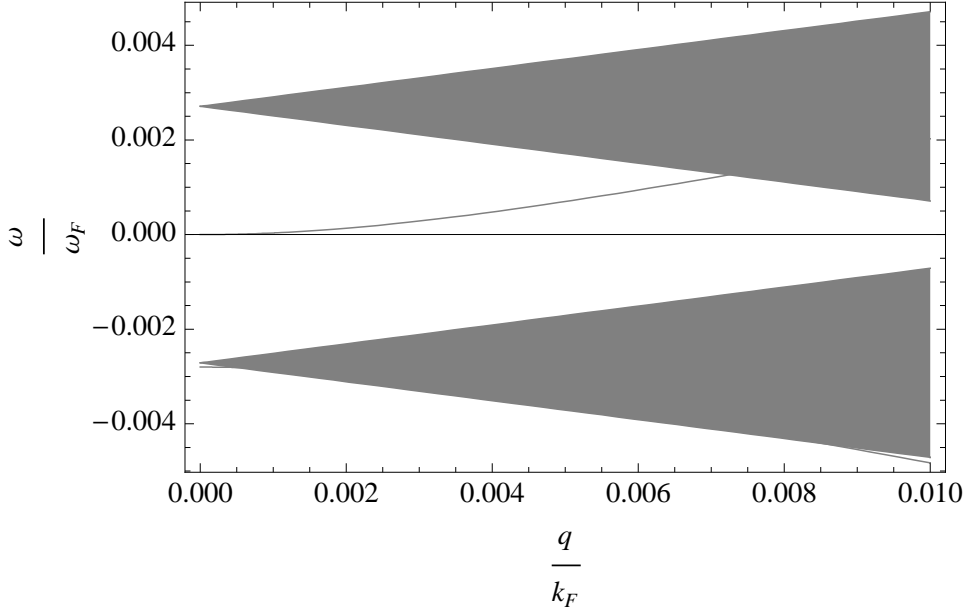


Figure 3.1: Theoretical ferromagnetic spin modes,  $\omega^+(q)$ , in an atomic gas of  ${}^6\text{Li}$  atoms.

microscopically derive them, e.g. [4], have only seen limited success. Therefore, numerical values for them must be obtained from experiment, where it is only possible to obtain values, with limited accuracy, for the first two Landau parameters [36]. Furthermore, the number of Landau parameters, of which there are an infinite number, that are nonzero in a certain system is not known. Two, the clean derivation of a hierarchy of modes, each corresponding to a harmonic moment of the distortion of the fermi surface, does not translate perfectly, as can be expected, to the case of a real piece of metal, given all of the imperfections and various interactions that can be present in the latter.

However, the direct observation of the molecular field (due to quasi particle interaction) is possible, thanks to the Leggett-Rice effect, which was derived by Anthony Leggett and Michael Rice in 1968 [24]. It is also via this

effect that an experimental measurement of the Landau parameter  $F_1^a$  can be made. The mechanism that is exploited by the Leggett-Rice effect is the spin echo effect.

The prospect of detecting these spin waves in a  $^6\text{Li}$  atomic gas is very feasible (this is discussed in more detail in the next chapter). Temperatures well below the fermi temperature are achievable in an atomic gas setup [35], and the experimental method of light scattering is capable of detecting spin waves in an atomic gas. It is also in such an experiment that we propose our new spin waves might be observable.

# Chapter 4

## New ground states in fermi liquid theory

In this chapter we present our results for new spin waves in a fermi liquid. The new results can be separated into two categories, corresponding to two different assumptions about the ground state from which we start. The first type of ground state comes from allowing the Fermi liquid to acquire a persistent spin current (PSC) in its ground state. Though this may seem unphysical, we will give evidence for the experimental realizability of such a situation. The second type of ground state is a non-homogeneous magnetic phase, e.g. a spiral or fan magnetic structure. Such ground states as these are known to exist in itinerant magnets such as MnSi, and have recently been proposed to be realizable in cold atom gases, as well [27]. We discuss these ground states and their corresponding spin waves in the following chapter, and the surprising characteristics of the spin wave dispersion. We then discuss the further surprising results that are found when these ground states

and modes are considered in the context of a Fermionic atomic gas near a Feshbach resonance, such as  $^6\text{Li}$  near its resonance at 834 Gauss.

## 4.1 Additional harmonics in the ground state

### 4.1.1 Spontaneous spin current in the ground state

In a Fermi liquid, the ground state is characterized by the distribution function, which in turn is determined by the quasi particle Hamiltonian. In a normal Fermi liquid (non-superfluid), the interaction of the quasi-particles must be repulsive for the Fermi surface to be stable against fluctuations. Furthermore, for stability of the system to be defined within Fermi liquid theory, the spin-symmetric and spin-antisymmetric dimensionless Landau parameters must satisfy the Pomeranchuk stability conditions, which are

$$F_l^{s,a} > -(2l + 1) \quad (4.1)$$

However, in a ferromagnetic Fermi liquid, the  $l = 0$  stability condition can be violated, and the stability of the Fermi surface is still achieved, because it is assumed that there is a fourth order term (quartic in the order parameter, which in our case is the magnetization  $\sigma \equiv \sum_p \sigma_p$ ) in the free energy that is greater than zero. Without this term, the fermi surface would evolve into a fully polarized state. With this positive quartic term, however, the order parameter, which, again, in our case is the magnetization, can be kept small, and a two-species ferromagnetic polarized Fermi liquid can be achieved in equilibrium.



In our new ferromagnetic Fermi liquid ground state, it is the  $l = 1$  instability that spontaneously generates a  $\sigma_1$  order parameter. Furthermore, it turns out that if we allow both the  $l = 0$  and  $l = 1$  instability to occur simultaneously, then the resultant spin waves are very different from the situation where only an  $l = 1$  instability occurs. A system in which both of these instabilities occurs would be a homogenous ferromagnet and would have a spontaneous spin current in the ground state. Surprisingly, such a ground state has been proposed to be realizable in a gas of  ${}^6\text{Li}$  atoms [40]. However, the manner in which this ground state is achieved is not via violation of the Pomeranchuk stability conditions in the context of Fermi liquid theory. Thus, we must be careful in applying too liberally the results we obtain for such a spontaneously-generated ground state. We can discuss theoretically the case where  $F_0^a < -1$  and  $F_1^a < -3$ , but to date these conditions have not been observed in an actual system. The theoretical discussion is not moot, however, since the generation of such a ground state, regardless of the values of the anti-symmetric Landau parameters, or the manner in which it is generated, would lead to the new spin waves.

The application of our results for spin waves in a system where ferromagnetism and a spin current have been spontaneously generated should be done delicately, however, for a different reason, which is that our modes assume only an exchange interaction, whereas the spin orbit interaction is usually associated with such a ground state. Therefore we must assume, in order to apply the results from this section, that the spin-orbit coupling between fermions is a perturbative effect, whereas the exchange modes that we derive would be a first order effect. Such an assumption is grounds for serious

objection to our results. However, it is still possible that these modes could be realized in a real system, and therefore we present them, knowing full well the limitations of only including exchange coupling.

### 4.1.2 Induced spin current in ground state

The generation of a spin current in the ground state of a fermi liquid without violating the  $l = 1$  Pomeranchuk stability condition is entirely possible experimentally, and the spin waves results obtained via Fermi liquid theory assuming only an exchange interaction need not be as delicately applied, as in the case of a spontaneously generated spin current. In order to induce a spin current in a cold atom gas, there are various approaches that, at least in theory, could be employed. The first is to induce the two spin species to move in opposite directions relative to each other by merely moving their respective potential minima towards and through each other. Another would be to begin with a fully polarized gas (as is usually done in experiment to begin with), and then optically pump a spin transition in one hemisphere of the gas into the other spin state, and let the two hemispheres diffuse through each other. Yet another method would be to use an external field that couples to the orbit of the fermions, in order to generate a spin current using the spin-orbit interaction. Then, turn off the external field, creating a quasi-equilibrium situation, but one that can still be treated with Fermi liquid theory. This quasi-equilibrium situation has been studied before [9], and the low collision frequency in a cold atom gas means that a quasi-equilibrium situation should be realizable. Thus, an  $l = 1$  instability would be able to be

simulated in any of the above ways, without violating the  $l = 1$  Pomeranchuk stability condition.

### 4.1.3 Induced spin current in ground state

Regardless of the method by which an  $l = 1$  distortion is generated in a Fermi liquid, we can look at the resulting shape of the spin distribution function in momentum space. The distortion can be expanded in terms of spherical harmonics, since the Fermi-Dirac distribution function is given by

$$n_{\mathbf{p}\vec{\sigma}} = \frac{1}{e^{-\varepsilon_{\mathbf{p}\vec{\sigma}}/k_B T} + 1} \quad (4.2)$$

and is thus approximately a sphere in momentum space at low temperatures,  $T \ll T_F$ , where  $T_F$  is the Fermi temperature. The spin distribution function is given by  $\vec{\sigma}_{\mathbf{p}} \equiv n_{\mathbf{p},\uparrow} - n_{\mathbf{p},\downarrow}$ , and is thus approximately a spherical shell for an itinerant magnet at low temperatures, with a thickness that is determined by the difference in the population of the spin species. Anyway, the spin distribution function is expanded in terms of spherical harmonics, as well, i.e.

$$\begin{aligned} \sigma_p &= \sigma_0 Y_0^0(\theta_p, \phi_p) + \sigma_1 Y_1^0(\theta_p, \phi_p) + \sigma_2 Y_2^0(\theta_p, \phi_p) + \dots \\ &= \frac{1}{\sqrt{4\pi}} \sigma_0 + \sqrt{\frac{3}{4\pi}} \cos \theta_p \sigma_1 + \sqrt{\frac{5}{16\pi}} (\cos^2 \theta_p - 1) \sigma_2 + \dots \end{aligned} \quad (4.3)$$

As many orders can be included in this expansion as are desired, however, since the expansion is usually truncated after the  $l = 0$  term, we truncate

the expansion after the  $l = 1$  term and explore the consequences. (We also explored including the  $l = 2$  term, but interestingly this term did not give any new results as compared to the  $l = 0$  term. We discuss this briefly at the end of this chapter, and derive the resulting spin waves in the appendix.)

The spin distribution function (SDF) for a homogeneous ferromagnet is a spherical shell, as shown representationally (as an annulus in two dimensions) in the 4.1. In a system that has a spin current, i.e. has an  $l = 1$  spherical harmonic component in its ground state, the SDF is a shell of thickness that varies as the function  $\cos \theta_p$ , where  $\theta_p$  is the polar angle. In Fig. 4.2, a two-dimensional representation of this SDF is shown. One can readily see that, with more polarization in the  $z > 0$  hemisphere of the SDF than in the  $z < 0$  hemisphere, there is a resulting spin current in the  $+z$ -direction. The spin current,  $j_\sigma$ , is calculated by integrating over the SDF in momentum space

$$j_\sigma = \int d^3p \vec{\sigma}_p \cdot \vec{p} \quad (4.4)$$

The details of this calculation are in the appendix. This spin current is frozen into the ground state, as a result of the  $l = 1$  spherical harmonic deformation of the SDF.

If the ground state SDF has only an  $l = 1$  deformation, without an  $l = 0$  deformation, then the system has no net polarization, but still has a spin current. This situation gives rise to the following net spin current

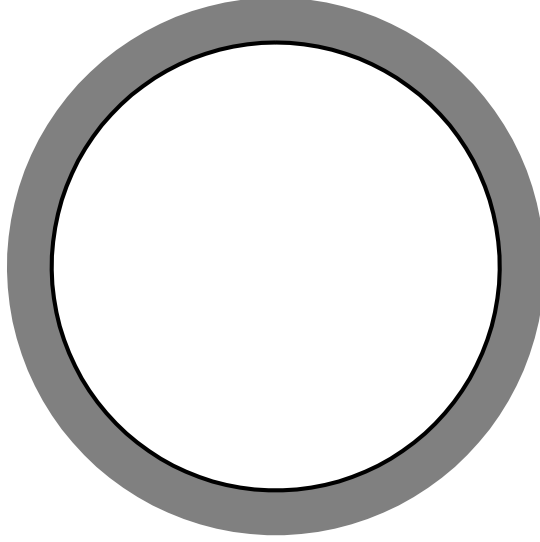


Figure 4.1: A spin distribution function (SDF) that contains only  $\sigma_0$ , and thus describes a system in a homogeneous magnetic state.

$$\begin{aligned}
 j_{\uparrow,z} &= \frac{2\pi p_F^4}{m^*(2\pi\hbar)^3} \sigma_1 \left(1 + \frac{F_1^a}{3}\right) \sqrt{\frac{3}{4\pi}} \\
 j_{\downarrow,z} &= -\frac{2\pi p_F^4}{m^*(2\pi\hbar)^3} \sigma_1 \left(1 + \frac{F_1^a}{3}\right) \sqrt{\frac{3}{4\pi}}
 \end{aligned}
 \tag{4.5}$$

Thus the spin currents of each spin species are equal in magnitude and opposite in direction in a persistent spin current (PSC) ground state, i.e. a ground state SDF that possesses a  $\sigma_1$ . As stated earlier, this situation is physically equivalent to a cloud of spin- $\uparrow$  fermions passing through a cloud of spin- $\downarrow$  fermions that is traveling in the opposite direction.

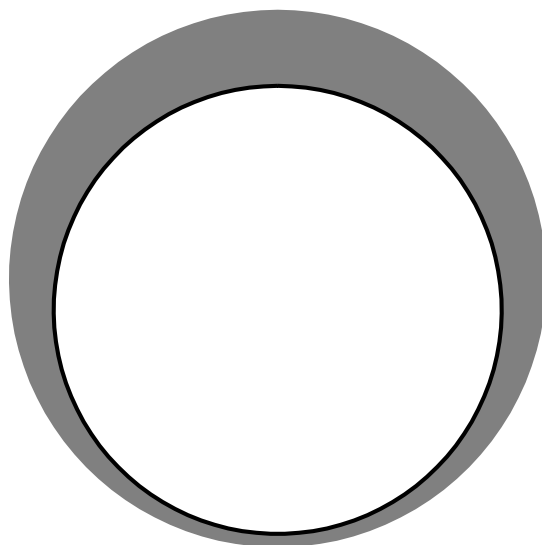


Figure 4.2: A spin distribution function (SDF) that contains  $\sigma_0$  and  $\sigma_1$ , and thus describes a system in a homogeneous magnetic state which also has a persistent spin current (PSC) in its ground state.

#### 4.1.4 $l=2$ spherical harmonic distortion in the ground state

As previously mentioned, further distortions of the fermi surface can be included in the ground state. However, the practical applications of such distortions in a fermi liquid is limited, because the fermi surface of a real system of fermions is unlikely to involve such harmonics to any meaningful degree. Also, the interaction parameters,  $F_l^a$ , are often assumed to be unnecessary for  $l > 1$ , as are the perturbative distortions of the FS (due to collisional damping [33]). Thus, a study of  $l = 2$  moments and higher is usually considered moot, since most of the physics of a fermi liquid is assumed to be captured in the  $l = 0$  and  $l = 1$  moments of the FS and LP's. Nevertheless, we include here a brief description of the  $l = 2$  distortion of the FS in the GS. Interestingly we found that an  $l = 2$  FS distortion turns out not to affect the spin wave dispersions at all.

The  $l = 2$  spherical harmonic is given by

$$Y_2^0 = \sqrt{\frac{5}{16\pi}}(\cos^2 \theta_p - 1) \quad (4.6)$$

Such a function of  $\theta_p$  has two zero crossings in the region of  $0 \leq \theta_p \leq \pi$ . A ground state SDF with  $l = 0$  and  $l = 2$  distortion is depicted in the Fig. 4.3. This ground state has no spin current, only a net polarization. The  $l = 2$  distortion does not affect either the polarization properties or the spin current properties of the system. While these properties make an  $l = 2$  distortion in the ground state attractive for investigation and probably easily realizable in a physical system, according to our calculations there is

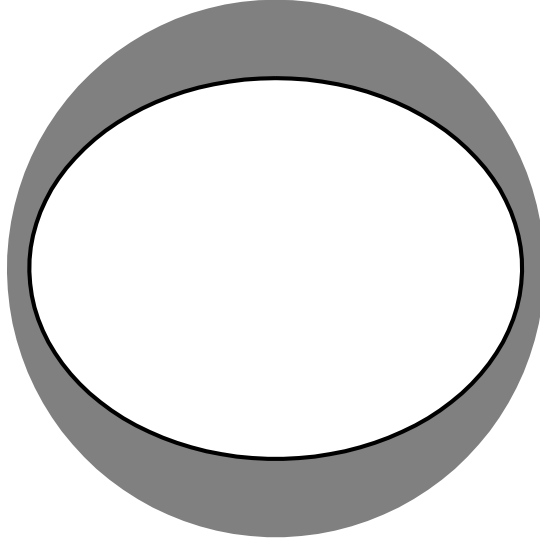


Figure 4.3: The SDF of a system with  $\sigma_0$  and  $\sigma_1$  in its ground state. The white surface is the spin- $\downarrow$  distribution function, and the shaded surface is the spin- $\uparrow$  distribution function.

no new physics introduced into the spin wave structure, at least when only considering exchange interactions (the results of these calculations are shown in the next chapter). Thus it is reasonable to ignore an  $l = 2$  distortion in the ground state SDF, and by extrapolation, the  $l = 3, 4, 5 \dots$  distortions, as well (though we have not verified this last assumption explicitly).

## 4.2 Non-homogeneous polarizations

Spin density waves (SDW), or a frozen-in non-homogeneous spin structure, occur in the ground states of some metals, such as MnSi, MnP,  $\text{Fe}_2\text{O}_3$ , etc... These are itinerant magnets have have a complex magnetic phase diagram.



At certain temperatures and pressures these materials exhibit a spin structure such as helical magnetism and fan magnetism. Phase diagrams and exemplary magnetic structures are shown in the Fig. 4.4 and Fig. 4.5. The itinerant nature of these magnetic phases can lead to SDW's that are incommensurate with the underlying lattice, i.e., the wavelength of the SDW is not just a multiple of a lattice constant. Incommensurability does not always imply itinerant origins of the magnetism, but further experiments have verified the itinerant nature of the above materials. Therefore, it should be valid to apply Fermi liquid theory to these materials. Now, again, it must be noted that spin-orbit coupling and/or crystal-field coupling usually play a role in the ground state properties of these systems, thus in the present work we assume the ground state to be naturally occurring, and then derive the spin waves that would result from a Hamiltonian that only includes exchange coupling. This approach is possibly validated by noting the well-documented spin wave structure of MnSi, which closely resembles the spin wave structure of a ferromagnet with only exchange interactions, as seen in the figure. The small gap in the spin structure at  $q = 0$  is a result of the small anisotropy of the ground state spin structure, and can be understood as a result of the breaking of full rotational symmetry that exists in a homogeneous ferromagnet.

in Fermi liquid theory one minimizes the free energy to derive the ground state of the distribution function. In the case of an SDW material, some sort of coupling other than an isotropic exchange must be included in the free energy, since isotropic exchange coupling only leads to a homogeneous magnetic ground state, at best. The inclusion of spin-orbit, crystal field,

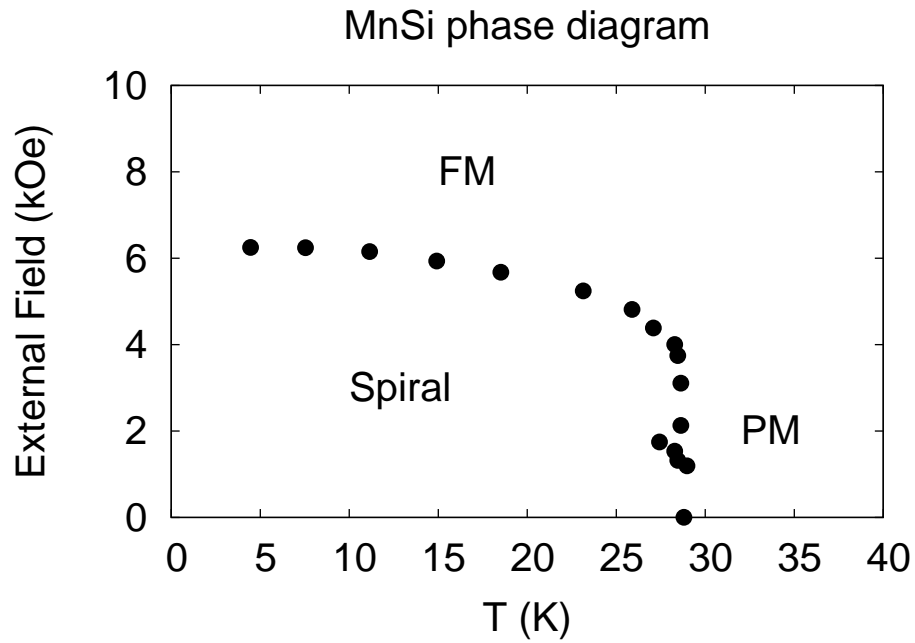


Figure 4.4: Phase diagram of MnSi. Data taken from Shirane (1983) [37].

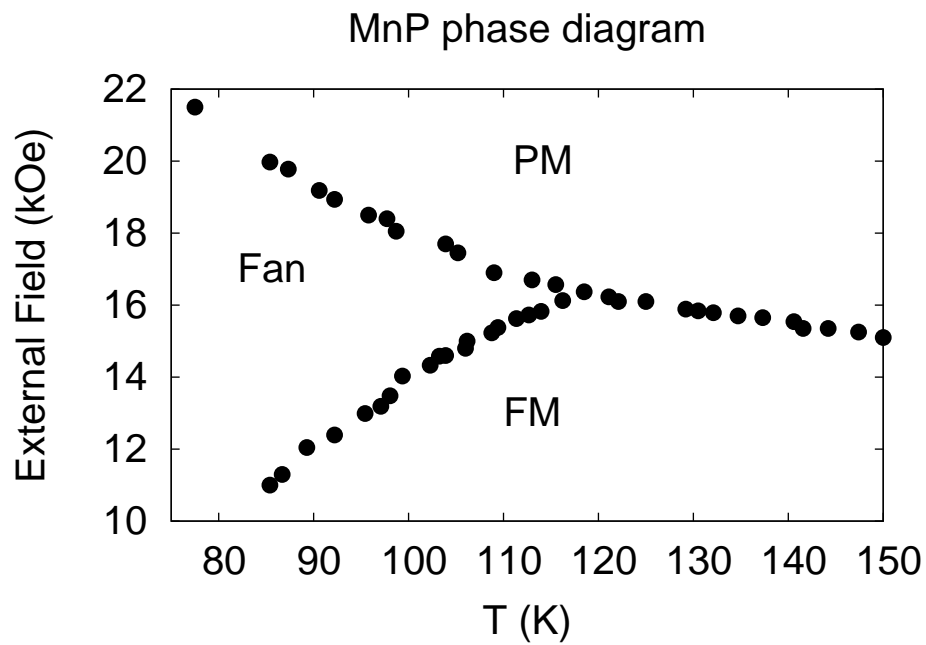
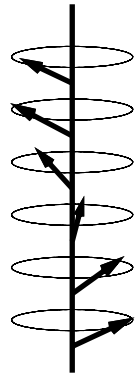


Figure 4.5: Phase diagram of MnP. Data taken from Becerra (1980) [7].

dipole, etc... coupling is possible, and has been explored in general terms []. However, in my estimation, complicating the theory with these interactions only serves to drive interest away from the results derived. Thus, while I wholly acknowledge that such an endeavor may be closer to the physics of SDW systems, and could yield interesting results, I don not include such interactions in my fermi liquid analysis of these systems for the above reason, and for the reason that this thesis is mainly concerned with the inclusion of higher spherical harmonics in the SDF, rather than SDW materials. So, in the following chapter I present results for the spin wave structure of such systems including only exchange coupling, and I leave the inclusion of anisotropic interactions for future consideration.

For an SDW material, the ground state spin distribution function,  $\vec{\sigma}_p(\vec{r})$ , varies in space, or more specifically, the vector components of the projection of the spin vary spatially. For example, in a spiral, or helical structure, the  $x$ - and  $y$ -projections of the polarization vary with  $z$  as  $\sigma_{p,x}(z) = \sigma_{\perp} e^{ikz}$  and  $\sigma_{p,y}(z) = \sigma_{\perp} e^{-ikz}$ , while the  $z$ -projection of the polarization is a constant  $\sigma_{p,z}(z) = \sigma^0$ . For a fan structure,  $\sigma_{p,x}(z) = \sigma_x \eta \cos kz - \pi$ ,  $\sigma_{p,y}(z) = \sigma_y \sin kz/2$ ,  $\sigma_{p,z}(z) = 0$ . These two cases, of a spiral and fan, are shown pictorially in Fig. 4.6. The spin waves of a spiral structure are studied in the following chapter, and the results are compared with experiment in MnSi and other materials.

Spiral



Screw

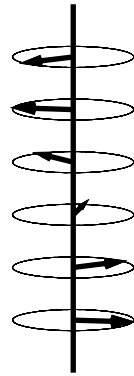


Figure 4.6: Representations of "spiral" and "screw" SDW magnetic structures.

# Chapter 5

## New spin waves

To reiterate, the idea for this research was conceived with the aim of finding a Fermi liquid description for a spiral ferromagnetic phase and describing the corresponding spin waves. It was believed that a ground state possessing an  $\sigma^\pm$  could be recast in the language of the  $\sigma_{1,\pm 1}$  spherical harmonic moments. While this connection has not been found to date, the general idea of allowing the ground state spin distribution function (SDF) to have an  $l = 1$  spherical harmonic distortion has been fruitful – leading to novel ground states and spin wave results.

It turns out that allowing the ground state to possess either an  $\sigma_{10}$  or  $\sigma_{1,\pm 1}$  harmonic moment leads to identical novel results for the ground state and spin wave excitations. This is not surprising, because the full rotational symmetry is broken in the same manner by any  $l = 1$  harmonic, the only difference is the axis with respect to which the symmetry is broken – and the axes for a rotationally invariant system are arbitrarily assigned from the beginning. Once the symmetry is broken, the direction of the momentum

transfer,  $\vec{q}$ , couples to the direction of the broken symmetry, and the transverse spin wave dispersion turns out to be the same whether there is an ( $l = 1, m = 0$ ) or ( $l = 1, m = \pm 1$ ) moment in the ground state.

## 5.1 Equilibrium and Quasi-equilibrium

To begin with, we discuss in general terms spin waves in equilibrium (EQ) Fermi liquid systems and spin waves in in quasi-equilibrium (QEQ) Fermi liquid systems. There are two main difference between EQ and QEQ spin waves. The first is that in EQ systems, there is either an external magnetic field, with which the system is in equilibrium, or the system is naturally in a ferromagnetic state. In a QEQ system, there is never an external field, and the system is also not a ferromagnet in its ground state, but instead has been artificially prepared in a magnetic state by external means, and then these external means have been shut off, so the system is in an excited state, but is said to be in quasi-equilibrium if the relaxation rate to equilibrium is much longer than the time scale of other dynamic phenomena, such as the propagation of spin waves. Of course, this condition may not always be satisfied. For instance, in the case of a Goldstone mode, where  $\omega \rightarrow 0$  as  $q \rightarrow 0$ , the time scale for the propagation of a long-wavelength spin wave (small  $q$ ) will be  $\tau \sim \frac{1}{\omega}$ , thus this time scale will be greater than the relaxation time scale of the system. Thus, QEQ modes must be carefully considered, especially in the case of a long-wavelength Goldstone mode. Still, as long as we are careful about time scales, a QEQ system can be assumed to support spin waves in a certain range of wavelengths, and perhaps all wavelengths,

in the case of a gapped (non-Goldstone) mode.

The second major difference between an EQ and a QEQ system is the nature of the magnetization fraction. In an EQ system, if the system is paramagnetic, the magnetization is either determined by the external magnetic field,  $\sigma = \chi H$ , where  $\chi = \frac{N(0)}{1+F_0^a}$ , and in a ferromagnetic system, the magnetization is determined by the stability of the Ginzburg-Landau free energy,  $\frac{\partial F}{\partial \sigma} = 0$ , and  $\frac{\partial^2 F}{\partial \sigma^2} > 0$ , where  $F = -|a|\sigma^2 + |b|\sigma^4$ , where  $a = \frac{1}{4} \frac{\hbar^2 \gamma^2 N(0)}{1+F_0^a}$ , and  $b$  is an unknown parameter (it is a fitting parameter, and is of little importance in the context of this thesis—see [43] for more information on Ginzburg-Landau theory and determination of critical parameters). In a QEQ system, the magnetization fraction is simply set by external means, and is not linked to any parameters of fermi liquid theory or Ginzburg-Landau theory. The only restriction on the magnetization fraction in a QEQ system is that it must be small,  $\sigma = (n_\uparrow - n_\downarrow)/(n_\uparrow + n_\downarrow) < 0.1$ , in order for one to ignore the dependence of the fermi liquid interaction parameters on the magnitude of the quasi-particle momentum. A polarization fraction of  $\sigma = 0.1$  would mean that  $(p_\uparrow - p_\downarrow)/(p_\uparrow + p_\downarrow) \sim \sigma^3 \sim 0.001$ , in which case the dependence of  $F_{\vec{p}\vec{p}'}$  on  $|\vec{p} - \vec{p}'|$  can most likely safely be ignored.

In this chapter, results for spin waves in EQ and QEQ systems are presented. As will be shown, some dispersions of the respective modes are qualitatively affected by the type of system in which they arise, whether EQ or QEQ. Thus, delineation and distinctions of these two types of ground states will heretofore be mentioned only as necessary in the particular circumstances where it is of importance.

## 5.2 Including $l=2$ in the perturbation

Before discussing our new modes, we discuss the effects of including the  $l = 2$  distortion of the fermi surface in the perturbation (last chapter we discussed including  $l = 2$  in the ground state, and there is a section to follow that deals with the corresponding spin waves in this situation), and we give a specific example, one in which the first three harmonics of the perturbation,  $\nu_0$ ,  $\nu_1$ , and  $\nu_2$ , and the first three of the landau parameters,  $F_0^a$ ,  $F_1^a$ , and  $F_2^a$  are included in the calculations of the spin waves, while only the  $l = 0$ , homogeneous magnetization, distortion,  $\sigma_0$ , is included in the ground state. We look at the exact cubic solutions to the landau kinetic equation, and we also examine the result obtained by Bedell and Blagoev [8] for  $qv_F \ll F_1^a$ . The reasoning for including the  $l = 2$  in the perturbation as stated in this article was to avoid divergence of the spin wave dispersion as  $F_0^a \rightarrow -1$ .

The three coupled equations that result in the inclusion of  $\nu_0$ ,  $\nu_1$ ,  $\nu_2$ ,  $F_0^a$ ,  $F_1^a$ , and  $F_2^a$  and  $\sigma_0$  are

$$\begin{aligned}
(l=0, m=0) \quad & \omega\nu_0 - \frac{1}{\sqrt{3}}(1 + \frac{F_1^a}{3})qv_F\nu_1 = 0 \\
(l=1, m=0) \quad & \omega\nu_1 - \frac{1}{\sqrt{3}}(1 + F_0^a)qv_F\nu_0 - \frac{2}{\sqrt{15}}(1 + \frac{F_2^a}{5})qv_F\nu_2 \\
& + \frac{2}{\hbar N(0)}(F_0^a - \frac{F_1^a}{3})\sigma_0\nu_1 = 0 \\
(l=2, m=0) \quad & \omega\nu_2 - \frac{2}{\sqrt{15}}(1 + \frac{F_1^a}{3})qv_F\nu_1 + \frac{2}{\hbar N(0)}(F_0^a - \frac{F_2^a}{5})\sigma_0\nu_2 = 0
\end{aligned} \tag{5.1}$$



This set of equations can be equivalently expressed as

$$\begin{bmatrix} \omega & -\frac{1}{\sqrt{3}}(1 + \frac{F_1^a}{3})qv_F & 0 \\ -\frac{1}{\sqrt{3}}(1 + F_0^a)qv_F & \omega + \frac{2}{\hbar N(0)}(F_0^a - \frac{F_1^a}{3})\sigma_0 & -\frac{2}{\sqrt{15}}(1 + \frac{F_2^a}{5})qv_F \\ 0 & -\frac{2}{\sqrt{15}}(1 + \frac{F_1^a}{3})qv_F & \omega + \frac{2}{\hbar N(0)}(F_0^a - \frac{F_2^a}{5})\sigma_0 \end{bmatrix} \begin{bmatrix} \nu_0 \\ \nu_1 \\ \nu_2 \end{bmatrix} = 0 \quad (5.2)$$

Thus, the solution to these coupled equations is obtained by setting the determinant of the coefficient matrix to zero.

$$\text{Det} \begin{bmatrix} \omega & -\frac{1}{\sqrt{3}}(1 + \frac{F_1^a}{3})qv_F & 0 \\ -\frac{1}{\sqrt{3}}(1 + F_0^a)qv_F & \omega + \frac{2}{\hbar N(0)}(F_0^a - \frac{F_1^a}{3})\sigma_0 & -\frac{2}{\sqrt{15}}(1 + \frac{F_2^a}{5})qv_F \\ 0 & -\frac{2}{\sqrt{15}}(1 + \frac{F_1^a}{3})qv_F & \omega + \frac{2}{\hbar N(0)}(F_0^a - \frac{F_2^a}{5})\sigma_0 \end{bmatrix} = 0 \quad (5.3)$$

The solution to a cubic equation is generally not analytically helpful, that is to say, its analytic solution is extremely long with a bunch of third roots, etc... Furthermore, there is no general approximation scheme to obtain any sort of analytic approximation to the exact solution. Therefore, in Fig. 5.2 we plot numerically the general solution to the cubic equation for a QEQ system. Plotted in Fig. 5.1 are the approximate solutions from [8] for  $qv_F \ll F_1^a$ , which are

$$\begin{aligned} \omega_0^+(q) &\approx \frac{c_s^2}{\omega_1^+} q^2 \\ \omega_1^+(q) &\approx \omega_1^+ - \left[ \frac{c_s^2}{\omega_1^+} + \frac{4N(0)v_F^2}{30\sigma_0} \left( \frac{3}{F_1^a} + 1 \right) \right] q^2 \end{aligned} \quad (5.4)$$

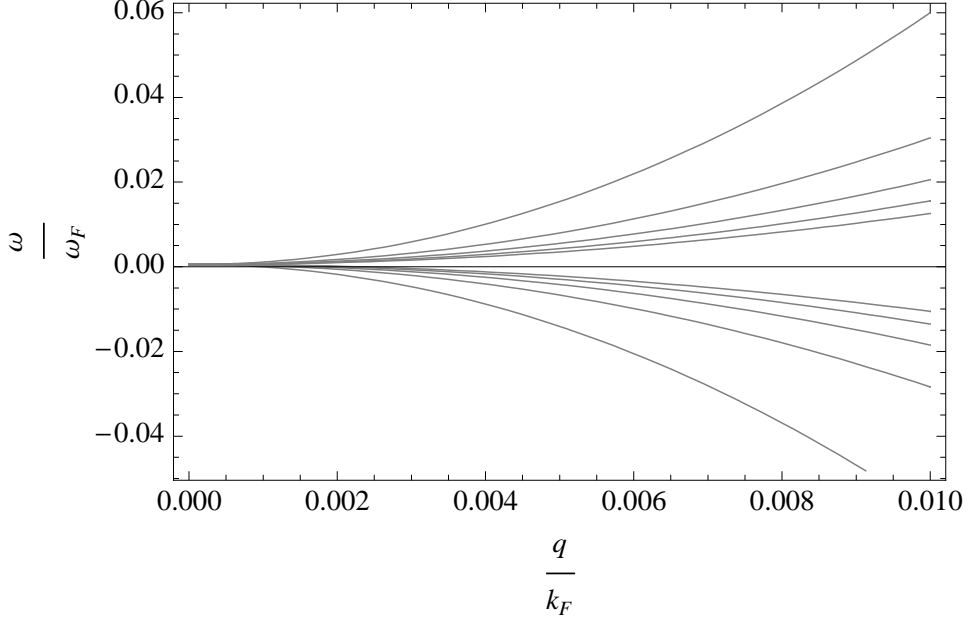


Figure 5.1: Approximate solutions from [8] for  $qv_F \ll F_1^a$ . The values of the LPs are  $F_1^a = 1$  and  $F_1^a = -0.5 \dots 0.5$ .

and in this limit, the approximation works quite well. However, as can be seen in the Fig. 5.2, when  $F_1^a \rightarrow 0$ , this approximation fails, and also if  $F_0^a < 0$ , the approximation doesn't capture the physics of the modes, which is to say, an imaginary root is not possible in the approximation.

To test the importance of including  $\nu_2$  and  $F_2^a$ , we compare the exact cubic solution to the exact solution when only  $\nu_0$ ,  $\nu_1$ ,  $F_0^a$ ,  $F_1^a$ , and  $\sigma_0$  are included. The analytic form of the latter dispersion is obtained from solving the two coupled equations

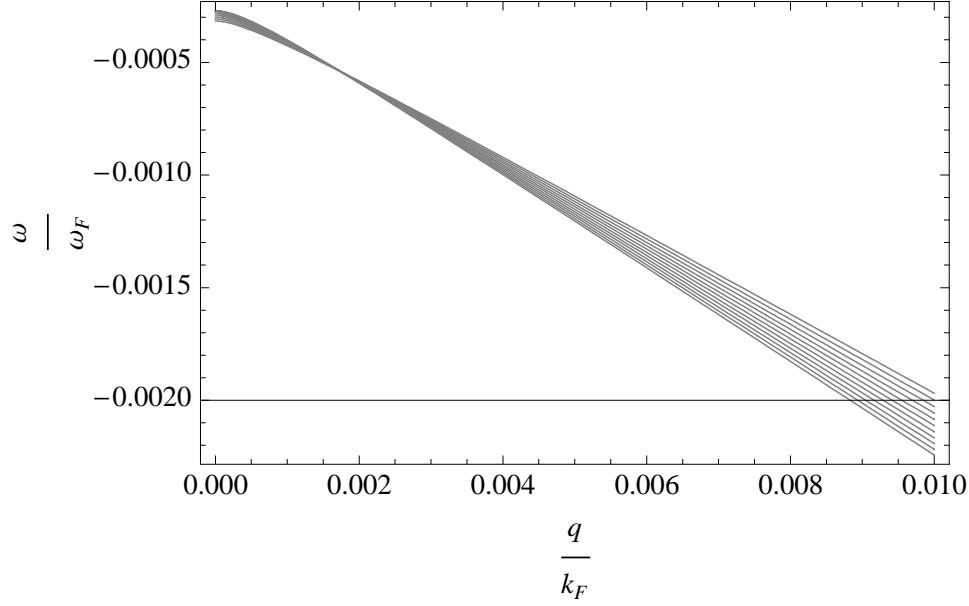


Figure 5.2: General solution to the cubic equation for the SC mode of a QEQ system, including  $l = 2$  in the perturbation. The values of the LPs are  $F_1^a = 1$  and  $F_1^a = -0.5 \dots 0.5$ .

$$\begin{aligned}
 (l = 0, m = 0) \quad & \omega \nu_0 - \frac{1}{\sqrt{3}} \left(1 + \frac{F_1^a}{3}\right) q v_F \nu_1 = 0 \\
 (l = 1, m = 0) \quad & \omega \nu_1 - \frac{1}{\sqrt{3}} (1 + F_0^a) q v_F \nu_0 + \frac{2}{\hbar N(0)} \left(F_0^a - \frac{F_1^a}{3}\right) \sigma_0 \nu_1 = 0
 \end{aligned} \tag{5.5}$$

The solution is

$$\begin{aligned}
 \omega = -\frac{1}{2} \frac{2}{\hbar N(0)} \left(F_0^a - \frac{F_1^a}{3}\right) \sigma_0 \pm \frac{1}{2} \left[ \left( \frac{2}{\hbar N(0)} \left(F_0^a - \frac{F_1^a}{3}\right) \sigma_0 \right)^2 \right. \\
 \left. - 4 \frac{1}{3} (1 + F_0^a) \left(1 + \frac{F_1^a}{3}\right) q^2 v_F^2 \right]^{1/2} \tag{5.6}
 \end{aligned}$$

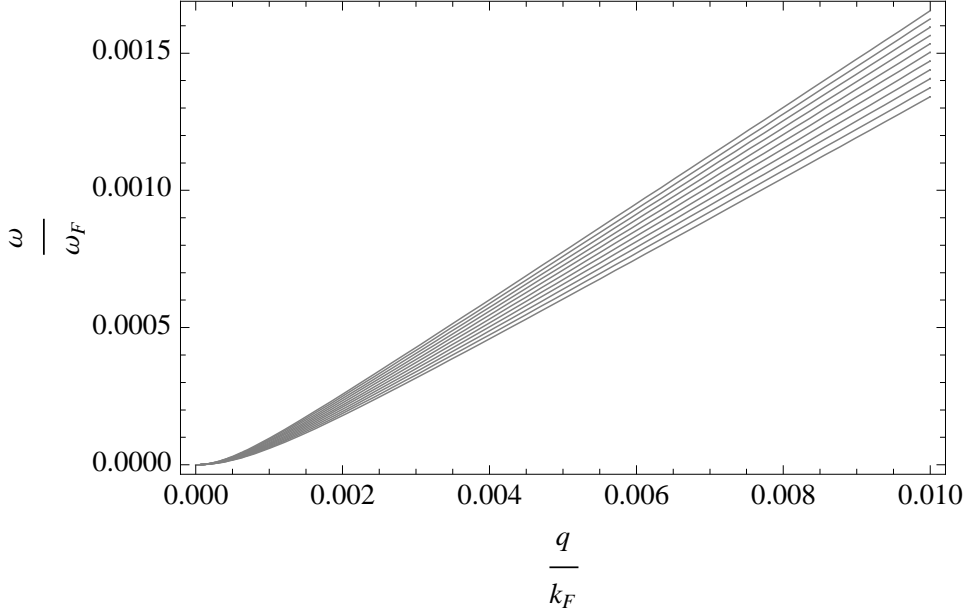


Figure 5.3:  $\omega_0^+(q)$  when only  $\nu_0$ ,  $\nu_1$ ,  $F_0^a$ ,  $F_1^a$ , and  $\sigma_0$  are included.  $F_0^a = 1$ , and  $F_1^a = -0.5 \dots 0.5$ .

In Fig. 5.3 and Fig. 5.4 we plot the exact solutions for a QEQ system to the  $l = 0, 1$  coupled equations, and in Fig. 5.5 and Fig. 5.6 we plot the exact solutions to the  $l = 0, 1, 2$  coupled equations. The curves are very similar, thus the inclusion of the  $l = 2$  moment in the perturbative response only leads to a new mode, the  $l = 2$  mode, as expected (not shown in figures). This mode is likely damped out in a real system, and is thus not important.

Now let's look at the behavior of the approximate solutions: a)  $\frac{1}{3}(1 + \frac{F_1^a}{3})(1 + F_0^a)qv_F \ll \frac{2}{\hbar N(0)}(F_0^a - \frac{F_1^a}{3})\sigma_0$ ; b)  $qv_F \ll F_1^a$  (Blagoev result). It is clear from Fig. 5.6 that these approximate solutions capture the physics of the spin wave dispersions in the respective limits and for certain values of  $F_0^a$  and  $F_1^a$ . However, their performance outside of these limits is not good, as expected.

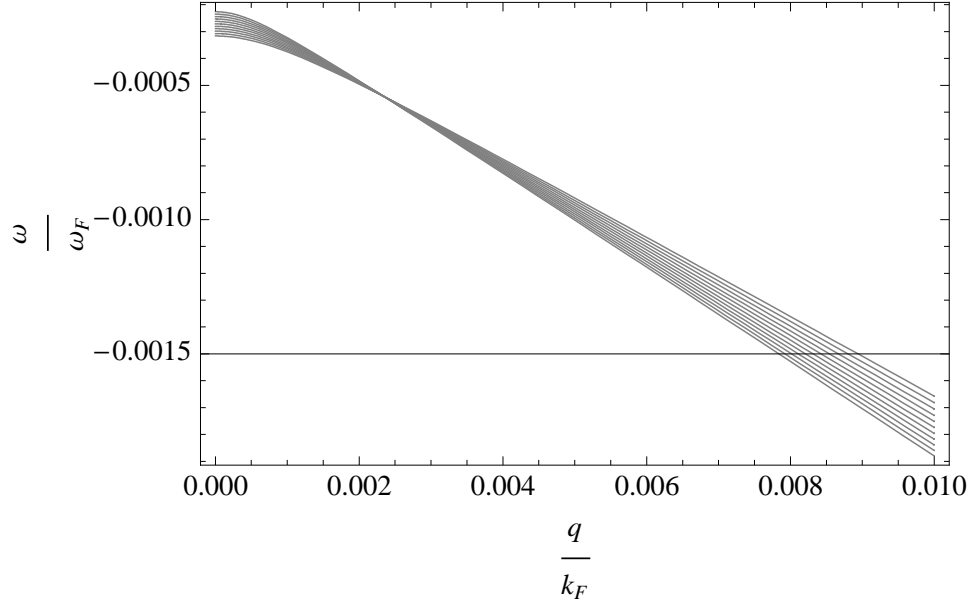


Figure 5.4:  $\omega_1^+(q)$  when only  $\nu_0$ ,  $\nu_1$ ,  $F_0^a$ ,  $F_1^a$ , and  $\sigma_0$  are included.  $F_0^a = 1$ , and  $F_1^a = -0.5 \dots 0.5$ .

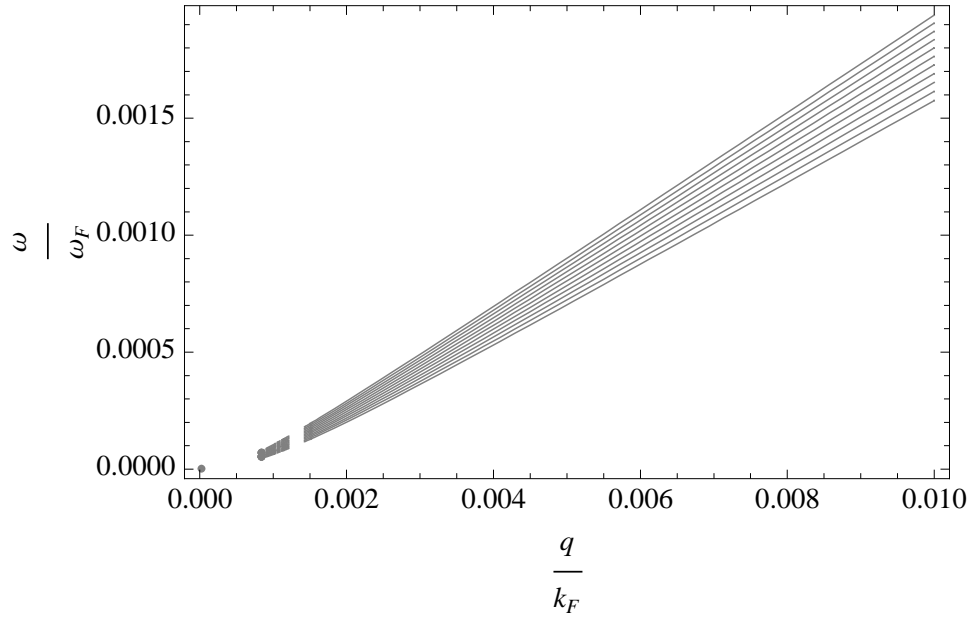


Figure 5.5:  $\omega_0^+(q)$  when  $\nu_0$ ,  $\nu_1$ ,  $\nu_2$ ,  $F_0^a$ ,  $F_1^a$ ,  $F_2^a$ , and  $\sigma_0$  are included.  $F_0^a = 1$ , and  $F_1^a = -0.5 \dots 0.5$ .

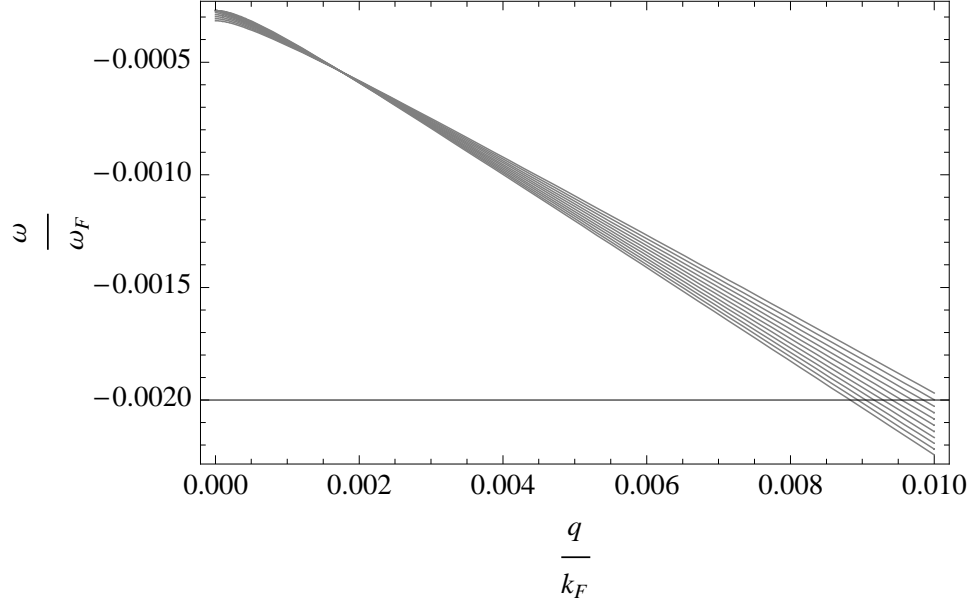


Figure 5.6:  $\omega_1^+(q)$  when  $\nu_0, \nu_1, \nu_2, F_0^a, F_1^a, F_2^a$ , and  $\sigma_0$  are included.  $F_0^a = 1$ , and  $F_1^a = -0.5 \dots 0.5$ .

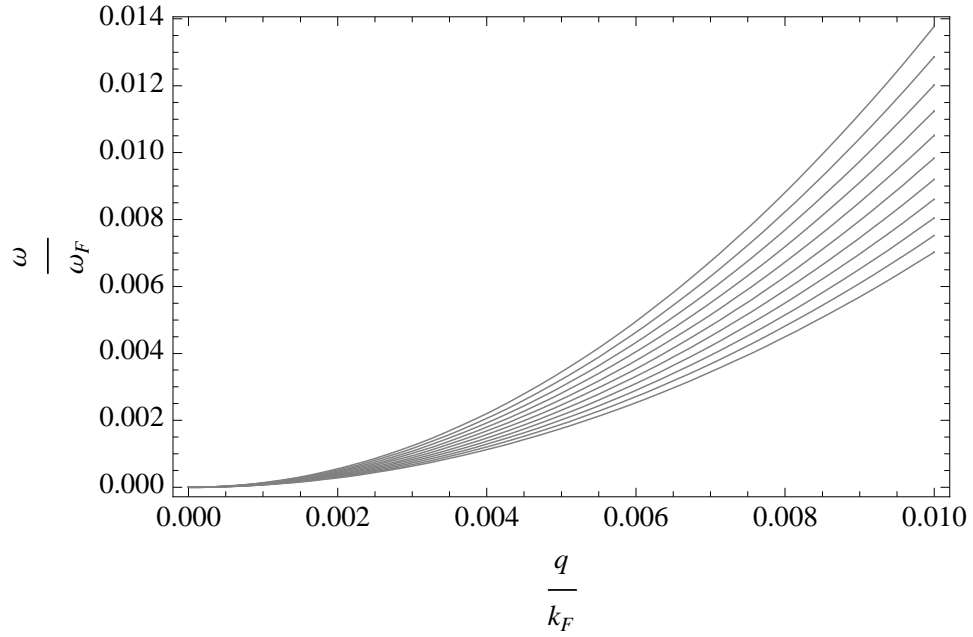


Figure 5.7:  $q^2$  approximation for  $\omega_1^+(q)$  when  $\nu_0, \nu_1, F_0^a, F_1^a$ , and  $\sigma_0$  are included.  $F_0^a = 1$ , and  $F_1^a = -0.5 \dots 0.5$ .

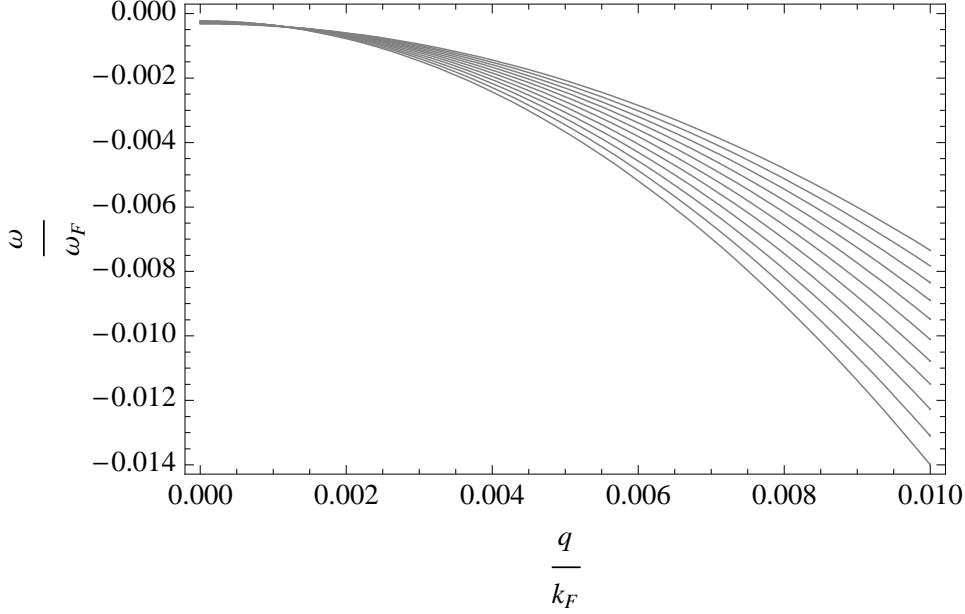


Figure 5.8:  $q^2$  approximation for  $\omega_1^+(q)$  when  $\nu_0$ ,  $\nu_1$ ,  $F_0^a$ ,  $F_1^a$ , and  $\sigma_0$  are included.  $F_0^a = 1$ , and  $F_1^a = -0.5 \dots 0.5$ .

As can also be seen in Fig. 5.7, the  $l = 2$  response is not necessary for capturing the physics of the spin precessional mode ( $l = 0$ ) and the spin current mode ( $l = 1$ ). Thus, for the remainder of this chapter only the  $l = 0$  and  $l = 1$  responses to the perturbation are utilized in deriving the spin wave dispersions.

### 5.3 Spin waves in a PSC system

As discussed in the previous chapter, fermi liquid theory has a convenient way of introducing a persistent spin current (PSC) into the ground state, which is to include the  $l = 1$  spherical harmonic,  $\sigma_1 Y_1^0(\theta_p, \phi_p)$  in the ground state SDF. The spin waves that result from perturbing such a PSC system can be studied via the spin kinetic equation.

The result of an  $l = 1$  harmonic contained in the ground state (calculations are shown in detail in the Appendix) is a dramatic change in the dispersion of the corresponding transverse spin waves. When  $\sigma_0$  and  $\sigma_1$  are present in the ground state, the coupled equations are

$$\begin{bmatrix} \omega & -\frac{1}{\sqrt{3}}(1 + \frac{F_1^a}{3})qv_F \\ -\frac{1}{\sqrt{3}}(1 + F_0^a)qv_F - \frac{2}{\hbar N(0)}(F_0^a - \frac{F_1^a}{3})\sigma_1 & \omega + \frac{2}{\hbar N(0)}(F_0^a - \frac{F_1^a}{3})\sigma_0 \end{bmatrix} \begin{bmatrix} \nu_0 \\ \nu_1 \end{bmatrix} = 0 \quad (5.7)$$

Examining these coupled equations, and comparing them to Eq. 5.2, it is clear that the effect on the spin wave of including  $\sigma_1$  in the ground state is to provide an additional coupling between the  $l = 0$  and  $l = 1$  projections of the kinetic equation (off-diagonal element in the matrix). This results in a linear term in  $q$  in the characteristic equation, along with the usual  $q^2$  term.

$$\begin{aligned} \omega^2 - \frac{2}{\hbar N(0)}(F_0^a - \frac{F_1^a}{3})\sigma_0\omega + \frac{1}{\sqrt{3}}(1 + \frac{F_1^a}{3})\frac{2}{\hbar N(0)}(F_0^a - \frac{F_1^a}{3})\sigma_0qv_F \\ - \frac{1}{3}(1 + F_0^a)(1 + \frac{F_1^a}{3})q^2v_F^2 = 0 \end{aligned} \quad (5.8)$$

Interestingly, the term  $\frac{1}{\sqrt{3}}(1 + \frac{F_1^a}{3})\frac{2}{\hbar N(0)}(F_0^a - \frac{F_1^a}{3})\sigma_0qv_F$  has characteristics of a spin-orbit coupling, since the polarization parameter  $\sigma_1$  is multiplied by the momentum transfer,  $q$ . Thus, even though only an exchange interaction has been assumed in the Hamiltonian, the inclusion of  $\sigma_1$  in the ground state SDF has led to an effective  $\sigma q$  term. This differs from the usual spin-orbit interaction, which is proportional to  $\sigma p$ , where  $p$  is the quasi particle



momentum. A possible physical interpretation of the  $\sigma_1 q$  term would be that the spin current,  $\sigma_1$ , couples to the spatial fluctuations of the perturbation,  $q$ .

Solving the quadratic characteristic equation leads to the two solutions

$$\begin{aligned}\omega_0^+(q) &= -\frac{1}{2} \frac{2}{\hbar N(0)} (F_0^a - \frac{F_1^a}{3}) \sigma_0 + \frac{1}{2} \left[ \left( \frac{2}{\hbar N(0)} (F_0^a - \frac{F_1^a}{3}) \sigma_0 \right)^2 - \right. \\ &\quad \left. \frac{4}{3} (1 + F_0^a) (1 + \frac{F_1^a}{3}) q^2 v_F^2 + 4 \frac{2}{\hbar N(0)} (F_0^a - \frac{F_1^a}{3}) \sigma_1 (1 + \frac{F_1^a}{3}) q v_F \right] \\ \omega_1^+(q) &= -\frac{1}{2} \frac{2}{\hbar N(0)} (F_0^a - \frac{F_1^a}{3}) \sigma_0 + \frac{1}{2} \left[ \left( \frac{2}{\hbar N(0)} (F_0^a - \frac{F_1^a}{3}) \sigma_0 \right)^2 - \right. \\ &\quad \left. \frac{4}{3} (1 + F_0^a) (1 + \frac{F_1^a}{3}) q^2 v_F^2 + \frac{2}{\hbar N(0)} (F_0^a - \frac{F_1^a}{3}) \sigma_1 (1 + \frac{F_1^a}{3}) q v_F \right]\end{aligned}\tag{5.9}$$

To leading order in  $q$ , these solutions become

$$\begin{aligned}\omega_0^+(q) &= \frac{-\frac{1}{3} (1 + F_0^a) (1 + \frac{F_1^a}{3}) q^2 v_F^2 + 4 \frac{2}{\hbar N(0)} (F_0^a - \frac{F_1^a}{3}) \sigma_1 (1 + \frac{F_1^a}{3}) q v_F}{\frac{2}{\hbar N(0)} (F_0^a - \frac{F_1^a}{3}) \sigma_0} \\ \omega_1^+(q) &= -\frac{2}{\hbar N(0)} (F_0^a - \frac{F_1^a}{3}) \sigma_0 + \\ &\quad \frac{-\frac{1}{3} (1 + F_0^a) (1 + \frac{F_1^a}{3}) q^2 v_F^2 + 4 \frac{2}{\hbar N(0)} (F_0^a - \frac{F_1^a}{3}) \sigma_1 (1 + \frac{F_1^a}{3}) q v_F}{\frac{2}{\hbar N(0)} (F_0^a - \frac{F_1^a}{3}) \sigma_0}\end{aligned}\tag{5.10}$$

Thus the dispersion of both the spin precessional mode and the spin current mode are linear to first order in  $q$ . This is a new result for a transverse spin wave in fermi liquid theory.

The particle hole continuum of single-particle excitations (Stoner continuum) is given by the following expression

$$\omega_{ph}^+ = \frac{2}{\hbar N(0)} F_0^a \sigma_0 + \left[ \frac{2}{\hbar N(0)} \frac{F_1^a}{3} \sigma_1 + v_F q \right] \cos \theta_p \quad (5.11)$$

An interesting feature of this single-particle excitation spectrum is that at  $q = 0$  the continuum has an extended range of excitation energies, as opposed to a single value, which is the usual (see Fig. C.24). This new feature is a result of the translation of the two fermi spheres relative to each other, which is of course due to  $\sigma_1$ .

The linear dispersion of the spin waves themselves suggests that a symmetry has been broken in the system by the inclusion of  $\sigma_1$ , because the  $q^2$  behavior of the Silin modes as  $q \rightarrow 0$  is not present. The stiffening to a linear dispersion means that the mode requires more energy to be activated at low  $q$ , and thus the spin current has broken the rotational symmetry of a homogeneous ferromagnet. This is not a surprise, since the direction of the spin current,  $\sigma_1$ , is the  $z$ -direction, thus polar symmetry has been broken.

## 5.4 Non-polarized PSC spin waves

In a system that has a persistent spin current but no net polarization, the ground state is characterized by the presence of a  $\sigma_1$  order parameter and the absence of a  $\sigma_0$  order parameter (i.e.  $n_\uparrow - n_\downarrow = 0$ ). In such a system, spin waves would still be excitable, just as they can be excited in a slab of paramagnetic aluminum with no external magnetic field present, and thus

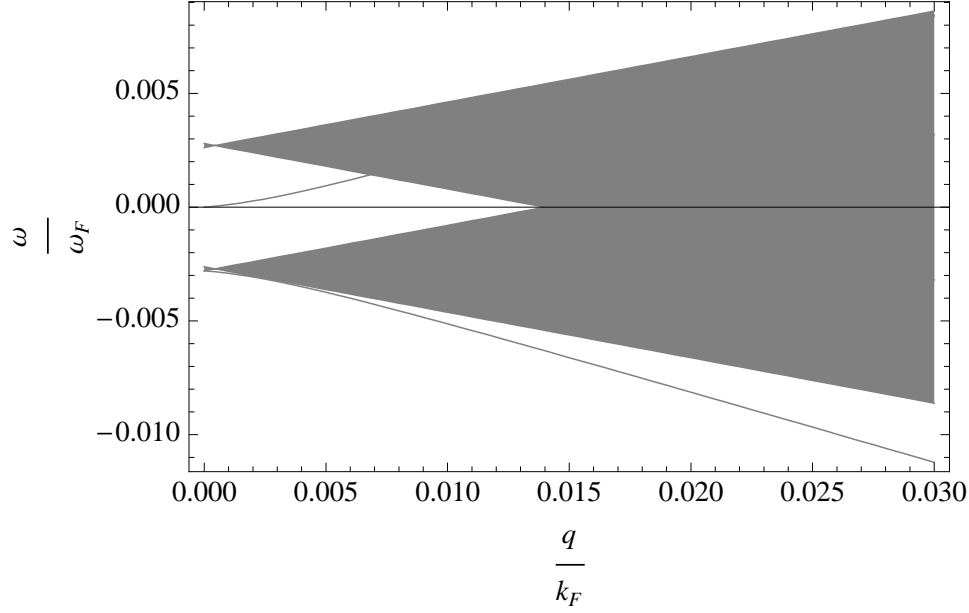


Figure 5.9: The  $l = 0$  and  $l = 1$  spin wave dispersions that result from a fermi liquid that is magnetic and has a spin current in its ground state. The dispersions are proportional to  $q^1$  to leading order in  $q$ .

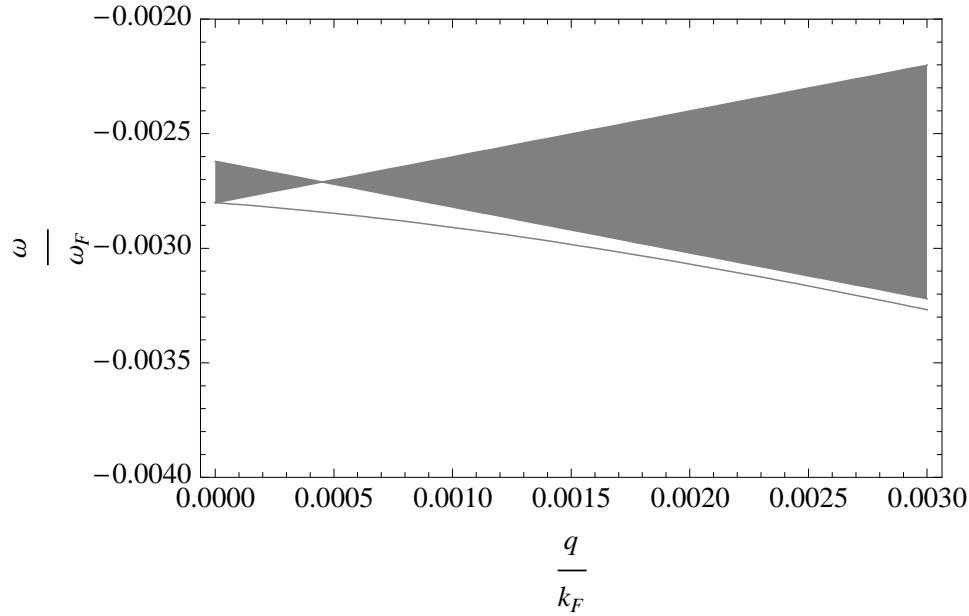


Figure 5.10: Showing the leading order  $q$  behavior of the spin current mode of a fermi liquid that is magnetic and has a spin current in its ground state. The dispersion is proportional to  $q^1$  as  $q \rightarrow 0$ .

no net polarization [17].

If only a  $\sigma_1$  exists in a system, then the coupled equations derived from the LKE are

$$\begin{bmatrix} \omega & -\frac{1}{\sqrt{3}}(1 + \frac{F_1^a}{3})qv_F \\ -\frac{1}{\sqrt{3}}(1 + F_0^a)qv_F - \frac{2}{\hbar N(0)}(F_0^a - \frac{F_1^a}{3})\sigma_1 & \omega \end{bmatrix} \begin{bmatrix} \nu_0 \\ \nu_1 \end{bmatrix} = 0 \quad (5.12)$$

These coupled equations lead to the characteristic equation

$$\omega^2 - \frac{1}{3}(1 + F_0^a)(1 + \frac{F_1^a}{3})q^2v_F^2 - \frac{2}{\hbar N(0)}(F_0^a - \frac{F_1^a}{3})\sigma_1 \frac{1}{\sqrt{3}}(1 + \frac{F_1^a}{3})qv_F = 0 \quad (5.13)$$

and the solutions to this equation are

$$\begin{aligned} \omega_0^+(q) &= \left[ \frac{2}{\hbar N(0)}(F_0^a - \frac{F_1^a}{3})\sigma_1 \frac{1}{\sqrt{3}}(1 + \frac{F_1^a}{3})qv_F \right. \\ &\quad \left. - \frac{1}{3}(1 + F_0^a)(1 + \frac{F_1^a}{3})q^2v_F^2 \right]^{1/2} \\ \omega_1^+(q) &= - \left[ \frac{2}{\hbar N(0)}(F_0^a - \frac{F_1^a}{3})\sigma_1 \frac{1}{\sqrt{3}}(1 + \frac{F_1^a}{3})qv_F \right. \\ &\quad \left. - \frac{1}{3}(1 + F_0^a)(1 + \frac{F_1^a}{3})q^2v_F^2 \right]^{1/2} \end{aligned} \quad (5.14)$$

If we expand the radical, assuming  $q \ll k_F$ , and thus  $(\dots)qv_F \ll \frac{2}{\hbar N(0)}(F_0^a - \frac{F_1^a}{3})\sigma_1$ , then the small- $q$  behavior of the modes is characterized by a  $q^{1/2}$  dispersion.

$$\begin{aligned}
\omega_0^+(q) &= \left( \frac{2}{\hbar N(0)} \left( F_0^a - \frac{F_1^a}{3} \right) \sigma_1 \frac{1}{\sqrt{3}} \left( 1 + \frac{F_1^a}{3} \right) \right) q^{1/2} v_F^{1/2} \\
&\quad - \frac{1}{\sqrt{3}} \frac{\left( 1 + \frac{F_1^a}{3} \right)}{\left( F_0^a - \frac{F_1^a}{3} \right) \sigma_1} q v_F \\
\omega_1^+(q) &= - \left( \frac{2}{\hbar N(0)} \left( F_0^a - \frac{F_1^a}{3} \right) \sigma_1 \frac{1}{\sqrt{3}} \left( 1 + \frac{F_1^a}{3} \right) \right) q^{1/2} v_F^{1/2} \\
&\quad + \frac{1}{\sqrt{3}} \frac{\left( 1 + \frac{F_1^a}{3} \right)}{\left( F_0^a - \frac{F_1^a}{3} \right) \sigma_1} q v_F
\end{aligned} \tag{5.15}$$

This square root behavior is novel for a transverse spin wave. Both modes are gapless, as well, which is the result of no net magnetization in the system.

The Stoner continuum for a  $\sigma_1$  system occupies the bounds

$$-\frac{F_1^a}{3} \sigma_1 \cos \theta_p q v_F \leq \omega_{ph} \leq +\frac{F_1^a}{3} \sigma_1 \cos \theta_p q v_F \tag{5.16}$$

An interesting feature of this continuum is that if  $F_1^a < 0$ , there exists a value of  $q$  for which the continuum vanishes. This leads to the disappearance of the single-particle continuum of excitations at a finite  $q$  value. This would mean that the collective modes spectrum, or spin waves, would monopolize the dynamic form factor, and thus saturate and frequency sum rule:

$$\int_0^\infty \omega S(q, \omega) d\omega = \frac{Nq^2}{2m} \tag{5.17}$$

where  $N$  is the number of particles in the system,  $m$  is their bare mass, and  $S(q, \omega)$  is the dynamic form factor [33]. This would make the spin precession mode very easy to detect experimentally, as the cross-section of incident light

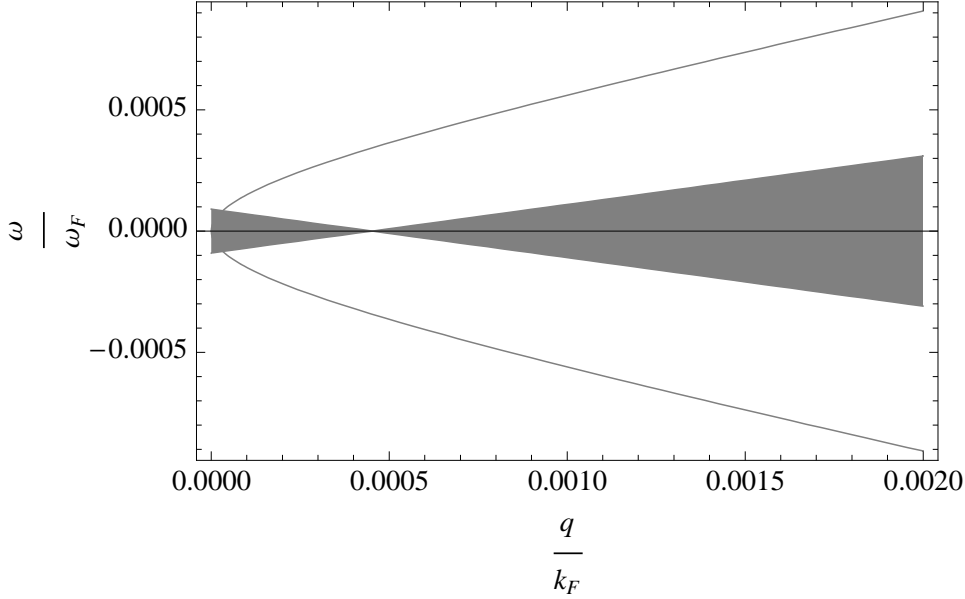


Figure 5.11: The two spin waves that arise from a spin current being in the ground state of a fermi liquid that does not have homogeneous magnetization. The dispersion is proportional to  $q^{1/2}$ .

(or neutrons) would only be determined by the presence or absence of this mode, at the  $q$  value

$$q = -\frac{F_1^a}{3} \frac{2\sigma_1}{\hbar N(0)} \frac{1}{v_F} \quad (5.18)$$

In the figure, the spin wave modes are shown with the Stoner continuum. As a result of the square root nature of the modes for small  $q$ , and the range of the Stoner continuum at  $q = 0$ , there exists a cutoff value of  $q$  below which the spin wave modes will not propagate, or equivalently, there is a maximum wavelength value,  $\lambda_{max} = \frac{2\pi}{q_{min}}$ , above which spin waves would not exist in such a system. This cutoff would greatly affect the thermodynamics of the system, since long-wavelength excitations in fermi systems contribute significantly to the specific heat [33].

## 5.5 Paramagnetic

If an external magnetic field is present, then the new spin waves that are shown above acquire an additional term in the expression for the dispersion, which is the Larmor frequency. This is the precession that a magnetic moment would have in an external field in the absence of quasi particle interaction, and is equal to  $\omega_L = \gamma H$ , where  $\gamma$  is the gyromagnetic ratio, and  $H$  is the external magnetic field. In an interacting fermi liquid, the frequency is modified by the quasi particle interaction,  $f_{pp'}^a$ , and the dispersions of the new spin waves, in the range of small  $q$ , that result from a transverse perturbation are: for the  $l = 0, 1$  distortion terms present for small  $q$

$$\begin{aligned}\omega_0^+(q) &= \omega_0 + \frac{1}{\sqrt{3}} \frac{\sigma_1}{\sigma_0} (1 + \frac{F_1^a}{3}) q v_F - \frac{1}{3} (1 + F_0^a) (1 + \frac{F_1^a}{3}) q^2 v_F^2 \\ \omega_1^+(q) &= \omega_0 + \frac{2}{\hbar} (F_0^a - \frac{F_1^a}{3}) \sigma_0 - \frac{1}{\sqrt{3}} \frac{\sigma_1}{\sigma_0} (1 + \frac{F_1^a}{3}) q v_F \\ &\quad + \frac{1}{3} (1 + F_0^a) (1 + \frac{F_1^a}{3}) q^2 v_F^2\end{aligned}\tag{5.19}$$

and for only the  $l = 1$  distortion term present for small  $q$ ,

$$\omega = \omega_0 + \pm ((1 + \frac{F_1^a}{3}) q v_F \frac{2}{\hbar} (F_0^a - \frac{F_1^a}{3}) \sigma_1)^{1/2} \pm \frac{(\frac{1}{3} (1 + F_0^a) (1 + \frac{F_1^a}{3}))^{1/2} q v_F}{(\frac{2}{\hbar} (F_0^a - \frac{F_1^a}{3}))^{1/2} \sigma_1^{1/2}}\tag{5.20}$$

The external field only changes the dispersions by a constant amount equal to the Larmor frequency. The paramagnetic spin waves are still characterized

by a  $q^1$  and  $q^{1/2}$  dispersions to leading order in  $q$ . The Stoner continuum also acquires an additional gap due to the presence of the external field, equal to  $\omega_0$ . Thus, the damping considerations mentioned in the previous section still apply to the current mode in a paramagnetic system.

## 5.6 Spin waves in dilute atomic gases

Spin waves in dilute atomic gases have been theoretically understood and observed in atomic gases since the early 1980's. Johnson, et al. [22] observed resonances in the NMR spectrum of polarized hydrogen gas,  $\text{H}\downarrow$  (at a density of  $10^{16} \text{ cm}^{-3}$  and temperature of  $0.8\text{K}$ ), that had been predicted theoretically by Levy and Ruckenstein [25]. The mechanism for these spin waves is different from those that are presented in this thesis, but the direct experimental observation of spin waves in  $\text{H}\downarrow$  makes it extremely plausible that spin waves could be observed in a partially polarized gas of  $^6\text{Li}$ , which would be those derived in this thesis.

Spin waves in dilute bosonic atomic gases has already been observed, as well. In 2002, McGuirk, et al. observed longitudinal and transverse spin waves in a gas of  $^{87}\text{Rb}$  atoms (at a density of  $10^{13} \text{ cm}^{-3}$  and temperature of  $800\text{nK}$ ) [29]. In this and similar experiments in dilute atomic gases, the spin states of the atoms are manipulated by using a two photon coupling transition scheme, which was stumbled upon in 2001 by Lewandowski, et al. [26]. Thus, the polarization fraction of the gas can be controlled without an external magnetic field. As mentioned before, the method of spin injection can also be used to control the polarization fraction [21].



## 5.7 Spin waves near a Feshbach resonance in an atomic gas

As mentioned above, dilute atomic gases are conducive for observing condensed matter phenomena, including spin waves. However, they also offer an additional degree of freedom, as compared to conventional solid state systems—the interaction between the atoms can be tuned at will, utilizing something known as a Feshbach resonance.

The inherent inhomogeneity of a three-dimensional confined atomic gas is not expected to affect the fermi liquid results significantly [30]. In very anisotropic traps approaching lower dimensions, however, the confining potential restricts the motion of the atoms in certain directions, thus fermi liquid excitations have been shown to change significantly [12]. In this paper we are not interested in quasi-one dimensional or quasi-bidimensional effects, thus all of the following calculations are done for the three-dimensional, homogeneous case.

The term Feshbach resonance describes the situation where the kinetic energy of a single particle becomes equal, or nearly equal, to the energy of a bound state between two particles. When this occurs, on one side of the resonance, particles may form bound states, with the scattering length of the two particles becoming negative. On the other side of the resonance, usually denoted the BCS side, the scattering length is positive, and there is also a quasi bound state, but with a much larger coherence length. If the atoms in the gas are fermions, for example  ${}^6\text{Li}$ , and the temperature is above the critical temperature but still below the fermi temperature on the BCS side

of the resonance, the atoms will comprise a fermi liquid. The strength of the interaction between the atoms can be tuned simply by changing the magnetic field.

For example, in a dilute gas of  $^6\text{Li}$ , it is possible to tune the fermi liquid parameter  $F_0^a$  near the Feshbach resonance of 834 Gauss. This was reported by Dahal, et al., in 2008 [14]. If this finding is substantiated by experiment, this would lead to many possibilities in the field of spin waves. On the flip side, the new spin waves that are reported above could provide a way to substantiate this tunability.

While the BCS and BEC states in atomic gases garner wide interest across many fields [3, 16, 41, 34], investigations into the normal state of atomic gases, i.e. above the superfluid phase transition, can also provide interesting results and important insights into the properties of these gases and other related systems. For instance, theoretical studies directed towards the density excitations of atomic gases in the hydrodynamic, collisionless, and intermediate regimes [11, 32, 28] paved the way for experimental investigations into the excitation spectra [23, 5] and the discovery of surprising features. Application of fermi liquid theory to density fluctuations of atomic gases has also led to interesting predictions and results [44, 2].

In [14], the induced interaction model [4] was used to theoretically calculate the fermi liquid parameters for an atomic gas as a Feshbach resonance (FBR) is approached. Dr. Sergio Gaudio wrote a Matlab program that used the IIM to numerically calculate the parameters, and I adapted the program to specifically calculate the parameters for a  $^6\text{Li}$  gas in a QEQ state near its 834 Gauss FBR at a temperature  $T_{BCS} < T \ll T_F$ , where  $T_{BCS}$  is the

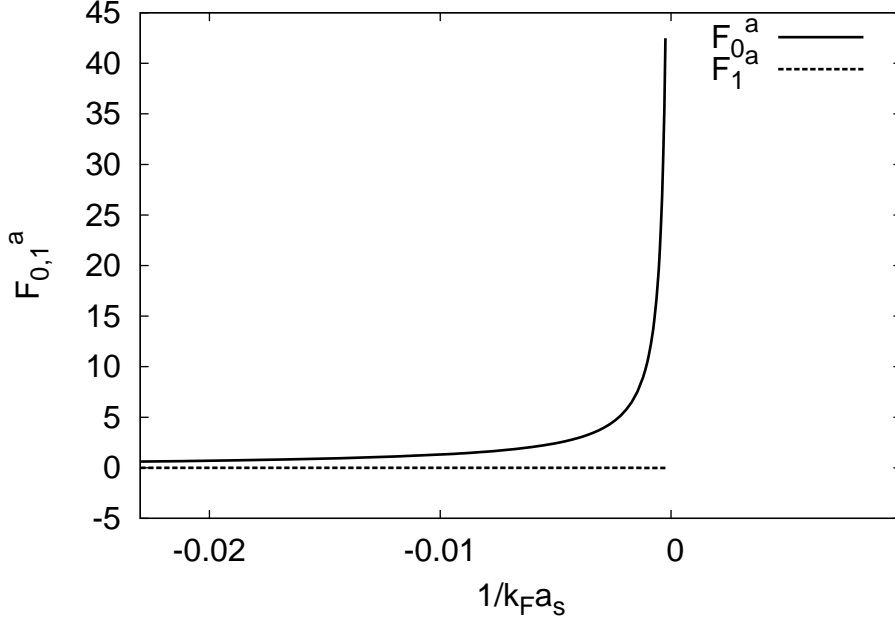


Figure 5.12: Calculated Landau parameters,  $F_0^a$  and  $F_1^a$ , for a gas of  ${}^6\text{Li}$  atoms in the appropriate high-field seeking spin states near the 834-Gauss Feshbach resonance. The horizontal axis is the inverse of the bare scattering length  $a_s$  times the fermi wave vector  $k_F$ . The quantities plotted are dimensionless.

critical temperature at which the BCS super-conducting state is realized. A chief characteristic of the FBR is the divergence of the bare s-wave scattering length as the external magnetic field is tuned towards the resonance. At low enough temperatures, only the s-wave scattering process is allowed, thus the characteristic scattering length is effectively determined by the s-wave scattering length alone. The parameters used for this calculation, specific to the  ${}^6\text{Li}$  FBR, are detailed in the appendix. The results of this calculation are shown in Fig. 5.12. For comparison, the FL parameters for  ${}^3\text{He}$  for varying pressure are shown in Fig. ???. The behavior of the LPs near the  ${}^6\text{Li}$  FBR lead to very interesting effects in the transverse spin waves.

First let's inspect the QEQ modes in a system that only has  $\sigma_0$  present in its ground state SDF, which is to say it is a homogeneous magnet, with no external field, and no spin current in its ground state. The form for the spin precessional (SP) mode and spin current (SC) mode is

$$\begin{aligned}\omega_0^+(q) &= -\frac{1}{2} \frac{2}{\hbar N(0)} (F_0^a - \frac{F_1^a}{3}) \sigma_0 + \frac{1}{2} \left[ \left( \frac{2}{\hbar N(0)} (F_0^a - \frac{F_1^a}{3}) \sigma_0 \right)^2 \right. \\ &\quad \left. - 4 \frac{1}{3} (1 + F_0^a) (1 + \frac{F_1^a}{3}) q^2 v_F^2 \right]^{1/2} \\ \omega_1^+(q) &= -\frac{1}{2} \frac{2}{\hbar N(0)} (F_0^a - \frac{F_1^a}{3}) \sigma_0 - \frac{1}{2} \left[ \left( \frac{2}{\hbar N(0)} (F_0^a - \frac{F_1^a}{3}) \sigma_0 \right)^2 \right. \\ &\quad \left. - 4 \frac{1}{3} (1 + F_0^a) (1 + \frac{F_1^a}{3}) q^2 v_F^2 \right]^{1/2}\end{aligned}\tag{5.21}$$

The main effect that occurs as  $F_0^a$  increases near the FBR is the  $q = 0$  gap of the SC mode increases linearly with  $F_0^a$ . This would have repercussions for the dynamic form factor for the collective modes, which is given by

$$S(q, \omega) = \sum_n |(\rho_q^+)_{n0}|^2 \delta(\omega - \omega_{n0})\tag{5.22}$$

which would show up in scattering experiments, since the dynamic form factor is the amplitude of the scattering cross section. The spin stiffness of these modes is also affected as  $F_0^a \rightarrow \infty$ —the dispersion would become more quadratic and less linear, as show in Fig. 5.13.

Now, looking at the form of the QEQ modes for a  $\sigma_1$  system,

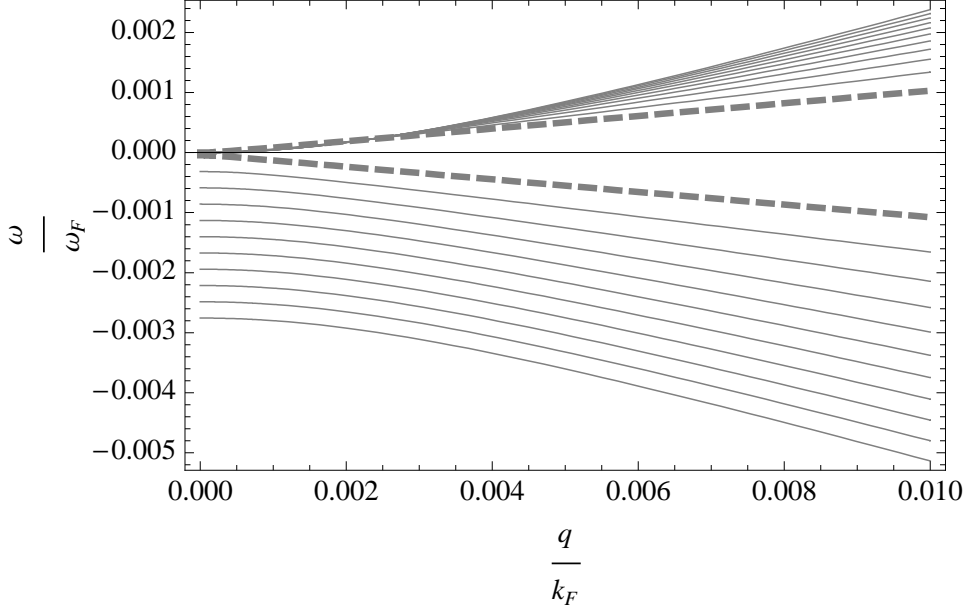


Figure 5.13: SC and SP modes near a Feshbach resonance for a polarized Fermi liquid, for  $F_0^a = 0 \dots 10$ . Dashed lines correspond to  $F_0^a = 0$ .

$$\begin{aligned}
 \omega_0^+(q) &= \left[ \left( \frac{2}{\hbar N(0)} \left( F_0^a - \frac{F_1^a}{3} \right) \sigma_1 \frac{1}{\sqrt{3}} \left( 1 + \frac{F_1^a}{3} \right) q v_F \right. \right. \\
 &\quad \left. \left. - \frac{1}{3} (1 + F_0^a) \left( 1 + \frac{F_1^a}{3} \right) q^2 v_F^2 \right]^{1/2} \\
 \omega_1^+(q) &= - \left[ \left( \frac{2}{\hbar N(0)} \left( F_0^a - \frac{F_1^a}{3} \right) \sigma_1 \frac{1}{\sqrt{3}} \left( 1 + \frac{F_1^a}{3} \right) q v_F \right. \right. \\
 &\quad \left. \left. - \frac{1}{3} (1 + F_0^a) \left( 1 + \frac{F_1^a}{3} \right) q^2 v_F^2 \right]^{1/2}
 \end{aligned} \tag{5.23}$$

the SP and SC modes are both gapless at  $q = 0$ , so  $q = 0$  behavior is not affected by a change in  $F_0^a$  near an FBR for these modes. However, the mode dispersions become more dramatically square root in behavior as  $F_0^a \rightarrow \infty$ , or as the spin-dependent interaction between the atoms increases, as shown

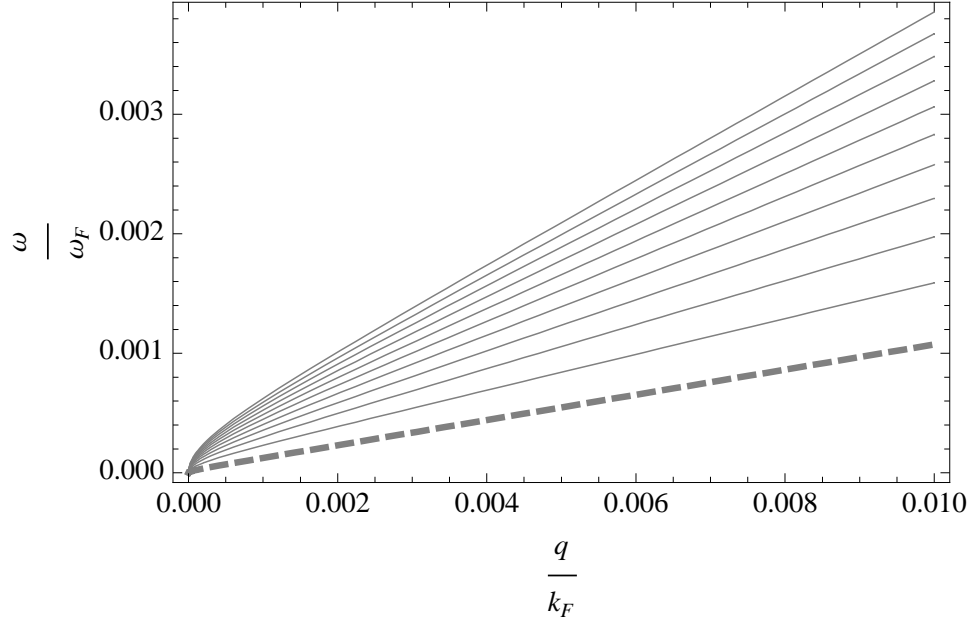


Figure 5.14: SP mode near a Feshbach resonance for an unpolarized PSC Fermi liquid, for  $F_0^a = 0 \dots 10$ . Dashed line corresponds to  $F_0^a = 0$ .

in Fig. 5.14 and Fig. 5.15. This would lower the lower-bound cutoff for propagation of the modes, i.e. the  $q_{min}$  value below which the modes would merge into the Stoner continuum would become smaller.

Lastly, in the case of a  $\sigma_0 + \sigma_1$  ground state SDF, the form of the modes is

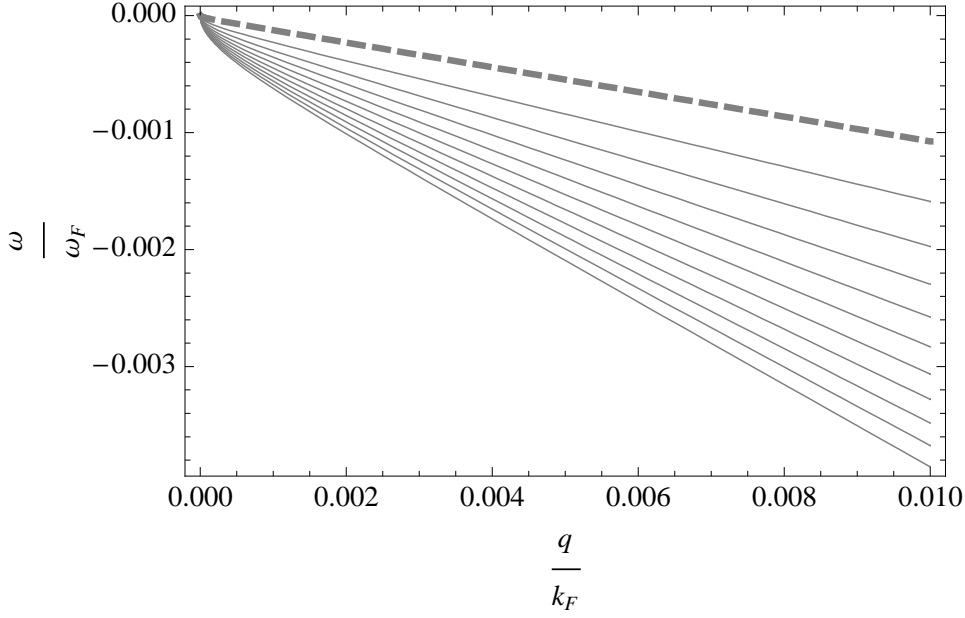


Figure 5.15: SC mode near a Feshbach resonance for an unpolarized PSC Fermi liquid, for  $F_0^a = 0 \dots 10$ . Dashed line corresponds to  $F_0^a = 0$ .

$$\begin{aligned}
 \omega_0^+(q) &= -\frac{1}{2} \frac{2}{\hbar N(0)} (F_0^a - \frac{F_1^a}{3}) \sigma_0 + \frac{1}{2} \left[ \left( \frac{2}{\hbar N(0)} (F_0^a - \frac{F_1^a}{3}) \sigma_0 \right)^2 \right. \\
 &\quad \left. - 4 \left( \frac{2}{\hbar N(0)} (F_0^a - \frac{F_1^a}{3}) \sigma_1 \frac{1}{\sqrt{3}} \left( 1 + \frac{F_1^a}{3} \right) q v_F - \frac{1}{3} (1 + F_0^a) \left( 1 + \frac{F_1^a}{3} \right) q^2 v_F^2 \right) \right]^{1/2} \\
 \omega_0^-(q) &= -\frac{1}{2} \frac{2}{\hbar N(0)} (F_0^a - \frac{F_1^a}{3}) \sigma_0 + \frac{1}{2} \left[ \left( \frac{2}{\hbar N(0)} (F_0^a - \frac{F_1^a}{3}) \sigma_0 \right)^2 \right. \\
 &\quad \left. - 4 \left( \frac{2}{\hbar N(0)} (F_0^a - \frac{F_1^a}{3}) \sigma_1 \frac{1}{\sqrt{3}} \left( 1 + \frac{F_1^a}{3} \right) q v_F - \frac{1}{3} (1 + F_0^a) \left( 1 + \frac{F_1^a}{3} \right) q^2 v_F^2 \right) \right]^{1/2}
 \end{aligned} \tag{5.24}$$

thus the gap of the SC mode would increase as the FBR were approached, and the dispersion of the SP mode and SC mode would become more quadratic. This behavior is shown in Fig. 5.16 and Fig. 5.17.

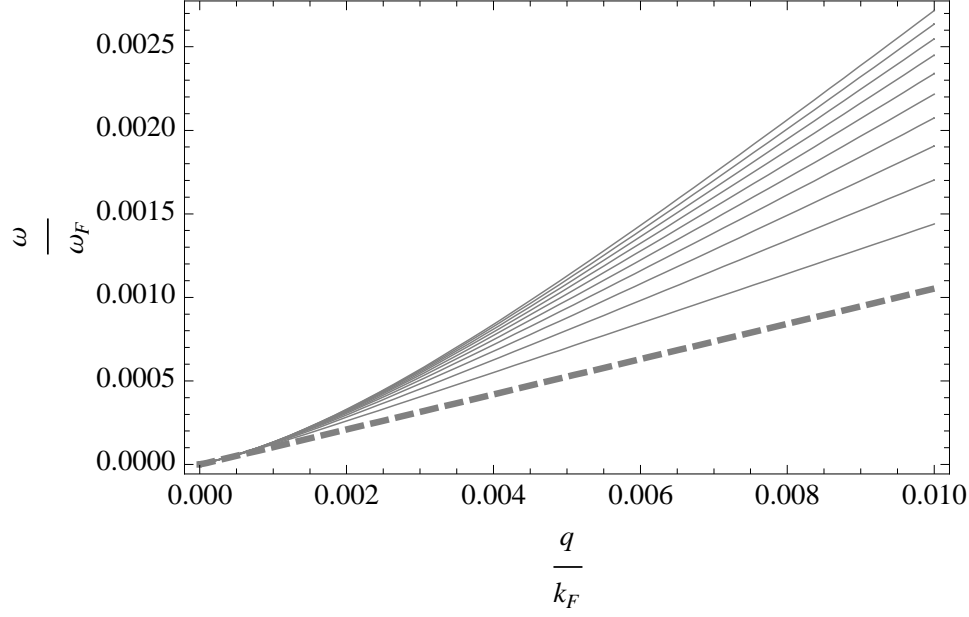


Figure 5.16: SP mode near a Feshbach resonance for a polarized PSC Fermi liquid, for  $F_0^a = 0 \dots 10$ . Dashed line corresponds to  $F_0^a = 0$ .

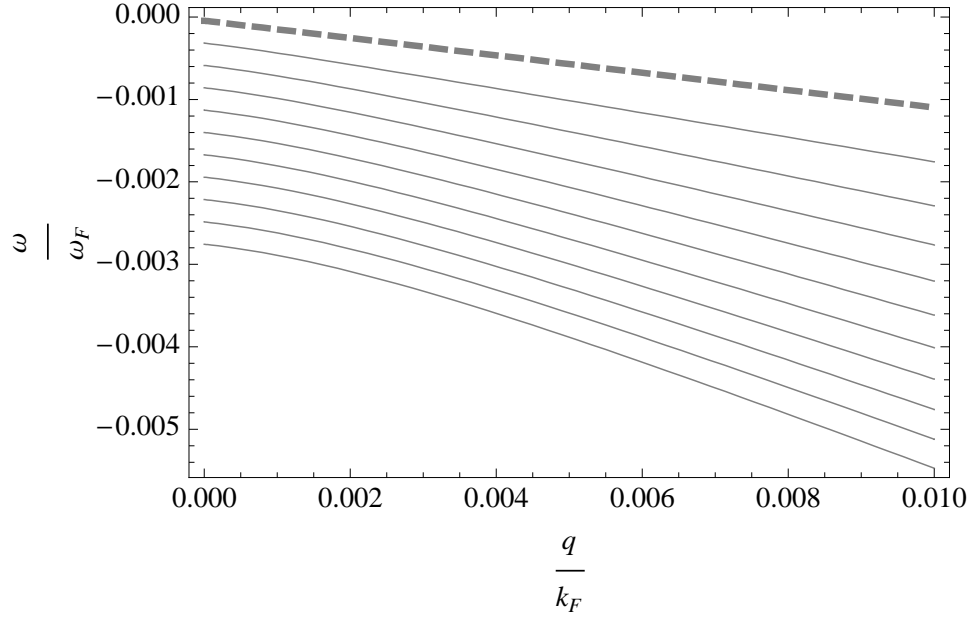


Figure 5.17: SC mode near a Feshbach resonance for a polarized PSC Fermi liquid, for  $F_0^a = 0 \dots 10$ . Dashed line corresponds to  $F_0^a = 0$ .



## 5.8 Spin waves in SDW materials

If a spin density wave (SDW) is present, e.g. a spiral or fan magnetic structure, in the ground state of an itinerant magnetic system, the transverse spin waves are affected by the magnetic anisotropy. Such a system is MnSi, and its spin wave, as detected by neutron scattering experiments, are characterized by a gapped quadratic dispersion [42]. The gap, in what is traditionally believed to be the spin precessional mode, arises from magnetic anisotropy. (The spin current mode is not believed to have been detected.)

In Fermi liquid theory, the spin waves of an itinerant SDW material are derived by assuming a spiral or fan magnetic structure, as the case may be, in the ground state of the system, and then employing the kinetic equation and fourier transform methods, just as in the case of Silin modes. With the details of the calculation presented in the appendix, we give below the results for the spin wave dispersions. (Below, a spiral structure is assumed in the ground state. A fan structure is not considered in this thesis – it is left for future consideration.)

The coupled equations for the spin waves of a spiral SDW are

$$\begin{aligned}
\boxed{+} \rightarrow 0,0 &\rightarrow \omega x^+ - By^+ = 0 \\
&\rightarrow 1,0 \rightarrow \omega y^+ - Ax^+ + Dm^z y^+ - Dm^+ y^z = 0 \\
\boxed{-} \rightarrow 0,0 &\rightarrow \omega x^- - By^- = 0 \\
&\rightarrow 1,0 \rightarrow \omega y^- - Ax^- - Dm^z y^- + Dm^- y^z = 0 \\
\boxed{z} \rightarrow 0,0 &\rightarrow \omega x^z - By^z = 0 \\
&\rightarrow 1,0 \rightarrow \omega y^z - Ax^z - \frac{1}{2}Dm^+ y^- + \frac{1}{2}Dm^- y^+ = 0
\end{aligned} \tag{5.25}$$

Upon simplification, the resultant characteristic equation of this matrix is

$$\omega^6 - \Gamma\omega^4 + \Gamma AB\omega^2 - A^3 B^3 = 0 \tag{5.26}$$

where  $\Gamma \equiv 3AB - D^2 m^z m^z + D^2 m^+ m^-$ . The solutions to this equation are

$$\begin{aligned}
\omega &= \pm (AB)^{1/2} \\
\omega &= \pm \left[ \frac{1}{2}(\Gamma - AB \pm [\Gamma^2 - 2AB\Gamma - 3A^2 B^2]^{1/2}) \right]^{1/2}
\end{aligned} \tag{5.27}$$

The definitions of A, B, C, D, and  $\Gamma$  are in the appendix. The six solutions are plotted in Fig. 5.18. Two are longitudinal paramagnon modes, and four are transverse spin wave modes.

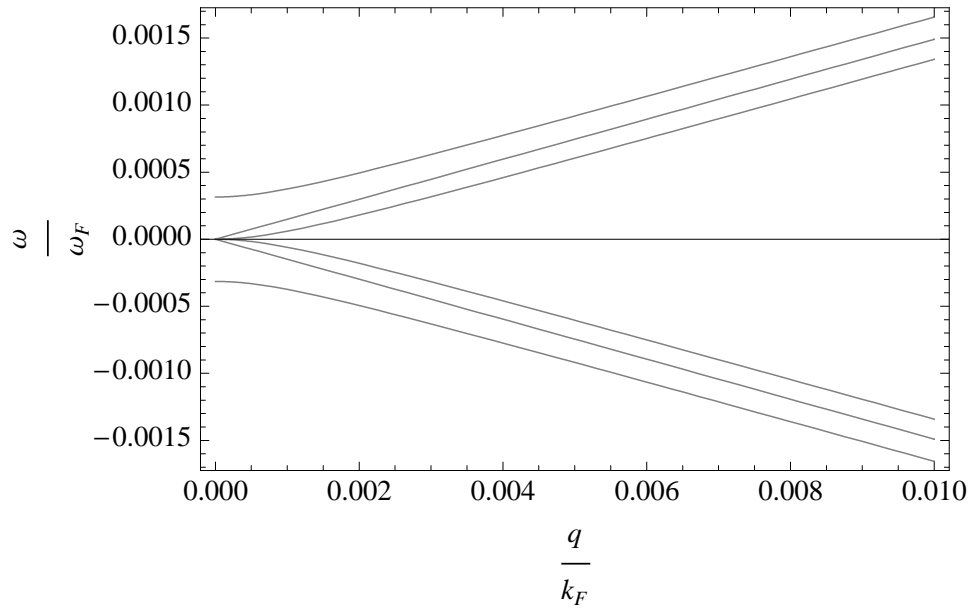


Figure 5.18: Spin wave modes of a spiral SDW fermi liquid. The linear modes are the paramagnon modes, and the quadratic modes are the SP and SC transverse spin wave modes.

# Chapter 6

## Summary and Conclusions

This thesis has presented our results for two new sets of transverse spin waves within fermi liquid theory, and discussed the ground states that would support them, as well. The dispersions of these transverse spin waves are proportional to  $q^1$  and  $q^{1/2}$  to leading order in  $q$ , which are new results for transverse spin waves in fermi liquid theory. Possible experimental conditions have been discussed for the observation of the new spin waves, including a dilute atomic gas of  $^6\text{Li}$  atoms near a Feshbach resonance, and solid state systems in which a persistent spin current exists in the ground state.

The spin waves reported in this thesis have a clear physical interpretation, and are grounded solidly within the framework of fermi liquid theory. The importance of the findings will be dictated by whether the conditions will turn out to be experimentally achievable, and whether the modes will be observable in such an experiment. The field of cold atom gases is expanding rapidly, and the possibilities in the field are thus expanding, as well. Thus, we expect that it will be soon that an experiment will be able to be performed

to easily observe the modes we have reported in this thesis.

Future theoretical work to be considered should be establishing, or disproving the possibility for, a connection between the spherical harmonic moments of the magnetization,  $\sigma_{1,0}$  and  $\sigma_{\pm 1,0}$ , and the perpendicular components of the magnetization of a spin density wave ground state,  $\sigma^{\pm}$ . The author and advisor have attempted to derive such a connection, but without success. However, it seems that there is a possibility that a connection could be made.

# Appendix A

## A.1 Substitutions

The following substitutions are defined for ease of notation, and are used throughout the appendices.

$$\begin{aligned}
 A &\equiv \frac{1}{\sqrt{3}}(1 + F_0^a)v_F q & x^\pm &\equiv \nu_0^\pm \\
 B &\equiv \frac{1}{\sqrt{3}}(1 + \frac{F_1^a}{3})v_F q & y^\pm &\equiv \nu_1^\pm \\
 B' &\equiv \frac{2}{\sqrt{15}}(1 + \frac{F_1^a}{3})v_F q & z^\pm &\equiv \nu_2^\pm \\
 C &\equiv \frac{2}{\sqrt{15}}(1 + \frac{F_2^a}{5})v_F q \\
 D &\equiv \frac{2}{\hbar N(0)}(F_0^a - \frac{F_1^a}{3}) \\
 E &\equiv \frac{2}{\hbar N(0)}(F_0^a - \frac{F_2^a}{5}) \\
 F &\equiv \frac{2}{\hbar N(0)}(\frac{F_1^a}{3} - \frac{F_2^a}{5})
 \end{aligned} \tag{A.1}$$

## A.2 Parameter Values

Unless otherwise stated, the following values for the Landau parameters, the density of states at the fermi level, the magnetization parameters  $\sigma_0$ ,  $\sigma_1$ , and  $\sigma_2$ , near a Feshbach resonance in a  ${}^6Li$  atomic gas are used throughout the thesis:

$$n = 1 \times 10^{19} m^{-3}$$

$$\sigma_0 = 5 \times 10^{17} m^{-3}$$

$$\sigma_1 = 5 \times 10^{17} m^{-3}$$

$$\sigma_2 = 5 \times 10^{17} m^{-3}$$

$$F_0^a = 10$$

$$F_1^a = -0.5$$

$$F_2^a = 0.1$$

$$N(0) = 7 \times 10^{48} J^{-1} m^{-3}$$

$$E_F = \hbar\omega_F$$

$$\omega_F = 5 \times 10^6 rad/s$$

$$k_F = 1 \times 10^7 m^{-1}$$

$$\gamma = -1.495 \times 10^{11}$$

$$H = 5 \times 10^{-5} Tesla$$

(A.2)

# Appendix B

Ginzburg-Landau free energy of a fermi liquid system possessing both  $l = 0$  and  $l = 1$  magnetic instabilities, thus  $F_0^a < -1$ , and  $F_1^a < -3$ .

We start by briefly copying down Baym and Pethick's derivation of thermodynamic stability of a fermi liquid (from page 15 of [6]). We do this, because it requires the same formalism as what we are doing with the deformation of the fermi surface of a spin species. The calculation we have done is formally exactly the same.

$$(E - \mu n) - (E - \mu n)_0 = \frac{1}{V} \sum_{\vec{p}, \sigma} (\varepsilon_p^0 - \mu) \delta n_{\vec{p}, \sigma} + \frac{1}{2V^2} \sum_{\vec{p}, \sigma, \vec{p}', \sigma'} f_{\vec{p}, \sigma, \vec{p}', \sigma'} \delta n_{\vec{p}, \sigma} \delta n_{\vec{p}', \sigma'} \quad (\text{B.1})$$

$$\delta n_{\vec{p}, \sigma} = n_{\vec{p}, \sigma} - n_{\vec{p}}^0 \quad (\text{B.2})$$

$$= (\delta p_f) \delta(p_f - p) - \frac{1}{2} (\delta p_f)^2 \frac{\partial}{\partial p} \delta(p_f - p) \quad (\text{B.3})$$

where



$$\delta p_f(\theta, \sigma) \equiv p_f(\theta, \sigma) - p_f^0 \quad (\text{B.4})$$

is the change in the fermi momentum from it's equilibrium value; in other words, it's the deformation of the fermi surface. Then evaluating Eq. (B.1) gives

$$\delta E - \mu \delta n = \sum_l \frac{N(0)}{8(2l+1)} [(\sigma_{l\uparrow} + \sigma_{l\downarrow})^2 (1 + \frac{F_l^s}{2l+1}) + (\sigma_{l\uparrow} - \sigma_{l\downarrow})^2 (1 + \frac{F_l^a}{2l+1})]. \quad (\text{B.5})$$

This is the derivation from Baym and Pethick [6]. Below I just show explicitly the intermediate steps. For the first term on the right hand side of Eq. (B.1), the integral to perform is

$$\begin{aligned} & \frac{1}{V} \sum_{\sigma} \int_0^{\infty} \int_0^{\pi} \int_0^{2\pi} p^2 \sin(\theta) dp d\theta d\phi (v_f(p - p_f)) \\ & [(\delta p_f) \delta(p_f - p) - \frac{1}{2} (\delta p_f)^2 \frac{\partial}{\partial p} \delta(p_f - p)]. \end{aligned} \quad (\text{B.6})$$

The single power of the delta function integrates to give zero, so the integral becomes

$$\begin{aligned} & -\frac{1}{2V} \sum_{\sigma} v_f \left[ \int_0^{\infty} p^3 dp \frac{\partial}{\partial p} \delta(p_f - p) - p_f \int_0^{\infty} p^2 dp \frac{\partial}{\partial p} \delta(p_f - p) \right] \\ & \int_0^{\pi} \int_0^{2\pi} \sin(\theta) d\theta d\phi (\delta p_f)^2. \end{aligned} \quad (\text{B.7})$$

Taking it one step further, evaluating the two magnitude integrals, which are easy (page 61 Shankar QM shows how to integrate over the derivative of a delta function), and substituting in the spherical harmonic expansion for  $\delta p_f$ , gives

$$\frac{1}{2V} \sum_{\sigma} v_f [3p_f^2 - 2p_f^2] \int_0^{\pi} \int_0^{2\pi} \sin(\theta) d\theta d\phi \left( \sum_{l,m} \sigma_{lm} Y_l^m(\theta, \phi) \right)^2. \quad (\text{B.8})$$

Now writing out explicitly the  $l = 0$  and  $l = 1$  spherical harmonic moments of the fermi surface distortion, the integral looks like

$$\begin{aligned} \frac{1}{2V} \sum_{\sigma} \frac{p_f^3}{m^*} \int_0^{\pi} \int_0^{2\pi} \sin(\theta) d\theta d\phi & \left( \left( \frac{1}{4\pi} \right)^{1/2} \sigma_{00} + \left( \frac{3}{4\pi} \right)^{1/2} \cos(\theta) \sigma_{10} \right. \\ & \left. - \left( \frac{3}{8\pi} \right)^{1/2} e^{i\theta} \sin(\theta) \sigma_{11} + \left( \frac{3}{8\pi} \right)^{1/2} e^{-i\theta} \sin(\theta) \sigma_{1-1} \right)^2 \end{aligned} \quad (\text{B.9})$$

Evaluating this integral gives

$$\frac{1}{2V} \sum_{\sigma} \frac{p_f^3}{m^*} [\sigma_{00}^2 + \sigma_{10}^2 - 2\sigma_{11}\sigma_{1-1}] \quad (\text{B.10})$$

Now to evaluate the second term of Eq. (B.1). Written out explicitly, this term looks like

$$\begin{aligned} \frac{1}{2V^2} \sum_{\sigma\sigma'} \int_0^{\infty} \int_0^{\pi} \int_0^{2\pi} \int_0^{\infty} \int_0^{\pi} \int_0^{2\pi} p^2 \sin(\theta) dp d\theta d\phi p'^2 \sin(\theta') dp' d\theta' d\phi' \\ f_{\vec{p}\sigma\vec{p}'\sigma'}(\delta p_f) \delta(p_f - p) (\delta p_f) \delta(p_f - p'). \end{aligned} \quad (\text{B.11})$$

The magnitude integrals over  $p$  and  $p'$  are the same as the magnitude integral in the first term, thus each giving  $\frac{p_f^3}{m^\star}$ . So, after performing these integrals, what is left is explicitly

$$\frac{1}{2V^2} \sum_{\sigma\sigma'} \left(\frac{p_f^3}{m^\star}\right)^2 \int_0^\pi \int_0^{2\pi} \int_0^\pi \int_0^{2\pi} \sin(\theta') d\theta' d\phi' \sum_l f_l P_l(\cos\gamma_{\vec{p}\vec{p}'}) \left(\sum_{l,m} \sigma_{lm} Y_l^m(\theta, \phi)\right) \left(\sum_{l,m} \sigma_{lm} Y_l^m(\theta', \phi')\right) \quad (\text{B.12})$$

This integral gives

$$\frac{4\pi}{2V^2} \sum_{\sigma\sigma'} \left(\frac{p_f^3}{m^\star}\right)^2 [f_0 \sigma_{00}^2 + \frac{f_1}{3} \sigma_{10}^2 - \frac{2f_1}{3} \sigma_{11} \sigma_{1-1}] \quad (\text{B.13})$$

Thus, combining the two terms, the final expression for the energy variation becomes

$$\delta E - \mu \delta n = \frac{1}{2V} \sum_{\sigma} \frac{p_f^3}{m^\star} [\sigma_{00}^2 + \sigma_{10}^2 - 2\sigma_{11} \sigma_{1-1}] + \frac{4\pi}{2V^2} \sum_{\sigma\sigma'} \left(\frac{p_f^3}{m^\star}\right)^2 [f_0 \sigma_{00}^2 + \frac{f_1}{3} \sigma_{10}^2 - \frac{2f_1}{3} \sigma_{11} \sigma_{1-1}]. \quad (\text{B.14})$$

This expression can be rewritten in a simpler-looking form:

$$F = N(0) [(1 + F_0^a) \sigma_{00}^2 + (1 + \frac{F_1^a}{3}) \sigma_{10}^2 - 2(1 + \frac{F_1^a}{3}) \sigma_{11} \sigma_{1-1}] \quad (\text{B.15})$$

# Appendix C

In this appendix, the calculations for the new spin waves are shown in detail. For completeness, we start out with the spin kinetic equation, which is the starting point for our spin wave calculations.

$$\frac{\partial}{\partial t} \vec{\sigma}_p + \vec{v}_p \cdot \vec{\nabla}_r \left( \vec{\sigma}_p - \frac{\partial n_p^0}{\partial \varepsilon_p} \int \frac{d^3 p'}{2\pi \hbar} f_{pp'}^a \vec{\sigma}_p' \right) = -\frac{2}{\hbar} \vec{\sigma}_p \times \vec{h}_p \quad (\text{C.1})$$

Now separate out  $\vec{\sigma}_p$  into ground state and first order deviation

$$\vec{\sigma}_p \equiv \vec{\sigma}_p^0 + \delta \vec{\sigma}_p \quad (\text{C.2})$$

Then the kinetic equation becomes

$$\frac{\partial}{\partial t} \delta \vec{\sigma}_p + \vec{v}_p \cdot \vec{\nabla}_r \left( \delta \vec{\sigma}_p - \frac{\partial n_p^0}{\partial \varepsilon_p} \int \frac{d^3 p'}{2\pi \hbar} f_{pp'}^a \delta \vec{\sigma}_p' \right) = -\frac{2}{\hbar} (\vec{\sigma}_p^0 \times \delta \vec{h}_p + \delta \vec{\sigma}_p \times \vec{h}_p^0) \quad (\text{C.3})$$

Then separating out the  $\hat{i}$ ,  $\hat{j}$ , and  $\hat{k}$  equations, we get for the  $\hat{i}$  equation

$$\frac{\partial}{\partial t}\delta\sigma_{px} + \vec{v}_p \cdot \vec{\nabla}_r \left( \delta\sigma_{px} - \frac{\partial n_p^0}{\partial \varepsilon_p} \int \frac{d^3 p'}{2\pi\hbar} f_{pp'}^a \delta\sigma_{p'x} \right) = -\frac{2}{\hbar} (-\sigma_{pz}^0 \delta h_{py} + \delta\sigma_{py} h_{pz}^0) \quad (\text{C.4})$$

and for the  $\hat{j}$  equation

$$\frac{\partial}{\partial t}\delta\sigma_{py} + \vec{v}_p \cdot \vec{\nabla}_r \left( \delta\sigma_{py} - \frac{\partial n_p^0}{\partial \varepsilon_p} \int \frac{d^3 p'}{2\pi\hbar} f_{pp'}^a \delta\sigma_{p'y} \right) = -\frac{2}{\hbar} (\sigma_{pz}^0 \delta h_{px} - \delta\sigma_{px} h_{pz}^0) \quad (\text{C.5})$$

and for the  $\hat{k}$  equation (though the  $\hat{k}$  equation is ignored in this derivation, because it does not constitute a transverse mode)

$$\frac{\partial}{\partial t}\delta\sigma_{pz} + \vec{v}_p \cdot \vec{\nabla}_r \left( \delta\sigma_{pz} - \frac{\partial n_p^0}{\partial \varepsilon_p} \int \frac{d^3 p'}{2\pi\hbar} f_{pp'}^a \delta\sigma_{p'z} \right) = -\frac{2}{\hbar} (\sigma_{px}^0 \delta h_{py} - \delta\sigma_{py} h_{px}^0) \quad (\text{C.6})$$

Achieving a solution to these coupled equations is facilitated by multiplying the  $\hat{j}$  equation by  $i$  (the square root of  $-1$ ), and then adding this to the  $\hat{i}$  equation to obtain one equation, and also subtracting this from the  $\hat{i}$  equation to obtain a second equation. Upon doing this, the two new equations are

$$\begin{aligned} \frac{\partial}{\partial t} (\delta\sigma_{px} + i\delta\sigma_{py}) + \vec{v}_p \cdot \vec{\nabla}_r \left( (\delta\sigma_{px} + i\delta\sigma_{py}) - \frac{\partial n_p^0}{\partial \varepsilon_p} \int \frac{d^3 p'}{2\pi\hbar} f_{pp'}^a (\delta\sigma_{p'x} + i\delta\sigma_{p'y}) \right) = \\ -\frac{2i}{\hbar} \left[ \sigma_{pz}^0 \int \frac{d^3 p'}{2\pi\hbar} f_{pp'}^a (\delta\sigma_{p'x} + i\delta\sigma_{p'y}) - (\delta\sigma_{px} + i\delta\sigma_{py}) \int \frac{d^3 p'}{2\pi\hbar} f_{pp'}^a \sigma_{p'z}^0 \right] \quad (\text{C.7}) \end{aligned}$$

and

$$\begin{aligned} \frac{\partial}{\partial t} (\delta\sigma_{px} - i\delta\sigma_{py}) + \vec{v}_p \cdot \vec{\nabla}_r \left( (\delta\sigma_{px} - i\delta\sigma_{py}) - \frac{\partial n_p^0}{\partial \varepsilon_p} \int \frac{d^3 p'}{2\pi\hbar} f_{pp'}^a (\delta\sigma_{p'x} - i\delta\sigma_{p'y}) \right) = \\ -\frac{2i}{\hbar} \left[ \sigma_{pz}^0 \int \frac{d^3 p'}{2\pi\hbar} f_{pp'}^a (\delta\sigma_{p'x} - i\delta\sigma_{p'y}) - (\delta\sigma_{px} - i\delta\sigma_{py}) \int \frac{d^3 p'}{2\pi\hbar} f_{pp'}^a \sigma_{p'z}^0 \right] \quad (\text{C.8}) \end{aligned}$$

Then, the substitutions,

$$\delta\sigma_p^+ \equiv \delta\sigma_{px} + i\delta\sigma_{py} \quad (\text{C.9})$$

$$\delta\sigma_p^- \equiv \delta\sigma_{px} - i\delta\sigma_{py} \quad (\text{C.10})$$

lead to the following equations,

$$\begin{aligned} \frac{\partial}{\partial t} \delta\sigma_p^+ + \vec{v}_p \cdot \vec{\nabla}_r \left( \delta\sigma_p^+ - \frac{\partial n_p^0}{\partial \varepsilon_p} \int \frac{d^3 p'}{2\pi\hbar} f_{pp'}^a \delta\sigma_{p'}^+ \right) = \\ -\frac{2i}{\hbar} \left[ \sigma_{pz}^0 \int \frac{d^3 p'}{2\pi\hbar} f_{pp'}^a \delta\sigma_{p'}^+ - \delta\sigma_p^+ \int \frac{d^3 p'}{2\pi\hbar} f_{pp'}^a \sigma_{p'z}^0 \right] \quad (\text{C.11}) \end{aligned}$$

and

$$\begin{aligned} \frac{\partial}{\partial t} \delta\sigma_p^- + \vec{v}_p \cdot \vec{\nabla}_r \left( \delta\sigma_p^- - \frac{\partial n_p^0}{\partial \varepsilon_p} \int \frac{d^3 p'}{2\pi\hbar} f_{pp'}^a \delta\sigma_{p'}^- \right) = \\ \frac{2i}{\hbar} \left[ \sigma_{pz}^0 \int \frac{d^3 p'}{2\pi\hbar} f_{pp'}^a \delta\sigma_{p'}^- - \delta\sigma_p^- \int \frac{d^3 p'}{2\pi\hbar} f_{pp'}^a \sigma_{p'z}^0 \right] \quad (\text{C.12}) \end{aligned}$$

The above equations are two uncoupled kinetic equations. The first de-

scribes the propagation of a spin wave that results from a spin being flipped from down to up, and the second describes the propagation of a spin wave the results from a spin being flipped from up to down. We will only derive the dispersion for the former case, and then give the result for both, since the dispersion for the flip down process is derived in exactly the same way.

Now, performing the substitutions

$$\delta\sigma_p^+ \equiv -\frac{\partial n_p^0}{\partial \varepsilon_p} \nu_p^+ \quad \delta\sigma_p^- \equiv -\frac{\partial n_p^0}{\partial \varepsilon_p} \nu_p^- \quad \sigma_{pz}^0 \equiv -\frac{\partial n_p^0}{\partial \varepsilon_p} \sigma_{pz} \quad (\text{C.13})$$

and dividing the equation by  $-\frac{\partial n_p^0}{\partial \varepsilon_p}$ , the "+" equation becomes

$$\begin{aligned} \frac{\partial}{\partial t} \nu_p^+ + \vec{v}_p \cdot \vec{\nabla}_r \left( \nu_p^+ + \int \frac{d^3 p'}{2\pi\hbar} f_{pp'}^a \left( -\frac{\partial n_p^0}{\partial \varepsilon_p} \nu_{p'}^+ \right) \right) = \\ -\frac{2i}{\hbar} \left[ \sigma_{pz} \int \frac{d^3 p'}{2\pi\hbar} f_{pp'}^a \left( -\frac{\partial n_p^0}{\partial \varepsilon_p} \nu_{p'}^+ \right) - \nu_p^+ \int \frac{d^3 p'}{2\pi\hbar} f_{pp'}^a \left( -\frac{\partial n_p^0}{\partial \varepsilon_p} \sigma_{p'z} \right) \right] \end{aligned} \quad (\text{C.14})$$

Fourier transforming  $\nu_p^+$ , such that

$$\nu_p^+(\vec{r}, t) = \sum_{\vec{q}, \omega} \nu_p^+(\vec{q}, \omega) e^{i(\vec{q} \cdot \vec{r} - \omega t)} \quad (\text{C.15})$$

and looking at only one Fourier component, dividing out  $e^{i(\vec{q} \cdot \vec{r} - \omega t)}$ , performing the temporal and spatial derivatives, multiplying the equation by  $i$ , and bringing everything over to the left side of the equation, the equation becomes,

$$\begin{aligned} & \omega \nu_p^+ - \vec{v}_p \cdot \vec{q} \nu_p^+ - \vec{v}_p \cdot \vec{q} \int \frac{d^3 p'}{2\pi\hbar} f_{pp'}^a \left( -\frac{\partial n_p^0}{\partial \varepsilon_p} \nu_{p'}^+ \right) + \\ & \frac{2}{\hbar} \left[ -\sigma_{pz} \int \frac{d^3 p'}{2\pi\hbar} f_{pp'}^a \left( -\frac{\partial n_p^0}{\partial \varepsilon_p} \nu_{p'}^+ \right) + \nu_p^+ \int \frac{d^3 p'}{2\pi\hbar} f_{pp'}^a \left( -\frac{\partial n_p^0}{\partial \varepsilon_p} \sigma_{p'z} \right) \right] = 0 \quad (\text{C.16}) \end{aligned}$$

Now expanding  $\nu_p^+$ ,  $\sigma_{pz}$  and  $f_{\mathbf{p}\mathbf{p}'}^a$  as

$$\sigma_{pz} = \sum_{l,m} \sigma_{l,m} Y_l^m(\theta_p, \phi_p) \quad (\text{C.17})$$

$$\nu_p^+ = \sum_{l,m} \nu_{l,m}^+ Y_l^m(\theta_p, \phi_p) \quad (\text{C.18})$$

$$f_{\mathbf{p}\mathbf{p}'}^a = \sum_{l,m} f_l^a P_l^m(\cos \theta_{pp'}) \quad (\text{C.19})$$

the kinetic equation becomes

$$\begin{aligned} & \omega \sum_{l,m} \nu_{l,m}^+ Y_l^m(\theta_p, \phi_p) - \vec{v}_p \cdot \vec{q} \sum_{l,m} \nu_{l,m}^+ Y_l^m(\theta_p, \phi_p) - \\ & \vec{v}_p \cdot \vec{q} \int \frac{d^3 p'}{2\pi\hbar} \sum_{l,m} f_l^a P_l^m(\cos \theta_{pp'}) \left( -\frac{\partial n_p^0}{\partial \varepsilon_p} \sum_{l,m} \nu_{l,m}^+ Y_l^m(\theta'_p, \phi'_p) \right) + \\ & \frac{2}{\hbar} \left[ -\sum_{l,m} \sigma_{l,m} Y_l^m(\theta_p, \phi_p) \int \frac{d^3 p'}{2\pi\hbar} \sum_{l,m} f_l^a P_l^m(\cos \theta_{pp'}) \left( -\frac{\partial n_p^0}{\partial \varepsilon_p} \sum_{l,m} \nu_{l,m}^+ Y_l^m(\theta'_p, \phi'_p) \right) + \right. \\ & \left. \sum_{l,m} \nu_{l,m}^+ Y_l^m(\theta_p, \phi_p) \int \frac{d^3 p'}{2\pi\hbar} \sum_{l,m} f_l^a P_l^m(\cos \theta_{pp'}) \left( -\frac{\partial n_p^0}{\partial \varepsilon_p} \sum_{l,m} \sigma_{l,m} Y_l^m(\theta'_p, \phi'_p) \right) \right] \\ & = 0 \quad (\text{C.20}) \end{aligned}$$



This equation is ready to be projected out into spherical harmonic components. In the next section we will perform the projections, thus obtaining the coupled harmonic equations for the spin waves. These calculations will be shown in complete detail.

### C.2.1 Spherical Harmonic Projection

The projections of the most general coupled equations that are presented in this thesis for spin waves in a fermi liquid are shown here. All other coupled equations for spin waves are a subset of these.

In what follows, the  $\nu_l^m$  are the spherical harmonics projections of the fermi surface distortion from the ground state, labeled by the polar order  $l$  and the azimuthal order  $m$ . Only  $m = 0$  harmonics need be considered, because the momentum transfer,  $\vec{q}$ , is assumed to be in the  $z$ -direction, and this results in the excitation of only the polar, or  $m = 0$ , moments of the spherical harmonics in the fermi surface distortion. The  $Y_l^m(\theta_p, \phi_p)$  are the usual normalized spherical harmonics. The first few spherical harmonics are

$$Y_0^0(\theta, \phi) = \frac{1}{\sqrt{4\pi}} \quad (\text{C.21})$$

$$Y_1^0(\theta, \phi) = \sqrt{\frac{3}{4\pi}} \cos \theta \quad (\text{C.22})$$

$$Y_2^0(\theta, \phi) = \sqrt{\frac{5}{16\pi}} (\cos^2 \theta - 1) \quad (\text{C.23})$$

The kinetic equation is

$$\begin{aligned}
& \omega(\nu_0^+ Y_0^0(p) + \nu_1^+ Y_1^0(p) + \nu_2^+ Y_2^0(p)) - \vec{v}_p \cdot \vec{q} (\nu_0^+ Y_0^0(p) + \nu_1^+ Y_1^0(p) + \nu_2^+ Y_2^0(p)) - \\
& \vec{v}_p \cdot \vec{q} \int \frac{d^3 p'}{2\pi\hbar} \sum_{l,m} f_l^a P_l^m(\cos \theta_{pp'}) \left( -\frac{\partial n_p^0}{\partial \varepsilon_p} (\nu_0^+ Y_0^0(p') + \nu_1^+ Y_1^0(p') + \nu_2^+ Y_2^0(p')) \right) + \\
& \frac{2}{\hbar} \left[ -(\sigma_0^+ Y_0^0(p) + \sigma_1^+ Y_1^0(p)) \int \frac{d^3 p'}{2\pi\hbar} \sum_{l,m} f_l^a P_l^m(\cos \theta_{pp'}) \left( -\frac{\partial n_p^0}{\partial \varepsilon_p} (\nu_0^+ Y_0^0(p') + \right. \right. \\
& \left. \left. \nu_1^+ Y_1^0(p') + \nu_2^+ Y_2^0(p')) \right) + (\nu_0^+ Y_0^0(p) + \nu_1^+ Y_1^0(p) + \nu_2^+ Y_2^0(p)) \right. \\
& \left. \int \frac{d^3 p'}{2\pi\hbar} \sum_{l,m} f_l^a P_l^m(\cos \theta_{pp'}) \left( -\frac{\partial n_p^0}{\partial \varepsilon_p} (\nu_0^+ Y_0^0(p') + \nu_1^+ Y_1^0(p') + \nu_2^+ Y_2^0(p')) \right) \right] \\
& = 0 \quad (\text{C.24})
\end{aligned}$$

The projections onto this equation are now done one term at a time, for clarity. The first term, which is  $\omega(\nu_0^+ Y_0^0(p) + \nu_1^+ Y_1^0(p) + \nu_2^+ Y_2^0(p))$ , has the following projections.

$$\begin{aligned}
(l=0, m=0) \quad & \int d\Omega_p Y_0^{0*}(p) \omega(\nu_0^+ Y_0^0(p) + \nu_1^+ Y_1^0(p) + \nu_2^+ Y_2^0(p)) \\
& = \int_0^{2\pi} \int_0^\pi d\phi_p d\theta_p \sin(\theta_p) \left( \frac{1}{\sqrt{4\pi}} \right) \omega \nu_0 \frac{1}{\sqrt{4\pi}} \\
& = \frac{1}{4\pi} 4\pi \omega \nu_0 = \omega \nu_0 \quad (\text{C.25})
\end{aligned}$$

$$\begin{aligned}
(l=1, m=0) \quad & \int d\Omega_p Y_0^{1*}(p) \omega((\nu_0^+ Y_0^0(p) + \nu_1^+ Y_1^0(p) + \nu_2^+ Y_2^0(p))) \\
& = \omega \nu_1 \quad (\text{C.26})
\end{aligned}$$

$$\begin{aligned}
(l=2, m=0) \quad & \int d\Omega_p \ Y_0^{2*}(p) \omega((\nu_0^+ Y_0^0(p) + \nu_1^+ Y_1^0(p) + \nu_2^+ Y_2^0(p))) \\
& = \omega \nu_2
\end{aligned} \tag{C.27}$$

The second term, which is  $-\vec{v}_p \cdot \vec{q}(\nu_0^+ Y_0^0(p) + \nu_1^+ Y_1^0(p) + \nu_2^+ Y_2^0(p))$ , has the following projections.

$$\begin{aligned}
(l=0, m=0) \quad & \int d\Omega_p \ Y_0^{0*}(p) \left( -\vec{v}_p \cdot \vec{q}(\nu_0^+ Y_0^0(p) + \nu_1^+ Y_1^0(p) + \nu_2^+ Y_2^0(p)) \right) \\
& = -\frac{1}{\sqrt{3}} v_F q \nu_1
\end{aligned} \tag{C.28}$$

$$\begin{aligned}
(l=1, m=0) \quad & \int d\Omega_p \ Y_0^{1*}(p) \left( -\vec{v}_p \cdot \vec{q}(\nu_0^+ Y_0^0(p) + \nu_1^+ Y_1^0(p) + \nu_2^+ Y_2^0(p)) \right) \\
& = -\frac{1}{\sqrt{3}} v_F q \nu_0 - \frac{2}{\sqrt{15}} v_F q \nu_2
\end{aligned} \tag{C.29}$$

$$\begin{aligned}
(l=2, m=0) \quad & \int d\Omega_p \ Y_0^{2*}(p) \left( -\vec{v}_p \cdot \vec{q}(\nu_0^+ Y_0^0(p) + \nu_1^+ Y_1^0(p) + \nu_2^+ Y_2^0(p)) \right) \\
& = -\frac{2}{\sqrt{15}} v_F q \nu_1
\end{aligned} \tag{C.30}$$

The third term, which is  $-\vec{v}_p \cdot \vec{q} \int \frac{d^3 p'}{2\pi\hbar} \sum_{l,m} f_l^a P_l^m(\cos \theta_{pp'}) (-\frac{\partial n_p^0}{\partial \varepsilon_p}(\nu_0^+ Y_0^0(p') + \nu_1^+ Y_1^0(p') + \nu_2^+ Y_2^0(p')))$ , has the following projections.

$$\begin{aligned}
(l=0, m=0) \quad \int d\Omega_p Y_0^{0*}(p) \Big( \dots \Big) &= -\frac{1}{\sqrt{3}} v_F q \frac{1}{3} F_1^a \nu_1 \\
(l=1, m=0) \quad \int d\Omega_p Y_0^{1*}(p) \Big( \dots \Big) &= -\frac{1}{\sqrt{3}} v_F q F_0^a \nu_0 - \frac{2}{\sqrt{15}} v_F q \frac{1}{5} F_2^a \nu_2 \\
(l=2, m=0) \quad \int d\Omega_p Y_0^{2*}(p) \Big( \dots \Big) &= -\frac{2}{\sqrt{15}} v_F q \frac{1}{3} F_1^a \nu_1
\end{aligned} \tag{C.31}$$

The fourth term, which is  $\frac{2}{\hbar} \left[ -(\sigma_0^+ Y_0^0(p) + \sigma_1^+ Y_1^0(p)) \int \frac{d^3 p'}{2\pi\hbar} \sum_{l,m} f_l^a P_l^m(\cos \theta_{pp'}) \right. \\ \left. (-\frac{\partial n_p^0}{\partial \varepsilon_p} (\nu_0^+ Y_0^0(p') + \nu_1^+ Y_1^0(p') + \nu_2^+ Y_2^0(p'))) \right]$ , has the following projections.

$$\begin{aligned}
(l=0, m=0) \quad \int d\Omega_p Y_0^{0*}(p) \Big( \dots \Big) &= -\frac{2}{\hbar} \frac{1}{\sqrt{4\pi}} \left[ \sigma_0 F_0^a \nu_0 + \frac{1}{3} \sigma_1 F_1^a \nu_1 \right] \\
(l=1, m=0) \quad \int d\Omega_p Y_0^{1*}(p) \Big( \dots \Big) &= -\frac{2}{\hbar} \frac{1}{\sqrt{4\pi}} \left[ \frac{1}{3} \sigma_0 F_1^a \nu_1 + \sigma_1 F_0^a \nu_0 \right] \\
(l=2, m=0) \quad \int d\Omega_p Y_0^{2*}(p) \Big( \dots \Big) &= -\frac{2}{\hbar} \frac{1}{\sqrt{5\pi}} \left[ \frac{1}{3} \sigma_1 F_1^a \nu_1 \right]
\end{aligned} \tag{C.32}$$

The fifth and final term, which is  $(\nu_0^+ Y_0^0(p) + \nu_1^+ Y_1^0(p) + \nu_2^+ Y_2^0(p)) \int \frac{d^3 p'}{2\pi\hbar} \sum_{l,m} f_l^a P_l^m(\cos \theta_{pp'}) (-\frac{\partial n_p^0}{\partial \varepsilon_p} (\nu_0^+ Y_0^0(p') + \nu_1^+ Y_1^0(p') + \nu_2^+ Y_2^0(p')))$ , has the following projections.

$$\begin{aligned}
(l=0, m=0) \quad \int d\Omega_p Y_0^{0*}(p) (\dots) &= \frac{2}{\hbar} \frac{1}{\sqrt{4\pi}} \left[ \sigma_0 F_0^a \nu_0 + \frac{1}{3} \sigma_1 F_1^a \nu_1 \right] \\
(l=1, m=0) \quad \int d\Omega_p Y_0^{1*}(p) (\dots) &= \frac{2}{\hbar} \frac{1}{\sqrt{4\pi}} \left[ \frac{1}{3} \sigma_1 F_1^a \nu_0 + \sigma_0 F_0^a \nu_1 + \frac{4}{\sqrt{5}} \frac{1}{3} \sigma_1 F_1^a \nu_2 \right] \\
(l=2, m=0) \quad \int d\Omega_p Y_0^{2*}(p) (\dots) &= \frac{2}{\hbar} \left[ \frac{1}{\sqrt{5\pi}} \frac{1}{3} \sigma_1 F_1^a \nu_1 + \frac{1}{\sqrt{4\pi}} \sigma_0 F_0^a \nu_2 \right]
\end{aligned} \tag{C.33}$$

Now, putting all of the terms together, the projections give the following coupled equations in  $\nu_0$ ,  $\nu_1$ , and  $\nu_2$ .

$$\begin{aligned}
(l=0, m=0) \quad \omega \nu_0 - \frac{1}{\sqrt{3}} v_F q \nu_1 - \frac{1}{\sqrt{3}} v_F q \frac{1}{3} F_1^a \nu_1 &= 0 \\
(l=1, m=0) \quad \omega \nu_1 - \frac{1}{\sqrt{3}} v_F q \nu_0 - \frac{2}{\sqrt{15}} v_F q \nu_2 - \frac{1}{\sqrt{3}} v_F q F_0^a \nu_0 \\
&\quad - \frac{2}{\hbar} \frac{1}{\sqrt{4\pi}} \left[ \frac{1}{3} \sigma_0 F_1^a \nu_1 + \sigma_1 F_0^a \nu_0 \right] \\
&\quad + \frac{2}{\hbar} \frac{1}{\sqrt{4\pi}} \left[ \frac{1}{3} \sigma_1 F_1^a \nu_0 + \sigma_0 F_0^a \nu_1 + \frac{2}{\sqrt{5}} \frac{1}{3} \sigma_1 F_1^a \nu_2 \right] = 0 \\
(l=2, m=0) \quad \omega \nu_2 - \frac{2}{\sqrt{15}} v_F q \nu_1 - \frac{2}{\sqrt{15}} v_F q F_1^a \nu_1 + \frac{1}{\sqrt{4\pi}} \sigma_0 F_0^a \nu_2 &= 0
\end{aligned} \tag{C.34}$$

Simplifying the equations by combining like terms,

$$\begin{aligned}
(l=0, m=0) \quad & \omega\nu_0 - \frac{1}{\sqrt{3}}(1 + \frac{F_1^a}{3})v_F q\nu_1 = 0 \\
(l=1, m=0) \quad & \omega\nu_1 - \frac{1}{\sqrt{3}}(1 + F_0^a)v_F q\nu_0 - \frac{2}{\sqrt{15}}v_F q\nu_2 \\
& + \frac{2}{\hbar} \frac{1}{\sqrt{4\pi}}(F_0^a - \frac{F_1^a}{3})(\sigma_0\nu_1 - \sigma_1\nu_0) + \frac{2}{\hbar} \frac{1}{\sqrt{4\pi}} \frac{1}{\sqrt{15}} \frac{1}{3} F_1^a \sigma_1 \nu_2 = 0 \\
(l=2, m=0) \quad & \omega\nu_2 - \frac{2}{\sqrt{15}}v_F q\nu_1 - \frac{2}{\sqrt{15}}v_F qF_1^a\nu_1 + \frac{1}{\sqrt{4\pi}}\sigma_0 F_0^a \nu_2 = 0
\end{aligned} \tag{C.35}$$

With the substitutions from Appendix A, the coupled equations become

$$\begin{aligned}
(l=0, m=0) \quad & \omega x - By = 0 \\
(l=1, m=0) \quad & \omega y - Ax - Cz + D(\sigma_0 y - \sigma_1 x) + \frac{2}{\sqrt{5}}F\sigma_1 z = 0 \\
(l=2, m=0) \quad & \omega z - B'y + E\sigma_0 z = 0
\end{aligned} \tag{C.36}$$

The solution of these equations is performed later. First, we look at the solutions to equations that have some of the above terms, but not all of them, beginning with the most simple set of equations, which were the equations that were first discovered by Abrikosov and Dzyaloshinski.

### C.2.2 $\nu_0, \nu_1, \sigma_0, f_0^a, f_1^a \neq 0$

The coupled equations are

$$\begin{aligned}
(l = 0, m = 0) \quad \omega x - By &= 0 \\
(l = 1, m = 0) \quad \omega y - Ax + D\sigma_0 y &= 0
\end{aligned} \tag{C.37}$$

This is a two-equation, two-unknown situation, and the characteristic equation is easily obtained by setting the determinant of the matrix equal to zero.

$$\text{Det} \begin{bmatrix} \omega & -B \\ -A & \omega + D\sigma_0 \end{bmatrix} = 0 \tag{C.38}$$

This gives the characteristic equation

$$\omega^2 + D\sigma_0\omega - AB = 0 \tag{C.39}$$

and the solution to this quadratic equation is

$$\omega = -\frac{1}{2}D\sigma_0 \pm \frac{1}{2} \left[ (D\sigma_0)^2 - 4(-AB) \right]^{1/2} \tag{C.40}$$

For  $q = 0$ , there is a gapless solution and a gapped solution, corresponding to the spin precessional mode ( $l = 0$ ) and the spin current mode ( $l = 1$ ). For small  $q$ , i.e.  $q \ll k_F$ , the two solutions are characterized by a quadratic dispersion,

$$\begin{aligned}
\omega_0 &= \frac{AB}{D\sigma_0} \\
\omega_1 &= -D\sigma_0 - \frac{AB}{D\sigma_0}
\end{aligned}
\tag{C.41}$$

### C.2.3 $\nu_0, \nu_1, \nu_2, \sigma_0, f_0^a, f_1^a, f_2^a \neq 0$

This section contains a review of the calculation and results of Bedell and Blagoev presented in [8], in which the authors obtained a result for a new term in the expression for a ferromagnetic spin wave in fermi liquid theory. The result can also be seen in [9]. The new term arises, as will be shown below, from the necessary inclusion of the  $l = 2$  harmonic of the fermi surface distortion.

The coupled equations are

$$\begin{aligned}
(l = 0, m = 0) \quad & \omega x - By = 0 \\
(l = 1, m = 0) \quad & \omega y - Ax - Cz + D\sigma_0 y = 0 \\
(l = 2, m = 0) \quad & \omega z - B'y + E\sigma_0 z = 0
\end{aligned}
\tag{C.42}$$

and the characteristic equation is



$$\omega^3 + (D + E)\sigma_0\omega^2 + (DE\sigma_0^2 - AB - B'C)\omega - ABE\sigma_0 = 0 \quad (\text{C.43})$$

This is a cubic equation in  $\omega$ , and it's direct solution is messy and not helpful analytically. This direct solution is plotted in the main body of the thesis, but it will not be given analytically here. Instead, we will focus on the new term that is introduced by the inclusion of the  $l = 2$  harmonics of the distortion of the fermi surface and the Landau parameters. For comparison, the characteristic equation from the previous subsection, where only  $l = 0, 1$  distortions and Landau parameters are allowed, is

$$\omega^2 - AB + D\sigma_0\omega = 0 \quad (\text{C.44})$$

while the new characteristic equation, after dividing by  $\omega + E$ , is

$$\omega^2 - AB - B'C \frac{\omega}{\omega + E} + D\sigma_0\omega = 0 \quad (\text{C.45})$$

From this it is clear that the new term that is introduced with the inclusion of the  $l = 2$  harmonics is

$$-B'C \frac{\omega}{\omega + E} \quad (\text{C.46})$$

If we can look at the limits of  $\omega$  that make this term easy to approximate as independent of  $\omega$ , then we will be left with a characteristic equation that is quadratic. Thus, let's inspect the following limits: 1)  $\omega \ll E\sigma_0$ ; 2)  $\omega \approx -D\sigma_0$ ; 3)  $\omega \approx -E\sigma_0$ . These three limits describe the

### C.2.4 $\nu_0, \nu_1, \sigma_0, \sigma_1, f_0^a, f_1^a \neq 0$

The coupled equations are

$$\omega\nu_0 - \frac{1}{\sqrt{3}}B\nu_1 = 0 \quad (\text{C.47})$$

$$\omega\nu_1 - \frac{1}{\sqrt{3}}A\nu_0 + C(\sigma_1\nu_0 - \sigma_0\nu_1) = 0 \quad (\text{C.48})$$

The characteristic equation is

$$\omega^2 - D\sigma_0\omega + \frac{1}{\sqrt{3}}BD\sigma_1 - \frac{1}{3}AB = 0 \quad (\text{C.49})$$

and the solution is

$$\omega = \frac{1}{2}D\sigma_0 \pm \frac{1}{2} \left[ D^2\sigma_0^2 - 4 \left( \frac{1}{\sqrt{3}}BD\sigma_1 - \frac{1}{3}AB \right) \right]^{1/2} \quad (\text{C.50})$$

Using a Taylor expansion,  $f(\xi) = \sum_n \frac{1}{n!} \frac{\partial^n}{\partial \xi} f(\xi)|_{\xi=0} \xi^n$ , and keeping only the two leading terms of this expansion, the two solutions for the dispersion for small  $q$  are

$$\omega = \frac{1}{\sqrt{3}} \frac{\sigma_1}{\sigma_0} B - \frac{1}{3} AB \quad (\text{C.51})$$

and

$$\omega = -D\sigma_0 - \frac{1}{\sqrt{3}} \frac{\sigma_1}{\sigma_0} B + \frac{1}{3} AB \quad (\text{C.52})$$

### C.2.5 $\nu_0, \nu_1, \sigma_1, f_0^a, f_1^a \neq 0$

In this section we show the new spin waves that result from only allowing the system to incur an  $l = 1$  instability in the ground state. In other words, there is no net magnetization in the ground state, there is only a spin current in the ground state. The calculation is similar to the more general situation, where a net magnetization occurs, as well, so only the differences in the calculations will be shown. The reader should refer to the above subsection of this appendix for a full derivation of the coupled equations.

The set of coupled equations to solve are given by

In terms of the simplified parameters, the equations are

$$(l = 0, m = 0) \quad \omega x - By = 0 \quad (\text{C.53})$$

$$(l = 1, m = 0) \quad \omega y - Ax - C\sigma_1 x = 0 \quad (\text{C.54})$$

Solving the first equation gives  $x = \frac{B}{\omega}y$ . Substituting this into the second equation, and solving,

$$\begin{aligned} \omega y - \frac{AB}{\omega}y - D\sigma_1 \frac{B}{\omega}y &= 0 \\ \omega - \frac{AB}{\omega} - \frac{BD}{\omega}\sigma_1 &= 0 \\ \omega^2 &= (AB + BC\sigma_1) \end{aligned} \quad (\text{C.55})$$

Now, we must enforce the condition that  $B < 0$ , which is the necessary condition for the  $l = 1$  instability that we are allowing to occur in the ground

state. Since  $B < 0$ , the above equation can be expanded for small  $q$ , and the spin wave that results has a dispersion that is real (not imaginary). If  $B$  were not less than zero, the spin wave would be purely imaginary for small  $q$ , because the term in the parentheses would be less than zero, and taking the square root of it would produce an imaginary mode. However, the signs work out correctly, and the mode is real.

Enforcing the condition  $B < 0$ , and expanding the square root gives an approximate solution for the spin modes for small  $q$ .

$$\omega = \pm(|B|D\sigma_1)^{1/2} \pm \frac{A|B|^{1/2}}{D^{1/2}\sigma_1^{1/2}} \quad (\text{C.56})$$

The leading order of this equation can be seen to be proportional to  $q^{1/2}$ , which is a novel result in itinerant spin wave theory.

### C.2.6 $\nu_0, \nu_1, \nu_2, \sigma_0, \sigma_1, f_0^a, f_1^a, f_2^a \neq 0$

The coupled equations are

$$\begin{aligned} (l=0, m=0) \quad & \omega x - By = 0 \\ (l=1, m=0) \quad & \omega y - Ax - Cz + D(\sigma_0 y - \sigma_1 x) + \frac{2}{\sqrt{5}}F\sigma_1 z = 0 \\ (l=2, m=0) \quad & \omega z - B'y + E\sigma_0 z = 0 \end{aligned} \quad (\text{C.57})$$

The characteristic equation is

$$\omega^2 - AB + C\sigma_0\omega - BC\sigma_1 + B'DE\frac{F_1^a}{3}\sigma_1\left(\frac{\omega}{\omega + DF_0^a\sigma_0}\right) = 0 \quad (\text{C.58})$$

This is a cubic equation, as can be seen by multiplying the equation by the denominator in the last term. However, it is easier to look at the limits of the equation in terms of this denominator, which will result in a quadratic equation, with the hope that solving the cubic equation exactly is unnecessary. Notice that  $DF_0^a\sigma_0$  is the Larmor frequency (TRUE??). First we look at the limit

$$\omega \gg DF_0^a\sigma_0 \quad (\text{C.59})$$

In this limit,

$$\frac{\omega}{\omega + DF_0^a\sigma_0} \approx \frac{\omega}{\omega} = 1 \quad (\text{C.60})$$

Solving Eq. (C.58) for  $\omega$ , the dispersions for the spin precession mode,  $\omega_0$ , and the spin current mode,  $\omega_1$ , in this limit are

$$\omega_0 = \frac{1}{C\sigma_0}2(AB + BC\sigma_1 - B'DE\frac{F_1^a}{3}\sigma_1) \quad (\text{C.61})$$

$$\omega_1 = -C\sigma_0 - \frac{1}{C\sigma_0}2(AB + BC\sigma_1 - B'DE\frac{F_1^a}{3}\sigma_1) \quad (\text{C.62})$$

Next, examining the limit  $\omega \approx DF_0^a\sigma_0$ , which is probably the most reasonable limit to assume to be closest to a real system, where

$$\frac{\omega}{\omega + DF_0^a \sigma_0} \approx \frac{\omega}{2\omega} = \frac{1}{2} \quad (\text{C.63})$$

the dispersions are

$$\omega_0 = \frac{1}{C\sigma_0} (AB + BC\sigma_1 - B'DE \frac{F_1^a}{3} \sigma_1) \quad (\text{C.64})$$

$$\omega_1 = -C\sigma_0 - \frac{1}{C\sigma_0} (AB + BC\sigma_1 - B'DE \frac{F_1^a}{3} \sigma_1) \quad (\text{C.65})$$

Finally, in the limit  $\omega \ll DF_0^a \sigma_0$ , and therefore,

$$\frac{\omega}{\omega + DF_0^a \sigma_0} \approx \frac{\omega}{DF_0^a \sigma_0} \quad (\text{C.66})$$

the dispersions are

$$\omega_0 = \frac{AB + BC\sigma_1}{C\sigma_0 + B'E \frac{F_1^a}{3} \sigma_1} \quad (\text{C.67})$$

$$\omega_1 = -(C\sigma_0 + B'E \frac{F_1^a}{3} \sigma_1) - \frac{AB + BC\sigma_1}{C\sigma_0 + B'E \frac{F_1^a}{3} \sigma_1} \quad (\text{C.68})$$

### **C.2.7** $\nu_0, \nu_1, \nu_2, \sigma_0, \sigma_1, f_0^a, f_1^a, f_2^a \neq 0$

The coupled equations are

$$\begin{aligned}
(l=0, m=0) \quad & \omega x - By = 0 \\
(l=1, m=0) \quad & \omega y - Ax - Cz + D(\sigma_0 y - \sigma_1 x) = 0 \\
(l=2, m=0) \quad & \omega z - B'y + E\sigma_0 z = 0
\end{aligned}
\tag{C.69}$$

**C.2.8**  $\nu_0, \nu_1, \nu_2, \sigma_1, f_0^a, f_1^a, f_2^a \neq 0$

The coupled equations are

$$\begin{aligned}
(l=0, m=0) \quad & \omega x - By = 0 \\
(l=1, m=0) \quad & \omega y - Ax - Cz - D\sigma_1 x + \frac{2}{\sqrt{5}}F\sigma_1 z = 0 \\
(l=2, m=0) \quad & \omega z - B'y = 0
\end{aligned}
\tag{C.70}$$

**C.2.9**  $\nu_0, \nu_1, \nu_2, \sigma_0, \sigma_2, f_0^a, f_1^a, f_2^a \neq 0$

The coupled equations are

$$\begin{aligned}
(l=0, m=0) \quad & \omega x - By = 0 \\
(l=1, m=0) \quad & \omega y - Ax - Cz + D\sigma_0 y - F\sigma_2 y = 0 \\
(l=2, m=0) \quad & \omega z - B'y + E(\sigma_0 z - \sigma_2 x) = 0
\end{aligned}
\tag{C.71}$$



# Appendix D

In this appendix, we show the full calculation of the new modes that arise from including a spiral spin density wave (SDW) in the ground state of a fermi liquid, with only an exchange interaction.

The LKE is given by

$$\begin{aligned}
& \frac{\partial}{\partial t} (\delta\sigma_x \hat{i} + \delta\sigma_y \hat{j} + \delta\sigma_z \hat{k}) \\
& + v_i \frac{\partial}{\partial r_i} \left[ \delta\sigma_x \hat{i} + \delta\sigma_y \hat{j} + \delta\sigma_z \hat{k} - \frac{\partial n_p^0}{\partial \varepsilon_p} (\delta h_x \hat{i} + \delta h_y \hat{j} + \delta h_z \hat{k}) \right] \\
& + \frac{2}{\hbar} \left[ (\sigma_x \delta h_y + \delta\sigma_x h_y - \sigma_y) \delta h_x \hat{k} \right. \\
& \quad + (\sigma_z \delta h_x + \delta\sigma_z h_x - \sigma_x \delta h_z - \delta\sigma_x h_z) \hat{j} \\
& \quad \left. + (\sigma_y \delta h_z + \delta\sigma_y h_z - \sigma_z \delta h_y - \delta\sigma_z h_y) \hat{i} \right]
\end{aligned} \tag{D.1}$$

First, these equations are separated into the component equations (which are the  $\hat{i}$ ,  $\hat{j}$ , and  $\hat{k}$  equations). Then the  $\hat{i}$  and  $\hat{j}$  equations are combined in two ways:  $\hat{i} \pm i\hat{j}$ . Then the following substitutions are made:

$$\begin{aligned}
\sigma^\pm &\equiv \sigma_x \pm i\sigma_y \\
\delta\sigma^\pm &\equiv \delta\sigma_x \pm i\delta\sigma_y
\end{aligned} \tag{D.2}$$

Next the substitution  $\delta\sigma_p^\pm \equiv -\frac{\partial n}{\partial \varepsilon} \nu_p^\pm$  is made.

$$\begin{aligned}
\boxed{+} &\rightarrow \frac{\partial}{\partial t} \delta\sigma_p^+ + v_i \frac{\partial}{\partial r_i} (\delta\sigma_p^+ - \frac{\partial n_p}{\partial \varepsilon_p} \delta h_p^+) + \frac{2i}{\hbar} (\sigma_p^+ \delta h_p^z - \delta\sigma_p^z h_p^+ + \delta\sigma_p^+ h_p^z - \sigma_p^z \delta h_p^+) = 0 \\
\boxed{-} &\rightarrow \frac{\partial}{\partial t} \delta\sigma_p^- + v_i \frac{\partial}{\partial r_i} (\delta\sigma_p^- - \frac{\partial n_p}{\partial \varepsilon_p} \delta h_p^-) - \frac{2i}{\hbar} (\sigma_p^- \delta h_p^z - \delta\sigma_p^z h_p^- + \delta\sigma_p^- h_p^z - \sigma_p^z \delta h_p^-) = 0 \\
\boxed{z} &\rightarrow \frac{\partial}{\partial t} \delta\sigma_p^z + v_i \frac{\partial}{\partial r_i} (\delta\sigma_p^z - \frac{\partial n_p}{\partial \varepsilon_p} \delta h_p^z) - \frac{i}{\hbar} (\sigma_p^+ \delta h_p^- - \sigma_p^- \delta h_p^+ + \delta\sigma_p^+ h_p^- - \delta\sigma_p^- h_p^+) = 0
\end{aligned} \tag{D.3}$$

Lastly, Fourier transforming, the equations for +, -, and z become

$$\begin{aligned}
\boxed{+} &\rightarrow \omega \nu_p^+ - \vec{v}_p \cdot \vec{q} (\nu_p^+ + \delta h_p^+) + \frac{2}{\hbar} (\sigma_p^+ \delta h_p^z - \delta\sigma_p^z h_p^+ + \delta\sigma_p^+ h_p^z - \sigma_p^z \delta h_p^+) = 0 \\
\boxed{-} &\rightarrow \omega \nu_p^- - \vec{v}_p \cdot \vec{q} (\nu_p^- + \delta h_p^-) - \frac{2}{\hbar} (\sigma_p^- \delta h_p^z - \delta\sigma_p^z h_p^- + \delta\sigma_p^- h_p^z - \sigma_p^z \delta h_p^-) = 0 \\
\boxed{z} &\rightarrow \omega \nu_p^z - \vec{v}_p \cdot \vec{q} (\nu_p^z + \delta h_p^z) - \frac{1}{\hbar} (\sigma_p^+ \delta h_p^- - \sigma_p^- \delta h_p^+ + \delta\sigma_p^+ h_p^- - \delta\sigma_p^- h_p^+) = 0
\end{aligned} \tag{D.4}$$

Projecting these equations onto spherical harmonic moments, the equations become

$$\begin{aligned}
\boxed{+} \rightarrow 0, 0 &\rightarrow \omega x^+ - B y^+ = 0 \\
&\rightarrow 1, 0 \rightarrow \omega y^+ - A x^+ + D m^z y^+ - D m^+ y^z = 0 \\
\boxed{-} \rightarrow 0, 0 &\rightarrow \omega x^- - B y^- = 0 \\
&\rightarrow 1, 0 \rightarrow \omega y^- - A x^- - D m^z y^- + D m^- y^z = 0 \\
\boxed{z} \rightarrow 0, 0 &\rightarrow \omega x^z - B y^z = 0 \\
&\rightarrow 1, 0 \rightarrow \omega y^z - A x^z - \frac{1}{2} D m^+ y^- + \frac{1}{2} D m^- y^+ = 0
\end{aligned} \tag{D.5}$$

The  $q = 0$  characteristic equation for these coupled equations can be obtained from the matrix that corresponds to this equation. The matrix is

$$\begin{bmatrix}
\omega + D m^z & 0 & -D m^+ \\
0 & \omega - D m^z & D m^- \\
\frac{1}{2} D m^- & -\frac{1}{2} D m^+ & \omega
\end{bmatrix} \tag{D.6}$$

Setting the determinant of this matrix to zero gives the characteristic equation for  $q = 0$ .

$$(\omega + D m^z) \left[ (\omega - D m^z) \omega + \frac{1}{2} D^2 m^+ m^- \right] - D m^+ \left[ -\frac{1}{2} D m^- (\omega - D m^z) \right] = 0 \tag{D.7}$$

A straightforward solution of this cubic equation gives the eigenvalues, which are

$$\begin{aligned}
\omega &= 0 \\
\omega &= \pm D(m^z m^z - m^+ m^-)^{1/2}
\end{aligned}
\tag{D.8}$$

These equations can be seen to be very similar to the Silin result for  $q = 0$ , which is

$$\begin{aligned}
\omega &= 0 \\
\omega &= \pm Dm^z
\end{aligned}
\tag{D.9}$$

The results for the spiral modes are consistent with the Silin result in the limit of  $m^\pm \rightarrow 0$ .

The  $q \neq 0$  matrix is given by

$$\begin{bmatrix}
\omega - \frac{AB}{\omega} + Dm^z & 0 & -Dm^+ \\
0 & \omega - \frac{AB}{\omega} - Dm^z & Dm^- \\
\frac{1}{2}Dm^- & -\frac{1}{2}Dm^+ & \omega - \frac{AB}{\omega}
\end{bmatrix}
\tag{D.10}$$

Upon simplification, the resultant characteristic equation of this matrix is

$$\omega^6 - \Gamma\omega^4 + \Gamma AB\omega^2 - A^3 B^3 = 0
\tag{D.11}$$

where  $\Gamma \equiv 3AB - D^2 m^z m^z + D^2 m^+ m^-$ . The solutions to this equation are

$$\begin{aligned}
\omega &= \pm (AB)^{1/2} \\
\omega &= \pm \left[ \frac{1}{2} (\Gamma - AB \pm [\Gamma^2 - 2AB\Gamma - 3A^2B^2]^{1/2}) \right]^{1/2}
\end{aligned} \tag{D.12}$$

The first solution is the longitudinal spin mode, and its dispersion is proportional to  $q$ .

Taking a closer look at the second solution, and plugging back in for  $\Gamma$ , the second solution becomes

$$\begin{aligned}
\omega &= \pm \left[ \frac{1}{2} (2AB + D^2[m^z m^z - m^+ m^-] \pm [-4A^2B^2 + \right. \\
&\quad \left. (-2AB - D^2[m^z m^z - m^+ m^-])^2]^{1/2}) \right]^{1/2}
\end{aligned} \tag{D.13}$$

For small  $q$ , the radicals can be expanded, and the leading order  $q$  behavior can be extracted. Upon performing the expansions, and after some algebra, the leading order solutions for the spiral mode are found to be proportional to  $q^{1/2}$ , and are given by

$$\begin{aligned}
\omega &= \pm 0 \\
\omega &= \pm D(m^z m^z - m^+ m^-) \pm \frac{AB}{D(m^z m^z - m^+ m^-)}
\end{aligned} \tag{D.14}$$

I included the  $\pm$  in the first solution to show explicitly that it is a double root, just for completeness. The second solution is the Silin result with the extra term,  $m^+m^-$ . Thus, the second solution would reduce to the Silin result in the limit of  $m^\pm \rightarrow 0$ . The first solution,  $\omega = 0$ , is discussed in the body of the thesis, where it is plotted as a function of  $q$ , without the restriction of keeping it small enough to expand the radical, which was only done for the sake of making the solution obtainable analytically. Obviously, by inspection, it is not really equal to zero – this is just in the small  $q$  limit.

# Appendix E

In this appendix, we show the calculation of the thermodynamics properties that arise from the new spin modes.

## E.3 Specific Heat

The specific heat contribution from a specific mechanism is determined by the amount of energy that is required to change the system's temperature via that mechanism by a unit of temperature, or in other words, the partial derivative of the energy of the mechanism with respect to temperature. In the case of a collective mode, the energy of a collective mode is calculated by an integral of that mode over  $\vec{q}$ ,

$$\varepsilon = \frac{2}{(2\pi)^3} \int q^2 \sin \theta \, dq \, d\theta \, d\phi \frac{\hbar\omega(q)}{e^{\frac{\hbar\omega(q)}{k_B T}} - 1} \quad (\text{E.1})$$

The angular part of this integral is  $4\pi$ , thus the integral becomes

$$\varepsilon = \frac{1}{\pi^2} \int_0^\infty q^2 \, dq \frac{\hbar\omega(q)}{e^{\frac{\hbar\omega(q)}{k_B T}} - 1} \quad (\text{E.2})$$

The specific heat is then calculated by the general formula  $C_V = (\frac{\partial \varepsilon}{\partial T})_V$ .

### E.3.1 Specific Heat for $\omega_0(q) \sim q^{1/2}$ spin mode

Now we turn to the specific heat calculations for the new collective modes that we are presenting in this thesis. For these calculations, we will be looking at the low-temperature region, and thus only the lowest order of  $q$  of a spin mode will be included in the specific heat calculation. This is valid, because the bosonic nature of the mode dictates that only the lowest energy states of the mode will be occupied at very low temperatures. So, for example, in the case of the  $q^{1/2}$  mode, only the  $q^{1/2}$  term will matter, since the  $q^{3/2}$  will not factor into the dispersion for very small  $q$ . First, for the ( $l = 0$ )  $q^{1/2}$  mode, the integral to calculate the energy density  $\varepsilon$  is

$$\varepsilon = \frac{1}{\pi^2} \int_0^\infty q^2 dq \frac{\hbar J q^{1/2}}{e^{\frac{\hbar J q^{1/2}}{k_B T}} - 1} \quad (\text{E.3})$$

where  $Jq^{1/2} \equiv (BD\sigma_1)^{1/2}$ . Recasting the integral in terms of a dimensionless variable,  $x \equiv \hbar J q^{1/2} / k_B T$ , the integral in terms of  $x$  is

$$\varepsilon = \frac{(k_B T)^7}{\pi^2 \hbar^6 B^6} \int_0^\infty dx \frac{x^6}{e^x - 1} \quad (\text{E.4})$$

where the integral over  $x$  can be done numerically,

$$\int_0^\infty dx \frac{x^6}{e^x - 1} \approx 726.011 \quad (\text{E.5})$$

Thus the contribution to the specific heat of this mode is

$$C_V \sim T^6 \quad (\text{E.6})$$



### E.3.2 Specific Heat for $\omega_0(q) \sim q^1$ spin mode

The specific heat contribution from the linear mode, which arises from including both  $\sigma_0$  and  $\sigma_1$  moments in the ground state, is given by

$$\varepsilon = \frac{1}{\pi^2} \int_0^\infty q^2 dq \frac{\hbar J q}{e^{\frac{\hbar J q}{k_B T}} - 1} \quad (\text{E.7})$$

after some similar algebra, the contribution to the specific heat of this mode is seen to be

$$C_V \sim T^3 \quad (\text{E.8})$$

# Bibliography

- [1] A. A. Abrikosov and I. E. Dzyaloshinski. Spin waves in a ferromagnetic metal. *Soviet Physics JETP*, 8(35):535–537, Nov 1959.
- [2] Z. Akdeniz, P. Vignolo, and M. P. Tosi. Collective dynamics of fermion clouds in cigar-shaped traps. *Physics Letters A*, 311:246–253, 2003.
- [3] M. H. Anderson, J. R. Ensher, M. R. Matthews, C. E. Wieman, and E. A. Cornell. Observation of Bose-Einstein Condensation in a Dilute Atomic Vapor. *Science*, 269(5221):198–201, 1995.
- [4] S. Babu and G. E. Brown. Quasiparticle interaction in liquid  $^3\text{He}$ . *Annals of Physics*, 78(1):1 – 38, 1973.
- [5] M. Bartenstein, A. Altmeyer, S. Riedl, S. Jochim, C. Chin, J. Hecker Denschlag, and R. Grimm. Crossover from a molecular bose-einstein condensate to a degenerate fermi gas. *Phys. Rev. Lett.*, 92(12):120401, Mar 2004.
- [6] Gordon Baym and Christopher Pethick. *Landau Fermi Liquid Theory*. John Wiley and Sons, Inc., 1991.
- [7] C. C. Becerra, Y. Shapira, N. F. Oliveira, and T. S. Chang. Lifshitz point in mnp. *Phys. Rev. Lett.*, 44(25):1692–1695, Jun 1980.
- [8] K. Bedell and K. Blagoev. Quantum spin hydrodynamics and a new spin current mode in ferromagnetic metals. *Phil. Mag. Lett*, 81(7):511–517, Apr 2001.
- [9] Kevin S. Bedell and Hari P. Dahal. Spin waves in quasiequilibrium spin systems. *Physical Review Letters*, 97(4):047204, 2006.
- [10] Krastan Blagoev. *Electron correlations in Fermi and non-Fermi liquids*. PhD thesis, Boston College, 1998.

- [11] Georg M. Bruun and Charles W. Clark. Hydrodynamic excitations of trapped fermi gases. *Phys. Rev. Lett.*, 83(26):5415–5418, Dec 1999.
- [12] P. Capuzzi, P. Vignolo, F. Federici, and M. P. Tosi. Sound wave propagation in strongly elongated fermion clouds at finite collisionality. *Journal of Physics B: Atomic, Molecular and Optical Physics*, 39:S25–S35, 2006.
- [13] L. R. Corruccini, D. D. Osheroff, D. M. Lee, and R. C. Richardson. Spin diffusion in liquid  $^3\text{he}$ : The effect of leggett and rice. *Phys. Rev. Lett.*, 27(10):650–653, Sep 1971.
- [14] H. P. Dahal, S. Gaudio, J. D. Feldmann, and K. S. Bedell. Spin collective modes of two-species fermi liquids:  $^3\text{he}$  and atomic gases near the feshbach resonance. *Physical Review A (Atomic, Molecular, and Optical Physics)*, 78(3):035601, 2008.
- [15] Hari Prasad Dahal. *Correlation effects in dilute Fermi liquids: nonequilibrium spin systems and graphene*. PhD thesis, Boston College, 2008.
- [16] K. B. Davis, M. O. Mewes, M. R. Andrews, N. J. van Druten, D. S. Durfee, D. M. Kurn, and W. Ketterle. Bose-einstein condensation in a gas of sodium atoms. *Phys. Rev. Lett.*, 75(22):3969–3973, Nov 1995.
- [17] Gerald L. Dunifer, Daniel Pinkel, and Sheldon Schultz. Experimental determination of the landau fermi-liquid-theory parameters: Spin waves in sodium and potassium. *Phys. Rev. B*, 10(8):3159–3185, Oct 1974.
- [18] Alexander Fetter and John Dirk Walecka. *Quantum Theory of Many Particle Systems*. Dover Publications, Inc., 2003.
- [19] Sergio Gaudio. *Consequences of Fermi liquid theory close to a diverging s-wave scattering length*. PhD thesis, Boston College, 2007.
- [20] Dennis S. Greywall. Specific heat of normal liquid  $^3\text{he}$ . *Phys. Rev. B*, 27(5):2747–2766, Mar 1983.
- [21] Igor Žutić, Jaroslav Fabian, and S. Das Sarma. Spintronics: Fundamentals and applications. *Rev. Mod. Phys.*, 76(2):323–410, Apr 2004.
- [22] B. R. Johnson, J. S. Denker, N. Bigelow, L. P. Lévy, J. H. Freed, and D. M. Lee. Observation of nuclear spin waves in spin-polarized atomic hydrogen gas. *Phys. Rev. Lett.*, 52(17):1508–1511, Apr 1984.

- [23] J. Kinast, S. L. Hemmer, M. E. Gehm, A. Turlapov, and J. E. Thomas. Evidence for superfluidity in a resonantly interacting fermi gas. *Phys. Rev. Lett.*, 92(15):150402, Apr 2004.
- [24] A. J. Leggett and M. J. Rice. Spin echoes in liquid  $^3\text{He}$  and mixtures: A predicted new effect. *Phys. Rev. Lett.*, 20(12):586–589, Mar 1968.
- [25] Laurent P. Lévy and Andrei E. Ruckenstein. Collective spin oscillations in spin-polarized gases: Spin-polarized hydrogen. *Phys. Rev. Lett.*, 52(17):1512–1515, Apr 1984.
- [26] H. J. Lewandowski, D. M. Harber, D. L. Whitaker, and E. A. Cornell. Observation of anomalous spin-state segregation in a trapped ultracold vapor. *Phys. Rev. Lett.*, 88(7):070403, Jan 2002.
- [27] Xiong-Jun Liu, Xin Liu, L. C. Kwek, and C. H. Oh. Optically induced spin-hall effect in atoms. *Physical Review Letters*, 98(2):026602, 2007.
- [28] P. Massignan, G. M. Bruun, and H. Smith. Viscous relaxation and collective oscillations in a trapped fermi gas near the unitarity limit. *Physical Review A (Atomic, Molecular, and Optical Physics)*, 71(3):033607, 2005.
- [29] J. M. McGuirk, H. J. Lewandowski, D. M. Harber, T. Nikuni, J. E. Williams, and E. A. Cornell. Spatial resolution of spin waves in an ultracold gas. *Phys. Rev. Lett.*, 89(9):090402, Aug 2002.
- [30] A. B. Migdal. *Nuclear theory: The quasiparticle method*. W. A. Benjamin, Inc., 1968.
- [31] Philippe Nozieres. *Theory of Interacting Fermi Systems*. Addison Wesley Longman, Inc., 1997.
- [32] P. Pedri, D. Guéry-Odelin, and S. Stringari. Dynamics of a classical gas including dissipative and mean-field effects. *Phys. Rev. A*, 68(4):043608, Oct 2003.
- [33] David Pines and Philippe Nozieres. *Theory of Quantum Liquids*. Perseus Books Publishing, L. L. C., 1999.
- [34] C. A. Regal, M. Greiner, and D. S. Jin. Observation of resonance condensation of fermionic atom pairs. *Phys. Rev. Lett.*, 92(4):040403, Jan 2004.

- [35] C. A. Regal and D. S. Jin. Measurement of positive and negative scattering lengths in a fermi gas of atoms. *Phys. Rev. Lett.*, 90(23):230404, Jun 2003.
- [36] Sheldon Schultz and Gerald Dunifer. Observation of spin waves in sodium and potassium. *Phys. Rev. Lett.*, 18(8):283–287, Feb 1967.
- [37] G. Shirane, R. Cowley, C. Majkrzak, J. B. Sokoloff, B. Pagonis, C. H. Perry, and Y. Ishikawa. Spiral magnetic correlation in cubic mnsi. *Phys. Rev. B*, 28(11):6251–6255, Dec 1983.
- [38] V. P. Silin. Oscillations of a fermi-liquid in a magnetic field. *Soviet Physics JETP*, 33(6):945–950, ?? 1958.
- [39] Skomski. *Simple Models of Magnetism*. Oxford University Press, 2008.
- [40] Jian-Jun Song and Bradley A. Foreman. Persistent currents in cold atoms. *Physical Review A (Atomic, Molecular, and Optical Physics)*, 80(3):033602, 2009.
- [41] H. T. C. Stoof, M. Houbiers, C. A. Sackett, and R. G. Hulet. Superfluidity of spin-polarized  $^6\text{Li}$ . *Phys. Rev. Lett.*, 76(1):10–13, Jan 1996.
- [42] J. A. Tarvin, G. Shirane, Y. Endoh, and Y. Ishikawa. Field dependence of spin dynamics in the itinerant ferromagnet mnsi. *Phys. Rev. B*, 18(9):4815–4820, Nov 1978.
- [43] Jean-Claude Toledano and Pierre Toledano. *Landau Theory of Phase Transitions*. World Scientific Publishing Co. Pte Ltd., 1987.
- [44] S.-K. Yip and Tin-Lun Ho. Zero sound modes of dilute fermi gases with arbitrary spin. *Phys. Rev. A*, 59(6):4653–4656, Jun 1999.